Nonlinear Control of Conventional Steam Power Plants

A DISSERTATION

SUBMITTED TO THE FACULTY OF THE GRADUATE SCHOOL

OF THE UNIVERSITY OF MINNESOTA

BY

Nahla Alamoodi

IN PARTIAL FULFILLMENT OF THE REQUIREMENTS

FOR THE DEGREE OF

Doctor of Philosophy

Advised by Prodromos Daoutidis

May 2016

Acknowledgements

First of all, I praise Allah the most Merciful for His blessings and gifts He sent me, for the person I am today, and for Him being My lord.

I would like to thank my advisor, Professor Prodromos Daoutidis, for his guidance, patience, and support. This thesis would have not been completed without his help. I should also thank Drs. Dimitrios Georgis and Ana Torres for their help during the early phase of my research.

I also express my gratitude to Abu Dhabi National Oil Company (ADNOC) for offering me the fellowship and for their full support during my course of study.

The Daoutidis group has always been a pleasant company. I would like to thank my lab mates Abdulla Malek, Udit Gupta, Nitish Mittal, Michael Zachar, Andrew Allman, Manjiri Moharir, Wentao Tang, Matthew Palys, and Lixia Kang for making the office enviroment friendly. Also I want to extend my thanking to Dr. Seongmin Heo for his valuable comments at different stages of my research.

My research was not going to succeed without the support of many of the people I lived among in the US. A special thank you to Dr. Alyaa Elramady for her care and support, Zeinab Alol, Hawanem UV, the Jamilat, GIAD and Alamaan families, and everyone who cared, supported, and offered help without waiting for me to ask.

Last and most, my deep gratitude to my family. My parents Dr. Saeed Alamoodi

and Noor Bin Naji for their continuous prayers and unconditional love, and my siblings Hatem, Lubna, and Khaled for their never ending care. I love you and will always do.

اللهم انفعني بما علمتني وعلمني ما ينفعني وزدني علماً ويقيناً وإيماناً وتسليما

"My Lord, benefit me with what You have taught me, teach me what will benefit me, and increase me in knowledge, certainty, faith, and submission"

Abstract

Conventional fossil fueled power plants are the leading power producers despite the existence of other energy sources and power generation technologies. As renewable power production is integrated into the grid, the operation of the conventional power plants faces new challenges that demand new control strategies. A key challenge is that the power demanded from conventional plants will continuously change to recover the production shortages caused by the intermittency of the renewable sources. This challenge demands an efficient control structure that is able to accommodate such power fluctuations, in addition to the inherent complexities of power plants such as the existence of deadtime associated with solid fuels. Coal, for example, is pulverized in real time prior to being transported to the furnace, which in turn, introduces deadtime to the power generation process.

This thesis proposes the use of deadtime compensated nonlinear controllers that are based on feedback linearization of models obtained from physical principles for the control of coal fired power plants. The designed control strategies aim to control power generation, boiler pressure, boiler drum level, and superheated and reheated steam temperatures. In the first part of this thesis, the control of the boiler pressure and power generation is considered. A single deadtime compensated model state feedback structure is developed to track variations in power demand and to reject applied disturbances.

The second part focuses on the development of a control strategy for the drum level dynamics in addition to the boiler pressure and power generation. The strategy proposed aims to decouple the manipulated variables of the boiler pressure and the drum level dynamics and applies a conventional three-element level controller with the deadtime nonlinear controller proposed in the first part.

In the last part of the thesis, the control of the boiler pressure, power generation, superheated steam temperatures is considered. The control strategy considers decoupling the performance of the boiler from the superheated steam temperature, the decomposition of the overall plant into three cascading subsystems and the application of deadtime compensated nonlinear controller for each subsystem.

Contents

List of Tables

List of Figures

Chapter 1

Introduction

Power generation continues to face challenges due to the simultaneous increase of demand and of environmental concerns regarding fossil fuels emissions. According to the U.S Energy Information Administration (EIA), the net worldwide power generation is expected to experience an annual increase of 2.2% until the year 2040 [1], most of which will be experienced in countries outside the Organization for Economic Cooperation and Development (OECD), such as India and China. The increase in power demand in these countries is driven by their strong, long-term economic growth [1]. However, countries that belong to the OECD have a rather slow average annual growth in power demand due to their economic stability, shifting to less energy-intensive industries, and the use of more efficient industrial equipment [2].

An increase in annual power generation necessitates an increase of fuel supply to the power industry. In efforts to decrease the environmental impact of fossil fuels emissions and due to governmental policies and incentives, the use of renewable sources for power generation is expected to increase at an annual rate of 2.8%, resulting in the production of 25% of the worldwide power by 2040 [1]. Despite this increase, coal remains the main fuel used. Contributing factors include its abundance and its low cost compared to other

fossil fuels [3]. Fossil fuels thus remain an essential source of fuel for power generation. Apart from their abundance and the well-established technologies of extracting energy form them, they serve as a standby energy source when renewable fuels availability recesses.

The operation of existing conventional power plants, i.e. fossil fuels fired power plants, faces several challenges as renewable power is incorporated into the grid. A key one is that the power demanded from conventional power plants will continuously change to recover the production shortages caused by the intermittent nature of renewable power sources. This challenge demands an efficient design of a control structure that is able to accommodate the fluctuations caused by the renewable power intermittency. In addition to this feature, the control structure is required to accommodate the inherent complexities of power plants. These complexities are the strong nonlinearity exhibited over a wide range of produced power, strong coupling between the different components of the plant, existence of unknown disturbances, variability of plant parameters [4], and in plants utilizing coal, the existence of a deadtime associated with the coal supply to the process when fuel flow adjustment is necessary [5].

1.1 Description of a conventional steam power plant

A power plant in its simplest form consists of a steam generator, turbine, electrical generator, condenser, and a pump. In the process of power generation, high-pressure superheated steam produced in the steam generator is sent to the turbine, or a set of turbines, through a steam governing valve. In the turbines, the steam expands converting its thermal energy into mechanical energy by rotating the shaft of the turbines, which in turn produce power through the electrical generator. The low-pressure saturated steam exiting the turbines is then received by the condenser and condenses to

saturated water. Following the condenser, a boiler feed pump raises the pressure of the condensed water to that of the steam generator causing the water to be in a subcooled state, and sends it back to the steam generator.

A steam generator is mainly composed of a furnace, steam drum and water walls, convection-type primary and secondary superheaters, a platen superheater and an economizer. The furnace is composed of a combustion chamber which includes the water walls and the platen superheater, and of a bypass duct. The bypass duct is divided into two sections, having convection-type superheaters in one section and a reheater in the other; at the end of the duct both divisions merge again and enclose the economizer. Utilizing the heat of combustion of the fuel in the furnace, boiling of saturated water is achieved in the water walls as well as final stage heating of superheated steam is achieved in the platen (radiant-type) superheater. The combustion effluent gas, which contains a large amount of energy, then travels to the bypass section and is divided to provide the required amount of energy to convert saturated steam to superheated one. In the superheaters division of the bypass duct, the secondary superheater is arranged such that it receives the flue gas prior to the primary superheater.

Following the steam path, saturated steam flows from the steam drum to the first stage of heating in the primary superheater where the flue gas in this position is at the lowest temperature in the bypass duct. The low temperature superheated steam then goes through a second stage of superheating in the secondary superheater and a final stage of superheating in the platen superheater. Once the steam leaves the steam generator through the platen superheater it is then utilized in a high pressure turbine (HP) for power generation. The partly expanded steam then returns to the reheater and leaves as low pressure superheated steam to a low pressure turbine (LP) where most power is being generated. Figure 1.1a illustrates a simplified thermal power plant block diagram and Figure 1.1b illustrates a detailed schematic of a steam generator.

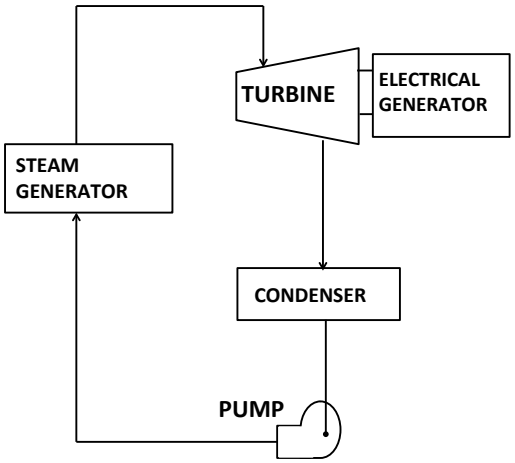

(a) Power plant block diagram

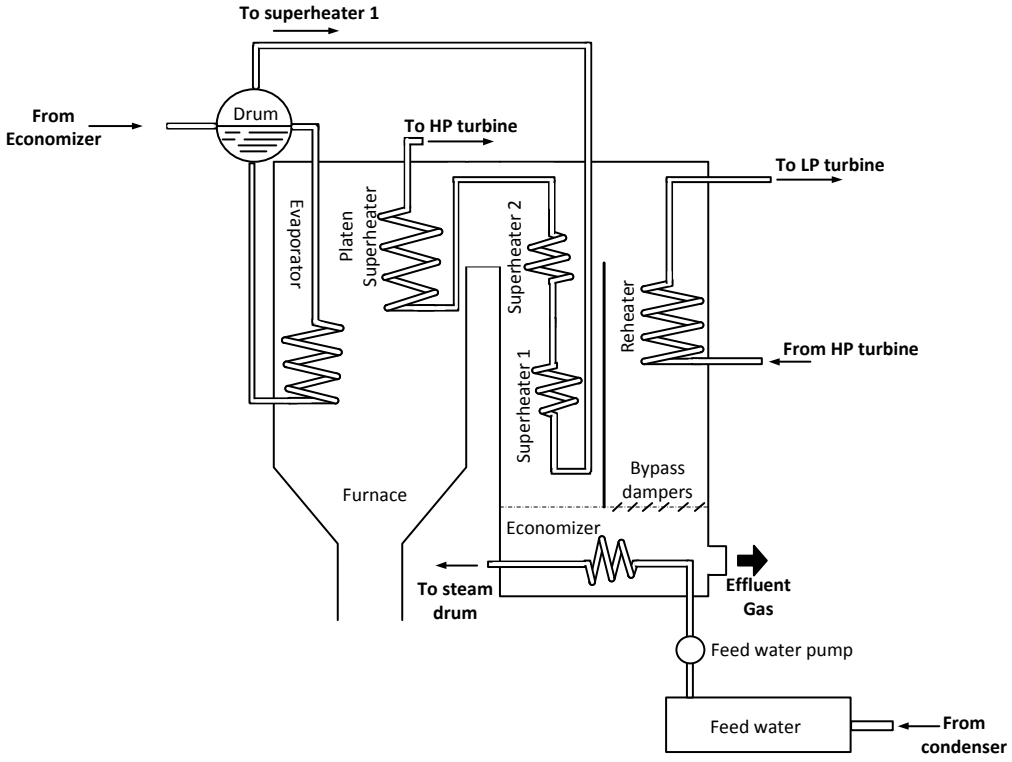

(b) Steam generator

Figure 1.1: Schematic of a conventional steam power plant

An upset in the operation of any part of the power plant will affect the operation of the other parts due to the intertwined functions among them. The furnace of the steam generator receives the fuel, combusts it with air, and supplies the required heat for the generation of superheated steam. For coal-fired power plants, the coal is first transported through conveyors from the feeders to the pulverizers, and upon pulverization the fine coal particles are carried by the combustion air to the furnace using forced draft fans. The air should be preheated to dry the coal but not to high enough temperature to start the combustion prior to reaching the furnace [6]. The process of coal transportation and grinding introduces a deadtime into the process of power generation. Changes in the operation of the coal handling system, forced draft fans, or pulverizers will increase the deadtime introduced into the process.

The boiler in the steam generator acts as an energy reserve, produces the required steam for power generation, and receives feedwater for continuous production of steam. Boilers generate steam at high pressures due to the reduced latent heat of vaporization of water at high pressures, and due to the high heat content of steam which results in an increase in the overall efficiency upon expansion in the turbine [7]. A decrease in the pressure will require an increase in the fuel consumption for a steady steam flow, an uncontrolled increase in the pressure might risk the life of the boiler and the lives of the operating staff, and a fluctuating boiler pressure can cause thermal stresses that ultimately result in boiler failure [8]. Hence, boiler pressure is a key variable in the control of power plants.

As steam is generated in the boiler, the level of water inside the boiler drum decreases and more feedwater is then required into the drum to compensate for the vaporized water. If the water level inside the drum is too low, boiler tubes will be damaged by overheating. On the contrary, if the steam generation is decreased and the water level is too high, separation of water and steam will be inefficient resulting in water

droplets to travel to the turbine. The increased moisture content of steam can lead to erosion, vibration, and water hammer in the turbine [9, 10]. These consequences of an unbalanced water level necessitate the control of drum level in the boiler.

Steam is also desired to be generated at a high temperature along with its high pressure to have a high heat content. An uncontrolled increase in temperature causes overheating and damages the steam generator, while a drop in the temperature decreases the overall efficiency of the power plant. Thus for an efficient operation, the temperatures of the superheated and reheated steam should be maintained closely at the desired temperatures.

1.2 Control of conventional steam power plants

Extensive studies have been carried out on the design of control strategies for conventional power plants. Model predictive control (MPC) is one of the preferred techniques due to its ability to accommodate constraints on the input and output variables, and its ability to accommodate processes that exhibit long time delay and processes that exhibit nonminimum phase characteristics such as the boiler drum level [11]. The predictive models utilized in the optimization problem dictate the complexity of the controller. The use of linear models for the control of the boiler pressure and power generation [13–16, 65] has been shown to lead to successful elimination of deadtime in the case of narrow operational range. For wide-range tracking of power demand and regulation of boiler pressure, drum level, and superheated and reheated steam temperatures, nonlinear physical models [17], fuzzy models based on iterative learning [18], Takagi-Sugeno fuzzy models based on fuzzy clustering and subspace identification [4, 19], neuro-fuzzy networks modeling [16], nonlinear exponential ARX [20], and switching multi linear [21]

models have been utilized. MPC has also been used as an upper control layer in a hierarchical control structure to determine economically optimal power demand trajectories with a lower control layer of PID controllers for the boiler-turbine system [22].

To overcome uncertainties in model parameters and variation of controller parameters, adaptive control has also been studied for the control of power generation. $\mathcal{L}_1$ adaptive control was applied to a boiler-turbine system that was modeled as a multi-input multi-output nonlinear system with unknown internal dynamics [23]. Nonlinear receding horizon control based on a genetic algorithm in combination with an H_∞ fuzzy state-feedback controller was also proposed for a boiler-turbine system. Based on a switching criterion, the adaptive control law switches between the genetic algorithm controller which handles large changes in set point, and the H_∞ fuzzy state-feedback controller which eliminates steady state errors [24]. Adaptive control based on the backstepping method was designed for boiler-turbine systems [25] and boiler-turbine-generator systems [26]. The backstepping method was applied due to its ability to account for the interactions between the generator unit and the boiler-turbine unit, for the parameter uncertainty, and to improve the power tracking under wide power variation range. For superheated temperature regulation, a predictive multistep multivariable adaptive regulator was proposed based on a stochastic model for the superheated steam temperature fluctuations [27].

Besides optimal control, analytical control approaches have also been proposed. Decentralized multivariable nonlinear controllers were considered based on their ability to achieve decoupling between the boiler pressure, drum level, and power generated, and asymptotic tracking of power set points [28]. A relative fuzzy PI controller was tested on a real-time process in a distributed control system for the control of boiler pressure [29]. The fuzzy rules were based on a neurofuzzy model of the boiler pressure. Coordinated control for a boiler- turbine system based on a sliding mode controller [30], and for

a boiler-turbine-generator system based on the backstepping method integrating coordinated passivation [31] were designed for asymptotic stability, improved performance of power regulation, mitigating interactions between power and boiler parameters, and protecting devices from thermodynamic tensions [31].

To include the dynamics of the power generation process in the controller design, feedback linearization was implemented with different types of linear controllers. The application of an active disturbance rejection controller (ADRC) designed based on feedback linearization was studied for the regulation of superheated steam temperature. The ADRC improves the control of superheated steam temperature by incorporating an extended state observer that can estimate the disturbances in real time [32]. Control of the boiler-turbine system based on feedback linearization was proposed by implementing the linearization on the boiler model and assuming the dynamics of the turbine to be negligible. The objective of the controller is tracking of power demand trajectory and of variable boiler pressure. Upon linearization of the boiler the boiler-turbine system is decoupled and single loop PI controllers were applied for each unit separately [33]. Similarly, set point tracking controller for tracking of power demand trajectory as well as variable boiler pressure was proposed based on approximate dynamic feedback linearization [34]. The dynamics of the boiler pressure, turbine mechanical power, and generator electrical power were considered. The partially linearized boiler-turbine-generator system was then controlled by an H_∞ robust controller. Adaptive feedback linearization was also studied for excitation control and regulation of synchronous generator operation. The synthesis of the controller constituted of an adaptive computation of an appropriate feedback linearizing control law to control the generator terminal voltage [35].

The majority of the proposed work mentioned above [18–26, 28, 30, 33, 34] bases the controller design on well known empirical models for the boiler designed by Astrom [36] and De Mello [37], or from input/output data of the plant. These models are weakly

nonlinear and are based on specific power plants. Although they capture the dominant boiler dynamics, they cannot capture the disturbances caused by a specific parameter change such as a change in the heating value of fuel, or fouling of boiler tubes. In addition, these model do not take into consideration the dynamics that are inherent in the boiler, such as the dynamics of water and steam enthalpies and densities.

Moreover, many of the proposed control strategies do not account for all the significant dynamics of the power plant. For example, in [32] the superheated steam temperature control was considered without considering the dynamics of the boiler. In [35] electric power generation control was considered without accounting for the dynamics of the boiler and the turbine.

Hence, a comprehensive study of power plant control that includes all significant dynamics contributing to power generation and is applicable to a wide range operation where process nonlinearity becomes significant is essential.

1.3 Thesis scope and organization

The goal of this thesis is to develop a nonlinear control strategy based on feedback linearization methods for controlling coal-fired conventional steam power plants. The work presented aims to develop a control strategy that :

- Utilizes nonlinear models that are obtained from physical principles.
- Mitigates the strong interactions between the different units of the power plant, specifically, the boiler, superheaters, reheater, and turbines.
- Accommodates wide variations in power demand and is able to reject the different sources of disturbances that may occur in a power plant.

The rest of the thesis is organized as follows. Chapter 2 demonstrates the application of a deadtime compensated model-state feedback control structure to control boiler-turbine systems, specifically controlling power generation and boiler pressure. Two different cases were tackled: tracking of narrow and wide variations in power demand and rejection of different disturbances applied to the power plant. For performance comparison, the results of the applied nonlinear control structure are compared to the performance of a linear multi-input multi-output (MIMO) controller composed of PI controller and a generalized multidelay compensator (GMDC).

In Chapter 3, the application of conventional three-element cascaded PI controllers for drum level control along with the nonlinear model-state feedback control structure developed in Chapter 2 is illustrated. The scenarios tackled are tracking of wide variations in power demand and rejection of different disturbances applied to the power plant. For performance comparison, the three-element drum level conventional PI controller is also applied with the linear multi-input multi-output PI-GMDC controller used for the control of power generation and boiler pressure.

Chapter 4 develops a control strategy that allows the use of nonlinear feedback control for temperature control despite the inverse response shown by the superheated temperature dynamics. The controlled variables are the boiler pressure, power generation, and superheated and reheated steam temperatures. Integrating the control structure developed in Chapter 2 within the proposed control strategy is assessed. The performance is illustrated within two main scenarios: tracking of wide variations in power demand and rejection of different disturbances applied to the power plant.

Finally, Chapter 5 summarizes the main results of this thesis, and proposes future research directions.

Chapter 2

Control of the boiler-turbine system [1]

2.1 Introduction

A controlled operation of a power plant resides in the successful control of the units that significantly affect power generation. The most significant system in the power generation process is the boiler-turbine system. A boiler-turbine system is composed of the steam generator and the turbine units. The strong interactions between these units, specifically between the boiler pressure and power generation, suggests the use of either a single multivariable controller or distributed controllers, where communication between the different controllers is established. Conventionally there are three strategies of controlling the boiler pressure and power generation of a boiler-turbine system [6]:

1. **Boiler Follow**: In the Boiler Follow strategy, two separate PID controllers are

[1] **Based on "Nonlinear Decoupling Control With Deadtime Compensation for Multirange Operation of Steam Power Plants", Nahla Alamoodi and Prodromos Daoutidis, *IEEE TRANSACTIONS ON CONTROL SYSTEMS TECHNOLOGY*, 24(1): 341-349, 2016 [5].**

utilized for the control of boiler pressure and power generation. Power demand is tracked by adjusting the turbine valve opening that admits steam to the turbine. As a consequence the pressure of the boiler experiences a disturbance. Depending on the boiler pressure change the boiler controller adjusts the flow of fuel entering the furnace. The drawback of this strategy is the delayed tracking of the power demand which is achieved after the boiler controller is activated, thus after the boiler pressure is disturbed.

2. **Turbine Follow**: Similar to the Boiler Follow strategy, in the Turbine Follow strategy, two separate PID controllers are utilized for the control of boiler pressure and power generation. The strategy is basically the reverse of the Boiler Follow one. Power demand is tracked by adjusting the fuel flow entering the furnace. As a consequence the pressure of the boiler experiences a disturbance. Depending on the boiler pressure change the boiler controller adjusts the turbine valve opening. Thus the amount of steam admitted to the turbine is adjusted. The disadvantage of this strategy is the adjustment of turbine valve opening only after the pressure inside the boiler is disturbed, which results in a very slow response to power demand changes.

3. **Coordinated Control**: The basic principle of the Coordinated Control strategy (CCS) is to have a supervisory control layer that regulates the set points sent to the boiler and turbine controllers. From the supervisory control, the power set point is sent as a feedforward signal to both the boiler and the turbine control systems. This configuration causes an immediate response of the turbine and the boiler to a power demand change. As the signal is received by the turbine controller, the turbine valve opening gets adjusted in response to any change in power demand. Simultaneously, the boiler controller receives the new set point and adjusts the

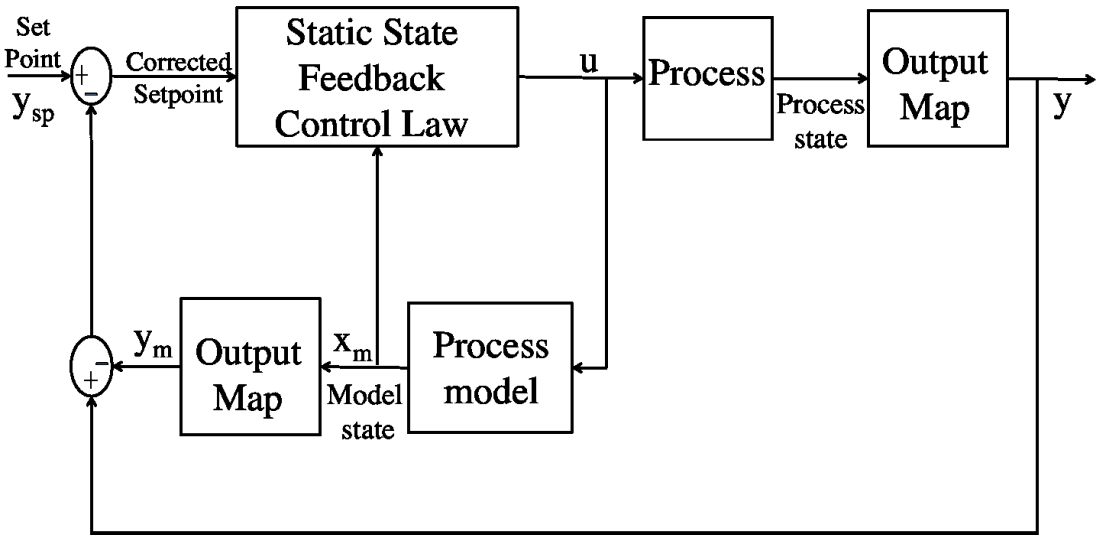

Figure 2.1: Model state feedback structure.

fuel flow entering the furnace. The supervisory layer is also responsible to adjust set points in response to measured and unmeasured disturbances that affects the boiler-turbine system.

These control strategies performs well for narrow range of power set point changes; however, as power set point changes significantly linear controllers will no longer be efficient due to the nonlinear nature of the power generation process.

The control strategy that we implement is a nonlinear decoupling control achieved by feedback linearization, along with deadtime compensation. Feedback linearization is an approach that involves the design of a state feedback control law that results in a fully linearized system or a linear input/output closed-loop response [38, 39]. Each input/output pair is then controlled using an external single-input single-output (SISO) controller with integral action. The model state feedback structure, an integration of static state feedback control with open-loop observers, involves utilizing an online simulation of the process model to estimate the model states [40]. Figure 2.1 illustrates a schematic of a model state feedback structure. The model state is then utilized in

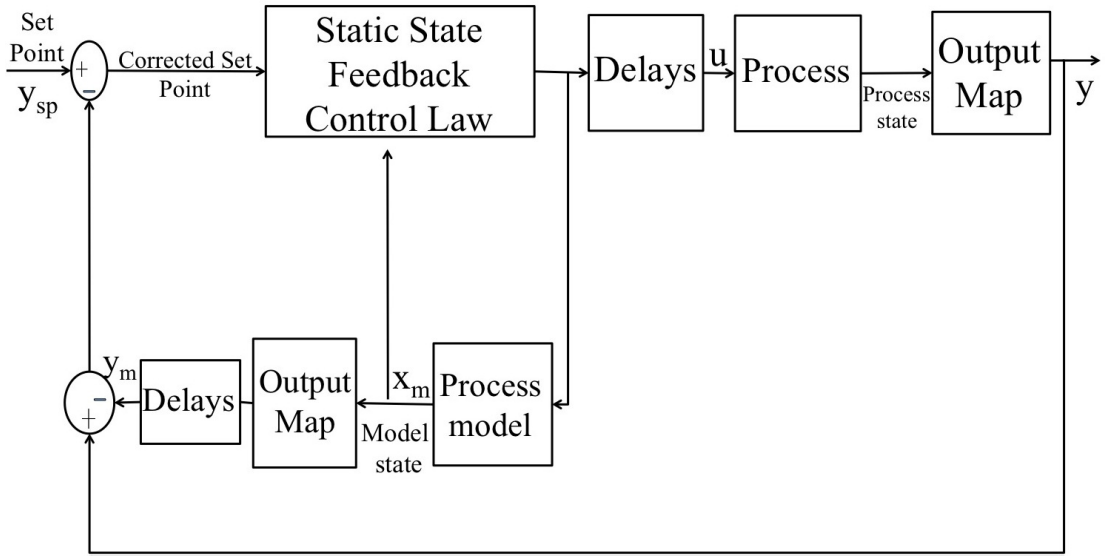

Figure 2.2: Model state feedback structure with deadtime compensation.

two ways: 1) it goes through the model output map to generate the model output and 2) it is fed back to the static-state feedback law. In the feedback loop, the difference between the model output and the process output corrects the required set point. The required control action is then generated from the static state feedback law utilizing the feedback model state and corrected set point. A detailed description of feedback linearization and model state feedback structure can be found in Appendix A.

The presence of deadtime in the system makes the control problem more challenging. Deadtime compensation for nonlinear SISO systems was first studied in [41], where the input/output map with deadtime is transformed to a linear one using a static-state feedback and a Smith-like predictor, and subsequently the control action is generated using a linear controller with integral action and deadtime compensation. However, in a MIMO system with unequal deadtimes, static- state feedback alone cannot obtain an input/output decoupled response because of the coupling of the different input/output

variables at different time instances. Much of the work tackling nonlinear MIMO systems with deadtime utilizes adaptive neural and adaptive fuzzy control [42–44]. In [45], a deadtime compensation strategy was proposed for a MIMO system that utilizes static-state feedback within the model state feedback structure discussed previously. In this strategy, decoupling is achieved by artificially delaying all the control actions sent to the process to have a deadtime equal to the largest deadtime that appears in the inputs. This allows the outputs of the process to be coupled at the same time instant. In addition, the simulated model outputs are also delayed to the largest deadtime in the inputs. This results in equal model and process outputs if there are no modeling errors. In this case, the corrected set point is simply the actual set point, and hence the deadtime is eliminated from the feedback loop. An illustration of the resulting control structure is given in Figure 2.2.

In this chapter, we focus on implementing the model state feedback structure with deadtime compensation for the control of the boiler-turbine system. In the following sections, the modeling of the boiler-turbine system is presented, the control problem considered is described, and a case study of the implementation and the results are presented and discussed.

2.2 Modeling

For the derivation of an effective control strategy it is important to have a dynamic model that captures the behavior of the units exhibiting dominant dynamics in the process. These units are the boiler and the turbine-generator system. For the remaining units, superheaters, economizer, reheaters, preheaters, and condenser, we assume that the temperatures of steam or water exiting them are kept constant by independent control subsystems.

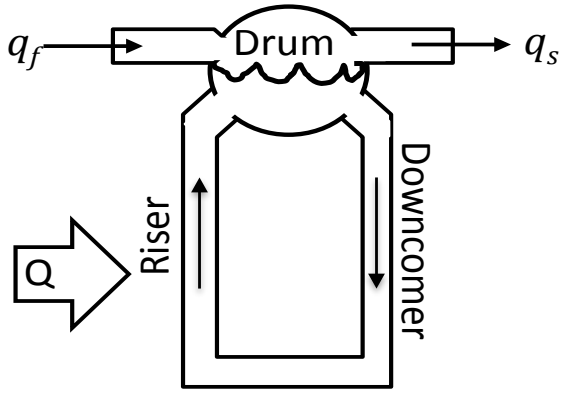

Figure 2.3: A schematic diagram of drum-type boiler

2.2.1 Drum-type boiler model

For the modeling of the dynamics of the boiler we follow a simplified model of the work of [46]. A drum-type boiler is composed of a drum and tube bundles of downcomers and risers. Risers are located inside the furnace where vaporization of the saturated water occurs. Due to the difference in density between the produced steam in the risers and the water inside the drum, a circulation loop between the riser-drum-downcomer is created [46]. The key property used for describing the dynamics of the boiler is the steam pressure. This choice is made to reflect the strong coupling between the boiler and the turbine-generator system.

The mass balance around the boiler is:

$$\frac{d(\rho_w V_{wt} + \rho_s V_s)}{dt} = q_f - q_s \tag{2.1}$$

where ρ denotes density, V denotes volume, and q denotes the mass flow rate of the fluid. The subscripts wt, s, f denote water, steam and feed respectively. Since ρ is a function of pressure, is it best to describe it in terms of its dependence on P [46]. Thus

by using $V_s = V_t - V_{wt}$ and the following relation:

$$\frac{d\rho}{dt} = \frac{\partial \rho}{\partial P}\frac{dP}{dt}$$

the mass balance becomes:

$$(\rho_w - \rho_s)\frac{dV_{wt}}{dt} + \left[V_{wt}\left(\frac{\partial \rho_w}{\partial P}\right) + V_s\left(\frac{\partial \rho_s}{\partial P}\right)\right]\frac{dP}{dt} = q_f - q_s \tag{2.2}$$

The mass flow rate of steam entering the turbine is manipulated using a governing steam valve, thus expressing q_s as a function of the steam valve opening gives [47]:

$$q_s = \frac{kP}{\sqrt{T^{sup}}}u_s \tag{2.3}$$

where k denotes the valve gain, T^{sup} denotes the temperature of the superheated steam, and u_s denotes the steam valve opening.

Since there is no mechanical work applied on the boiler and changes in potential and kinetic energy are assumed to be negligible, the energy balance is [46]:

$$\left[V_s\left(\rho_s\frac{\partial h_s}{\partial P}\right) + V_{wt}\left(\rho_w\frac{\partial h_w}{\partial P}\right) - V_t + m_t C_p\frac{\partial T^{sat}}{\partial P}\right]\frac{dP}{dt}$$

$$+(h_s - h_w)\frac{d(\rho_s V_s)}{dt} = q_f(h_f - h_w) - q_s h_c + \eta_b \Delta H q_e \tag{2.4}$$

where h is the specific enthalpy of the fluid, m_t is the total mass, C_p is the heat capacitance of boiler, T^{sat} is the saturation temperature, ΔH is the fuel heat of combustion, q_e is the fuel flow rate, η_b is the thermal efficiency of the boiler, $h_c = h_s - h_w$ is the vaporization enthalpy, and $V_t = V_{wt} + V_s$ is the total volume of the boiler.

The system is further simplified by making the following assumptions:

- Water level in the boiler is assumed to be constant at the centerline of the drum inside the boiler. This means that the feedwater flowing into the boiler is assumed to be equal to the steam flow leaving it.
- The steam valve opening is proportional to the open valve area.
- $\Delta P = 0$ across all superheaters.

The model in (3) is then reduced to:

$$\left[V_s\left(\rho_s\frac{\partial h_s}{\partial P}\right) + V_{wt}\left(\rho_w\frac{\partial h_w}{\partial P}\right) - V_t + m_t C_p\frac{\partial T^{sat}}{\partial P}\right]\frac{dP}{dt}$$

$$= \frac{kP}{\sqrt{T^{sup}}}u_s(h_f - h_s) + \eta_b \Delta H q_e \tag{2.5}$$

2.2.2 Turbine-generator model

It is convenient to represent the performance of the system of turbines and generator lumped into one system in order to avoid the complications that are present in the generator modeling. A dynamic model of the turbine-generator system can be represented by a first order differential equation [48] as a function of the enthalpy change in the turbine, thus the model becomes:

$$\tau\frac{dE}{dt} = \eta_T q_s(h^{sup}(T^{sup}, P_b^{sat}) - h^{ise}(P_{cond}^{sat})) - E \tag{2.6}$$

where τ denotes the time constant for the turbine-generator system, E is the power generated, η_T is the isentropic efficiency, h^{ise} is the isentropic enthalpy at the pressure of the condenser, P_b^{sat} is the boiler pressure at saturation, and P_{cond}^{sat} is the condenser pressure at saturation.

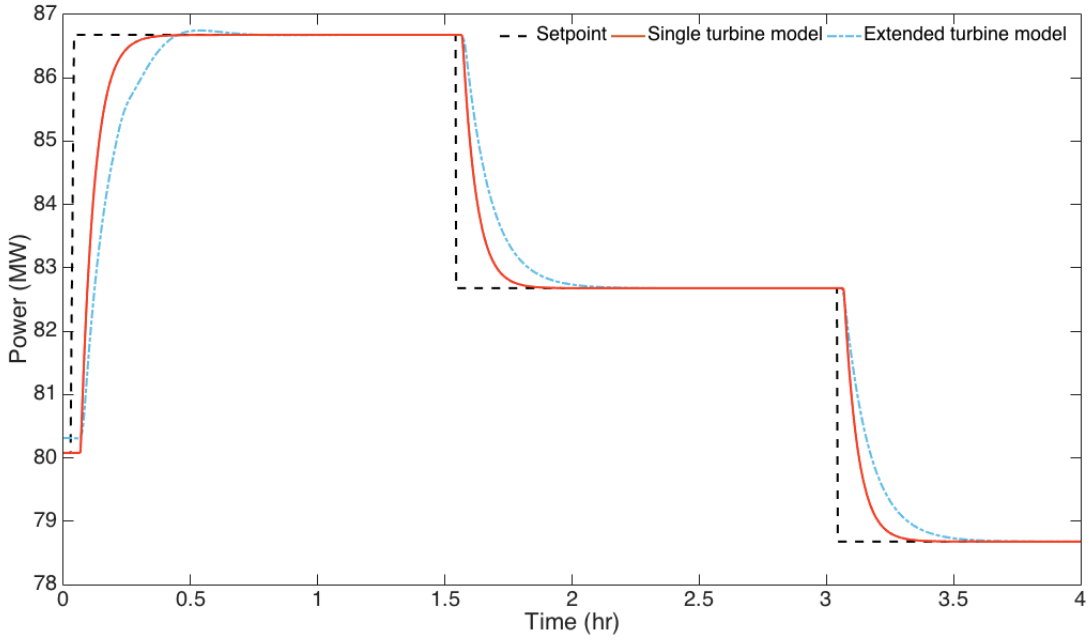

Figure 2.4: Set point tracking performance for turbine model considering a single turbine (solid) and multiple turbines (dashed-dot).

In practice, the system of turbines includes high, intermediate and low pressure turbines, however, lumping them into one model does not qualitatively change the dynamics of the system. This is illustrated in Figure 2.4. The figure shows the set point tracking performance for considering a single turbine versus multiple turbines.

2.3 Control problem description

As discussed previously, the vaporization of saturated water inside the boiler occurs in the furnace. Depending on the fuel flow, the amount of vaporization and thus the boiler pressure can be varied. However, due to the time needed for coal to be transported and ground, the pressure change due to a change in fuel flow will be delayed. To account for this delay in the model, a time delay, θ, is added to the fuel flow rate.

The system to be controlled then becomes:

$$\left[V_s\left(\rho_s\frac{\partial h_s}{\partial P}\right)+V_{wt}\left(\rho_w\frac{\partial h_w}{\partial P}\right)-V_t+m_tC_p\frac{\partial T^{sat}}{\partial P}\right]\frac{dP}{dt}$$

$$=\frac{kP}{\sqrt{T^{sup}}}u_s(h_f-h_s)+\eta_b\Delta Hq_e(t-\theta)$$

$$\tau\frac{dE}{dt}=\eta_T\frac{kP}{\sqrt{T^{sup}}}u_s(h^{sup}(T^{sup},P_b^{sat})-h^{ise}(P_{cond}^{sat}))-E \tag{2.7}$$

Equations for $\frac{\partial T^{sat}}{\partial P}$, $\frac{\partial h_w}{\partial P}$, $\frac{\partial h_s}{\partial P}$, h_s, and ρ_w were evaluated using the standard formulas given by the International Association for the Properties of Water IAPWS-IF97 using a MATLAB coded file [49] . The units used are: P $[kPa]$, T $[K]$, h $[\frac{kJ}{kg}]$, and ρ_w $[\frac{m^3}{kg}]$.

The enthalpy of superheated steam correlation used is developed by [50] and has the form:

$$h(T^{sup},P)=h_{cr}\sum_k^N\left(\frac{T_c}{T_{sup}}\right)^{m_k}\left(\frac{P}{P_c}\right)^{n_k} \tag{2.8}$$

where h_{cr}, T_c, P_c denote critical enthalpy, temperature, and pressure of water, respectively, N is the number of terms, and m_k and n_k are fitting parameters. This equation is simplified to account for terms that significantly contribute to the calculation of enthalpy and to take into consideration that the superheated temperature is assumed to be constant. The resulting correlation is reduced to a second order function of pressure. Parameters for the reduced correlation are found in Table 2.1 and the nominal parameters used for the power plant are found in Table 2.2. The nominal parameters are based on the Swedish 160 MW coal-fired power plant that was studied in [48].

Based on the derived power plant model the following observations can be made:

- The pressure of the boiler can be controlled by the steam flow leaving the boiler

Table 2.1: Steam superheated enthalpy correlation parameters

k	m_k	n_k
1	-5	1
2	-4	1
3	-2	0
4	-1	0
5	-1	1
6	0	0
7	1	0
8	3	1
9	7	1
10	9	2

Table 2.2: Nominal Parameters for the Steam Power Plant

m_t	300×10^3 kg	P_{cond}	0.0118 MPa
C_p	0.5 kJ/(kg C)	τ	0.4 s
ΔH	24 MJ/kg	η_b	0.88
h_f	1030.15 kJ/kg	η_T	0.725
V_w	63.9 m^3	T_c	374 C
T^{sup}	535 C	P_c	22.05 MPa

and a delayed fuel flow entering the furnace.

- Power generation can be controlled by the steam flow entering the turbine.
- Strong coupling of the power generation model and that of the boiler is a result of two factors: 1) the common manipulated variable, the steam flow. 2) The dependence of the quality of steam on the pressure of the boiler.

2.4 Case study

Referring to the power plant model in (2.7), there are two manipulated variables, q_e and u_s, and two state variables, P and E, which are the same as the outputs. The deadtime appears only in the fuel flow rate. The following MIMO nonlinear decoupling controller is used:

Process Model:

$$\left[V_s\left(\rho_s\frac{\partial h_s}{\partial P_m}\right)+V_{wt}\left(\rho_w\frac{\partial h_w}{\partial P_m}\right)-V_t+m_tC_p\frac{\partial T^{sat}}{\partial P_m}\right]\frac{dP_m}{dt}$$

$$=\frac{kP_m}{\sqrt{T^{sup}}}u_s(h_f-h_s)+\eta_b\Delta Hq_e(t-\theta)$$

$$\tau\frac{dE_m}{dt}=\eta_T\frac{kP_m}{\sqrt{T^{sup}}}u_s(h^{sup}(T^{sup},P_m)-h^{ise}(P^{sat}_{cond}))-E_m$$

where the subscript m denotes a model state.

Static-state feedback:

– Characteristic matrix:

$$C(x)=\begin{bmatrix}\dfrac{\dfrac{kP_m}{\sqrt{T^{sup}}}(h_f-h_s)}{V_s\left(\rho_s\dfrac{\partial h_s}{\partial P_m}\right)+V_{wt}\left(\rho_w\dfrac{\partial h_w}{\partial P_m}\right)-V_t+m_tC_p\dfrac{\partial T^{sat}}{\partial P_m}\dfrac{dP_m}{dt}}\\ \\ \dfrac{kP_m\eta_T}{\tau\sqrt{T^{sup}}}(h^{sup}-h^{sat}_{cond})\end{bmatrix}$$

$$\frac{(\eta_b \Delta H)}{V_s\left(\rho_s \frac{\partial h_s}{\partial P_m}\right) + V_{wt}\left(\rho_w \frac{\partial h_w}{\partial P_m}\right) - V_t + m_t C_p \frac{\partial T^{sat}}{\partial P_m}\frac{dP_m}{dt}}$$

$$0$$

$\bigg]$

– Control law:

$$u = C(x)^{-1}\left[\begin{array}{c} \frac{v_1 - P_m}{\beta_{11}} \\ \frac{v_2 - \left(1 - \frac{\beta_{21}}{\tau}\right) E_m}{\beta_{21}} \end{array}\right]$$

The artificial delay of the steam flow as well as the delay of the model outputs, P_m and E_m, is equal to the deadtime that appears in q_e. Therefore the corrected set points are:

$$v_1(t) = P_{sp}(t) - P(t-\theta) + P_m(t-\theta)$$

$$v_2(t) = E_{sp}(t) - E(t-\theta) + E_m(t-\theta)$$

and the closed-loop system under nominal conditions is fully linearized and has the form:

$$P(t) + \beta_{11}\frac{dP(t)}{dt} = P_{sp}(t-\theta)$$

$$E(t) + \beta_{21}\frac{dE(t)}{dt} = E_{sp}(t-\theta)$$

Choosing the parameters β_{11} and β_{21} to place the poles of the above responses in the left hand side of the complex plane results in a stable closed loop system.

The power plant to be assessed is a 160 MW coal-fired power plant with constant

operation of boiler pressure. The nominal operational conditions of the boiler pressure and power generation at 50% of its rated power are 13.73 MPa and 80.0 MW, respectively, whereas the deadtime is chosen to be 90 seconds from a typical range of 80-120 seconds [14]. The steam valve actuator was subjected to the following rate limits $-2 \leq \dot{u}_s \leq 0.2$ [48]. In order to examine the performance of the controller two operational modes of set point tracking are selected; a narrow range of set point changes and a wide one. The description of both modes is as follows.

2.4.1 Narrow range operational mode

For the narrow range of set point changes, the system was validated to be open loop stable around the nominal values of 13.73 MPa and 80.0 MW. Next the controller was tested to meet the following objectives:

- Set point tracking for multiple step changes in power demand ranging from 80 to 87 MW.
- Disturbance rejection for a 5% decrease in the heating value of the fuel.
- Disturbance rejection for a 5% decrease in the turbine efficiency.

Table 2.3: Controller Parameters for the Steam Power Plant

Controller	**Parameter**	
Nonlinear DT compensated	β_{11}	500 s
	β_{21}	200 s
PI-GMDC	k_{c1}	$1.9 \times 10^{-4} MW^{-1}$
	τ_{I1}	50 s
	k_{c2}	0.01 $\frac{kg/s}{MPa}$
	τ_{I2}	5 s

2.4.2 Wide range operational mode

The objective of this operational mode is to examine the ability of the controller to respond rapidly to large set point changes that can result from different reasons, one of which is power production using renewable energy. The intermittency of renewable energy will require conventional power plants to compensate for shortages that occur from renewable power generation. Therefore, the power plant control system was tested over a wide operating range of 50-100% of the rated power of the plant, for the robustness of the transient response, and the efficiency in achieving the required power set point. The controller performance was tested for the following tasks:

- Set point tracking for a power change rate of 2% per minute to rated power.
- Set point tracking for ±32MW (20% of the Maximum Continuous Rate) step changes in power set point at 20 minutes intervals with simultaneous random fluctuations in deadtime associated with the fuel flow [17].

The power change rate is selected from a range of 2-3% per minute that is a typical range for power plants with drum boilers [51].

For performance comparison purposes a linear MIMO controller composed of a PI controller and a Generalized Multidelay Compensator (GMDC) is derived following the work of [52]. The GMDC derivation involves developing a Smith-like predictor utilizing a linearized form of the model in (2.7). Parallel to the proposed controller, artificial delays are introduced to the control actions as well as to the predicted model with deadtimes in the Smith-like predictor. The output of the predictor is then added to the process output to generate a correction for the desired set point. This construction of the Smith-like predictor together with the PI controller ensures the PI-GMDC to be causal. Figure 2.5 depicts the PI-GMDC structure. The values of the controller

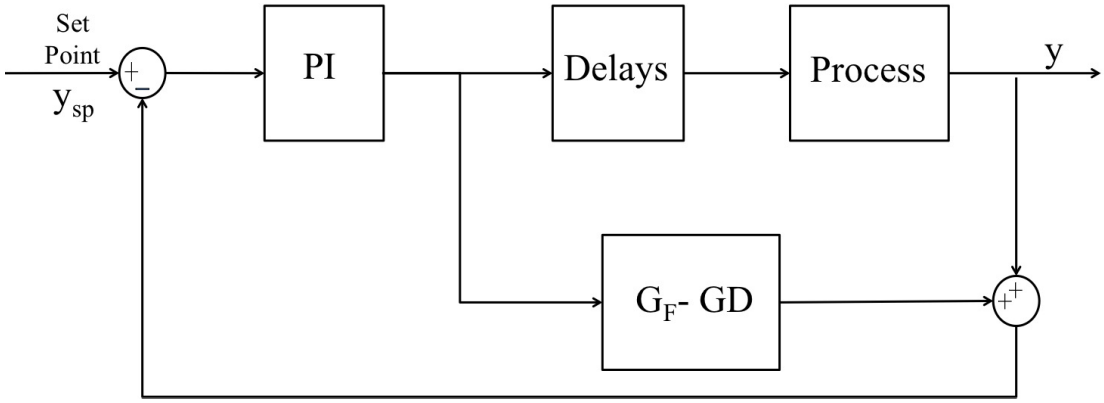

Figure 2.5: PI-GMDC structure. G-linearized process model, G_F-linearized process model without deadtime, D-Delays

parameters used are summarized in Table 3.2 where k_{ci} is the controller gain and τ_{Ii} is the integral action time constant.

2.5 Simulation results

2.5.1 Narrow range operational mode

The performance of the controller for set point tracking of power demand was first investigated for multiple step changes. The implemented step changes are (+6.8, -4.3, -4.0) MW respectively. The controllers are tuned to provide a fast and stable response with no oscillations. Figures 2.6 and 2.9 show the response of the nonlinear decoupling controller with deadtime compensation compared to that of the PI-GMDC to the multiple step changes in power set point. Both controllers track the changes in power set point according to the postulated trajectory (Figure 2.6), however, a much faster response is achieved by the nonlinear controller. To examine the behavior of the PI-GMDC controller further, the controller was retuned to achieve a faster response. The response of the controller, shown by dotted line in Figures 2.6, results in an oscillatory generation of power and reaches the set points at the same time as the controller with the original

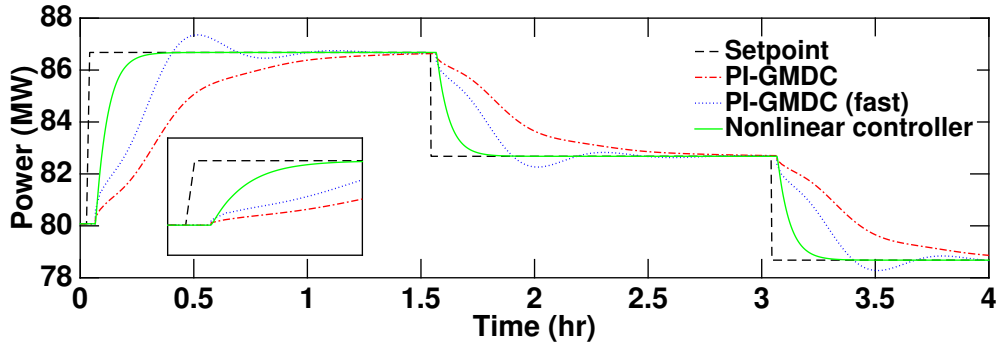

Figure 2.6: Response of power generation to multiple step changes in set point.

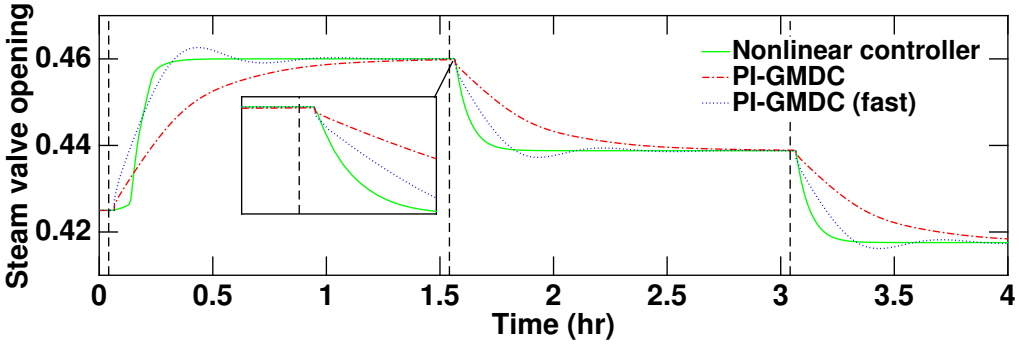

Figure 2.7: Steam valve opening control actions to a step change in power set point.

tuning. Since the time to reach the set points remains unchanged and oscillatory responses are undesirable, the original tuning parameters were kept unchanged for the rest of the studies.

The effect of artificially delaying the steam flow entering the turbine is reflected in the delayed response of the power generation of both controllers as shown in the inset of Figure 2.6. The artificial delays in the actions of the turbine valve opening are illustrated in Figure 2.7; the vertical dashed lines indicate the time at which the step changes are applied.

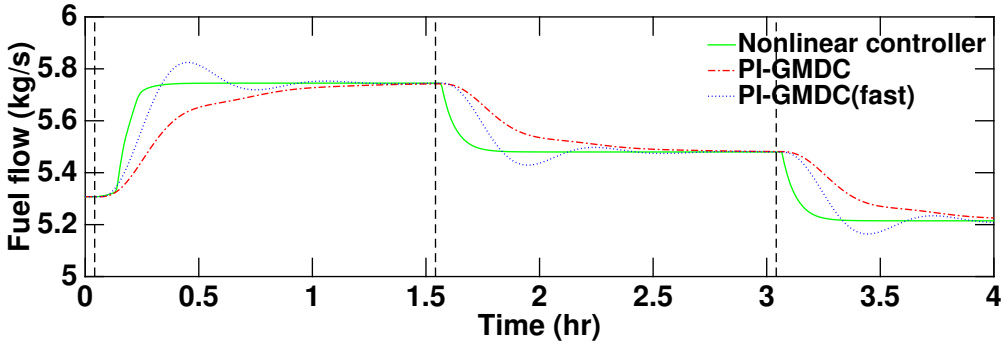

Figure 2.8: Fuel flow control actions to a step change in power set point.

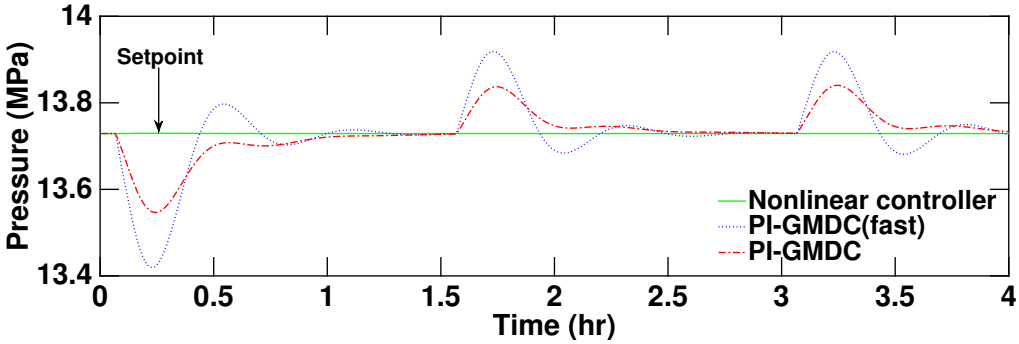

Figure 2.9: Response of boiler pressure to multiple step changes in power set point.

Figure 2.8 compares the behavior of the turbine valve opening and fuel flow of both controllers. The control actions produced by the nonlinear controller are fast but non aggressive whereas the ones produced by the PI-GMDC are sluggish. Figure 2.9 illustrates the pressure response to the step changes in the power set point. Due to the decoupling enforced the response is unaffected in the case of the nonlinear controller. However, a disturbance is introduced in the pressure of the boiler at every step change with the PI-GMDC controller. The disturbed response is due to the resulting control scheme of the PI-GMDC, which is a multi-loop SISO control system. Therefore a change in set point in one of the loops results in a disturbance in the other loop.

The disturbance rejection capability of the controllers is compared upon an unmeasured 5% decrease in the heating value of the fuel. The responses of power generation and boiler pressure as shown in Figures 2.10 and 2.11 show a fast, zero offset, and oscillation-free rejection for the nonlinear controller, indicating the ability of the controllers to accommodate problems of unsteady heating value of coal, or using another type of solid fuels. The PI-GMDC shows an oscillatory rejection of the resulted disturbance in the boiler pressure and power generation. As a final test for the narrow range operational mode, the performance of the controllers is also tested for a 5% decrease in the efficiency of the turbine-generator system. The results (Figures 2.12-2.13) show superior disturbance rejection of the nonlinear controller for power generation. Moreover, in Figure 2.13 the disturbance had no effect on the boiler pressure with the nonlinear controller; this decoupled response appears because the artificial delay applied to the steam flow allows the turbine valve opening and fuel flow rate to change at the same instant.

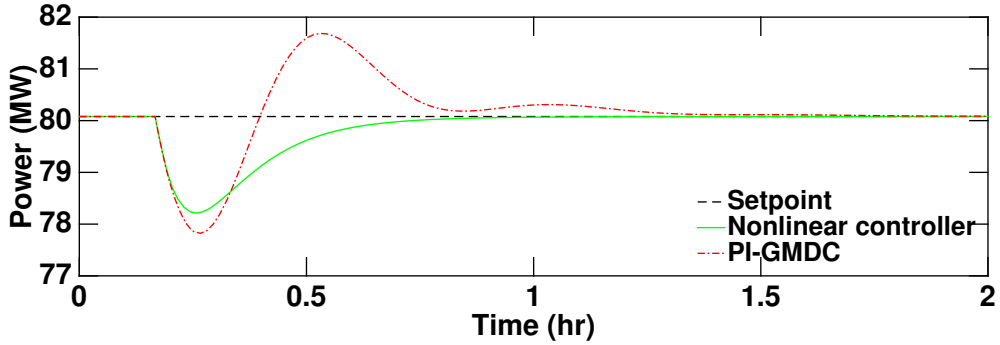

Figure 2.10: Response of power generation to a 5% decrease in the heating value of the fuel.

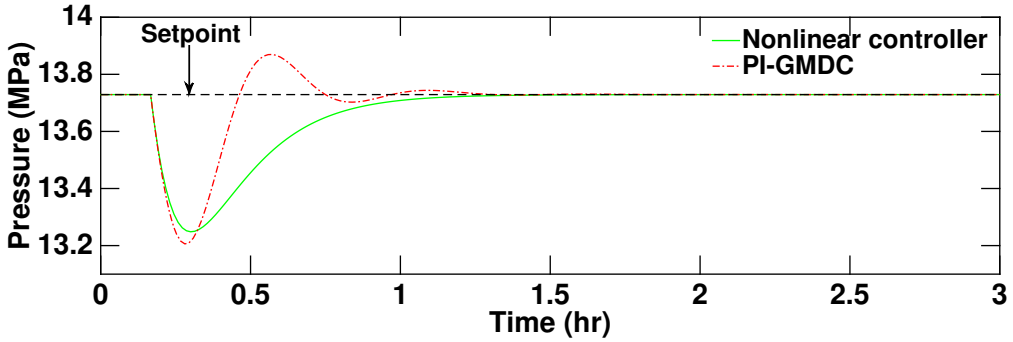

Figure 2.11: Response of boiler pressure to a 5% decrease in the heating value of the fuel.

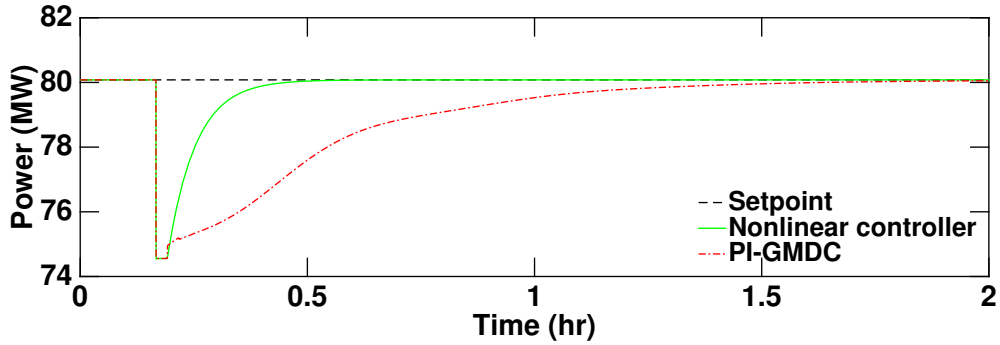

Figure 2.12: Response of power generation to a 5% decrease in the turbine efficiency of the turbine-generator system.

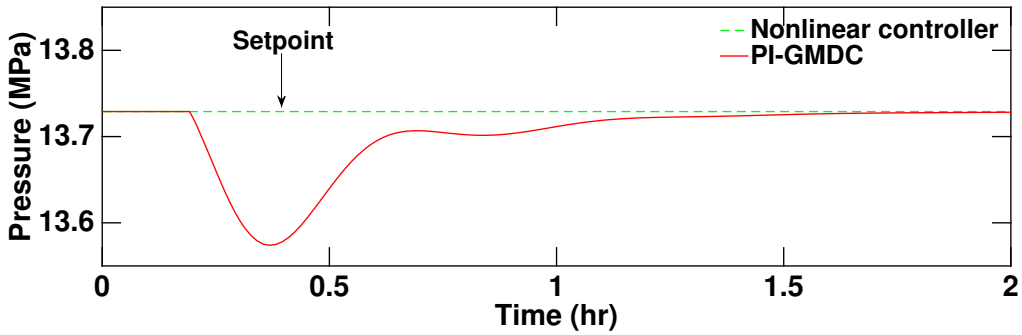

Figure 2.13: Response of boiler pressure to a 5% decrease in the turbine efficiency of the turbine-generator system.

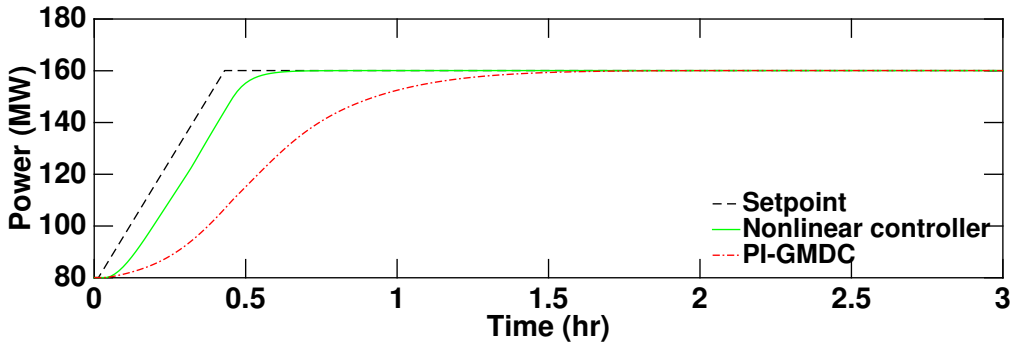

Figure 2.14: Response of power generation to a 2%/min ramping of power set point.

2.5.2 Wide range operational mode

In order to test the performance of the controller under a wide range operation, the power set point is ramped at a rate of 2%/min from 80 MW to 160 MW. The tuning parameters of both controllers are unchanged from the ones chosen for the narrow range operation. Figure 2.14 shows the power generation response to the change in set point for both controllers. The nonlinear controller provides a fast power generation response, tracking the required set point in about 22 minutes. The response of the PI-GMDC is four times slower than the nonlinear controller requiring 80 minutes for set point tracking. Figure 2.15 shows the effect of ramping the power set point on the boiler pressure. Due to the decoupling of the nonlinear controller the boiler pressure remains unaffected, conversely, a disturbance is resulted in the boiler pressure controlled by the PI-GMDC, requiring 90 minutes for complete rejection. The stability of both controllers for power set point tracking and stabilizing boiler pressure is well illustrated.

The controllers are lastly tested for their robustness. A "worst case" scenario performance test of large step changes of ±32MW in power set point at 20 minute intervals, with simultaneous random fluctuations in deadtime associated with the fuel flow at the

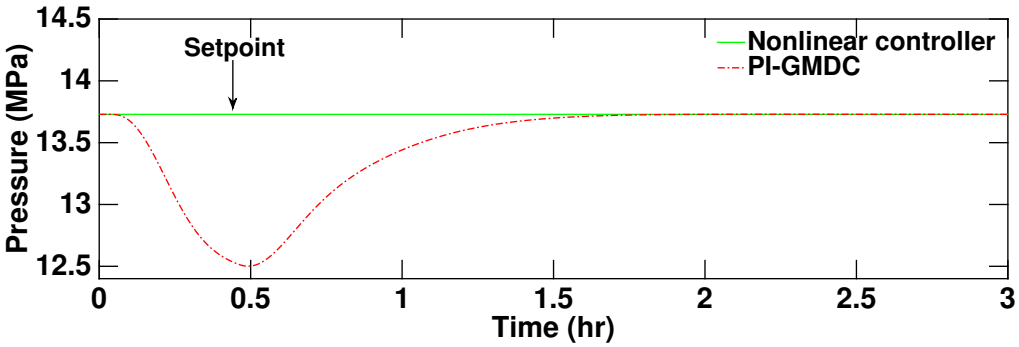

Figure 2.15: Response of boiler pressure to ramping in power set point.

range of 80-120 seconds, are applied. This test is performed in a power plant in UK to test new controllers before real-time implementation [17]. Figure 2.16 shows the applied deadtime. The tuning parameters of both controllers are unchanged. Figures 2.17 and 2.18 illustrates the results of the "worst case" scenario performance test. The response of the controllers reflects the ability of the nonlinear controller to track the power set point within the 20 minutes interval tests in a zero-offset, stable, and timely manner while the PI-GMDC fails. The pressure response shows that the fluctuation in deadtime causes small disturbances in boiler pressure using the nonlinear controller, indicating that the decoupling between the boiler and the turbine units is not affected significantly by uncertainties in the deadtime. The response of the boiler pressure under the PI-GMDC controller reflects large cyclic disturbances as a result of the large step changes and deadtime fluctuations. This cyclic behavior in pressure can risk the life of the boiler due to the resulting fluctuating thermal stresses.

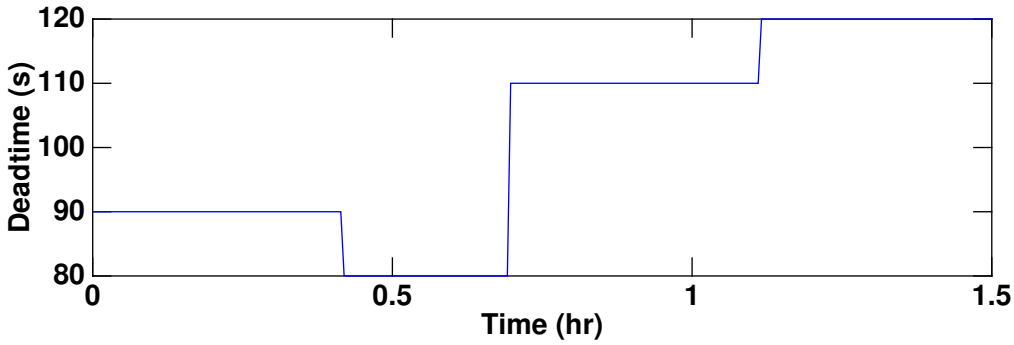

Figure 2.16: Applied deadtime values.

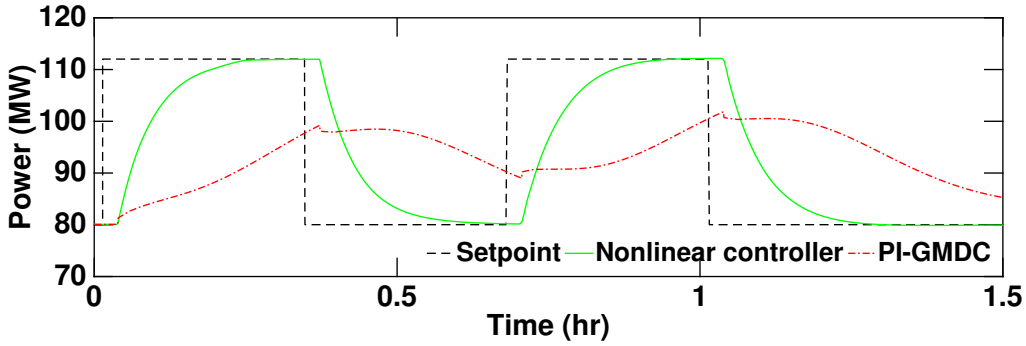

Figure 2.17: Response of power generation to large step changes in power set point and fluctuating deadtime values.

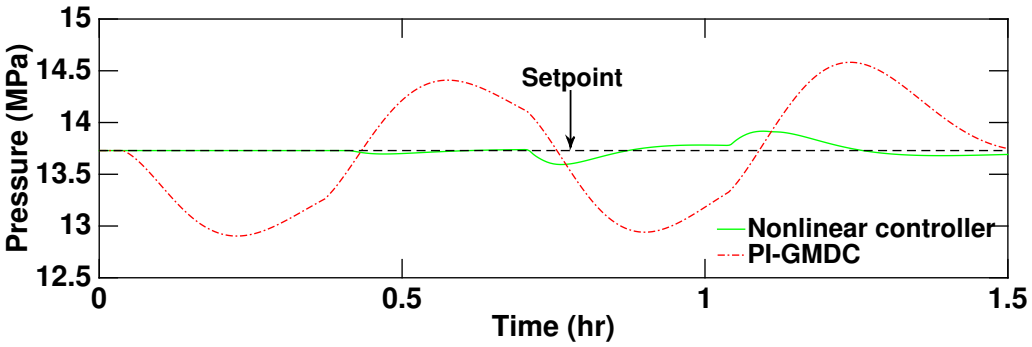

Figure 2.18: Response of boiler pressure to large step changes in power set point and fuel flow deadtime.

2.6 Conclusions

In this chapter, the application of a nonlinear model state feedback controller with deadtime compensation for power plant control was proposed. The results show complete decoupling of the boiler pressure and power generated with a stable and efficient operation under narrow and wide range changes in power demand. Sensitivity analysis results show robustness of the power plant performance utilizing the applied controller.

Chapter 3

Drum level control

3.1 Introduction

The simplest form of controlling the drum level is by regulating the feedwater flow to compensate for a deviation of the water level from the centerline of the drum. In a power plant, pressure is a key variable that affects the dynamics of the drum level. An increase in power demand requires more steam to flow to the turbines, which results in a pressure drop inside the steam drum. The pressure decrease then causes the steam bubbles entrained under the water level to expand [6]. In addition, due to the decrease in the steam saturation temperature more steam vaporizes under the water level [53]. Therefore, the drum level experiences a "swell" instead of decreasing. Once the pressure is controlled the drum level decreases if the feedwater is not adjusted. If the power demand decreases and the pressure inside the steam drum increases, the dynamics will reverse. The steam bubbles entrained under the water level will decrease in volume and the increase in the steam saturation temperature will decrease the amount of steam vaporized. The drum level then experiences a "shrink" instead of increasing. Hence the drum level dynamics exhibit an inverse response for a change in power demand. Due

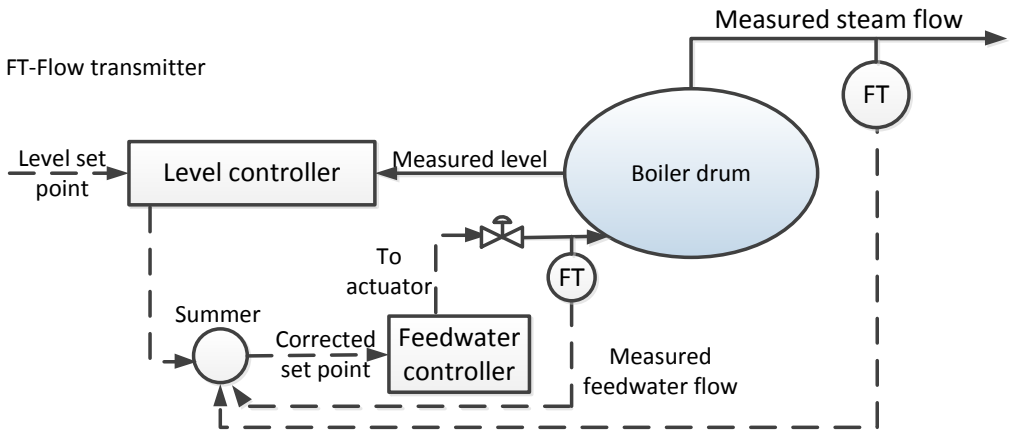

Figure 3.1: Conventional three-element drum level controller

to this inverse response, a simple drum level controller is not efficient for regulation. A three-element controller composed of a cascade and a feedforward control is the standard practice used to control this system. The three elements are the drum level, steam flow, and feedwater flow. The measured drum level deviation from the centerline of the boiler is sent to a primary "drum level" PI controller. The controller then compares the transmitted signal to the assigned set point and produces a control action that serves as a set point to a secondary "feedwater" PI controller. At this point, the steam flow rate is fed forward and is combined with the control action of the drum level controller. The feedwater controller then compares the feedwater flow with the cascaded set point and generates the required control action. Figure 3.1 is a schematic of the three-element drum level controller.

In this approach, the forward feeding of the steam flow serves as a measure of the amount of feedwater that should be allowed into the boiler, i.e. for every unit of steam flow change an equal unit of feedwater change should be made [54]. Therefore, the drum level controller compensates for the deviation of the drum level from the centerline of

the drum and the feedwater controller adjusts the feedwater control valve to maintain the feedwater flow at its set point [54].

We focus in this chapter on implementing the conventional three-element drum level controller along with the deadtime compensated model state feedback structure discussed in Chapter 2 for the control of the boiler-turbine system. Our interest is to investigate the effect of this control structure on the interactions between the different dynamics associated with the boiler and on the power generation. In the following sections, the modeling of the boiler-turbine system is revisited to account for the dynamics of the boiler drum level, the control problem considered is described, and a case study of the implementation and the results is presented and discussed.

3.2 Modeling

For the modeling of the boiler dynamics we adapt the work of [46]. To capture the dynamics of the drum level it is important to account for the distribution of steam and water in the boiler. This is because the distribution of steam and water is one of the factors responsible for the nonminimum-phase behavior of the level dynamics.

3.2.1 Boiler Pressure dynamics

The modeling of the boiler pressure dynamics follows the same steps discussed in 2.2.1, however, the assumptions of constant water level at the centerline and small steam volume variations are not considered. Thus, the dynamics of the boiler is expressed in terms of the boiler pressure and the water volume inside the boiler. Applying global mass and energy balances around the boiler yields the following model:

$$k_{11}\frac{dV_{wt}}{dt} + k_{12}\frac{dP}{dt} = q_f - q_s \tag{3.1}$$

$$k_{21}\frac{dV_{wt}}{dt} + k_{22}\frac{dP}{dt} = \eta_b \Delta H q_e + q_f h_f - q_s h_s \tag{3.2}$$

where

$k_{11} = \rho_w - \rho_s$

$k_{12} = V_{wt}\frac{\partial \rho_w}{\partial P} + V_s \frac{\partial \rho_s}{\partial P}$

$k_{21} = \rho_w h_w - \rho_s h_s$

$k_{22} = V_{wt}\left(h_w \frac{\partial \rho_w}{\partial P} + \rho_w \frac{\partial h_w}{\partial P}\right) + V_s \left(h_s \frac{\partial \rho_s}{\partial P} + \rho_s \frac{\partial h_s}{\partial P}\right) - V_t + m_t c_p \frac{\partial T^{sat}}{\partial P}$

Notice that in contrast to the model in (2.5), the model above takes into consideration the dynamics of the water volume inside the boiler. The model also reflects the effect of the change in feedwater flow rate, q_f, on the boiler pressure, along with the effects caused by a change in the steam and fuel flow rates.

3.2.2 Drum level dynamics

To have an accurate model of the drum level, it is necessary to quantify the total amount of steam in the riser section and under the liquid level inside the drum. Following the work of [46] the main variables capable of closely describing the drum level dynamics in the boiler are the steam quality at the riser outlet, α_r, and the steam distribution under the water level inside the drum, V_{sd}.

The amount of steam in the riser is obtained by finding the average volume fraction in the riser section, $\bar{\alpha_v}$. Assuming that the mass fraction is linear along the tubes of the riser section, the average volume fraction can be expressed explicitly as a function

of α_r, thus α_r is chosen as a state variable for describing the drum level dynamics. The amount of steam under the water level of the drum is obtained by performing a mass balance around the drum level, taking into consideration the flow rate of steam through the water surface in the drum, q_{sd}, and the condensation flow into the water surface, q_{cd}.

Assuming that the conditions and properties of steam are the same in a cross section of the riser tubes, and that the mass fraction distribution is linear along the riser tubes in the static and dynamic conditions, performing mass and energy balances for the riser section and the steam under the water level gives:

$$k_{32}\frac{dP}{dt} + k_{33}\frac{d\alpha_r}{dt} = \eta_b \Delta H q_e - \alpha_r h_v q_{dc}$$

$$k_{42}\frac{dP}{dt} + k_{43}\frac{d\alpha_r}{dt} + k_{44}\frac{dV_{sd}}{dt} = \frac{\rho_s}{T_d}(V_{sd}^0 - V_{sd}) + \frac{(h_f - h_w)}{h_v}q_f \tag{3.3}$$

where

$$k_{32} = \left(\rho_w \frac{\partial h_w}{\partial P} - \alpha_r h_v \frac{\partial \rho_w}{\partial P}\right)(1-\bar{\alpha_v})V_r + \left((1-\alpha_r)h_v\frac{\partial \rho_s}{\partial P} + \rho_s \frac{\partial h_s}{\partial P}\right)\bar{\alpha_v}V_r +$$

$$(\rho_s + (\rho_w - \rho_s)\alpha_r)h_v V_r \frac{\partial \bar{\alpha_v}}{\partial P} - V_r + m_r c_p \frac{\partial T^{sat}}{\partial P}$$

$$k_{33} = ((1-\alpha_r)\rho_s + \alpha_r \rho_w)h_v V_r \frac{\partial \bar{\alpha_v}}{\partial \alpha_r}$$

$$k_{42} = V_{sd}\frac{\partial \rho_s}{\partial P} + \frac{1}{h_v}\left(\rho_s V_{sd}\frac{\partial h_s}{\partial P} + \rho_w V_{wd}\frac{\partial h_w}{\partial P} - V_{sd} - V_{wd} + m_d c_p \frac{\partial T^{sat}}{\partial P}\right) +$$

$$\alpha_r(1+\beta)V_r\left(\bar{\alpha_v}\frac{\partial \rho_s}{\partial P} + (1-\bar{\alpha_v})\frac{\partial \rho_w}{\partial P} + (\rho_s - \rho_w)\frac{\partial \rho_s}{\partial P}\right)$$

$$k_{43} = \alpha_r(1+\beta)(\rho_s - \rho_w)V_r\frac{\partial \bar{\alpha_v}}{\partial \alpha_r}$$

$$k_{44} = \rho_s$$

ΔH is the fuel heat of combustion, q_e is the fuel flow rate, η_b is the thermal efficiency of the boiler, h_v is the vaporization enthalpy, q_{dc} is the downcomer flow rate, T_d is the residence time of the steam in the drum, V_{sd}^0 is the volume of steam in the drum in the hypothetical case when there is no condensation of steam in the drum, V_r is the volume of the riser section, V_{wd} is the volume of water in the drum, h is the specific enthalpy of the fluid, m_t is the total mass, m_r is the mass of the riser section, m_d is the mass of the boiler drum, c_p is the heat capacitance of boiler, T^{sat} is the saturation temperature of the steam, and β is a parameter related to the empirical model of q_{sd}.

The average volume fraction is expressed as a function of the steam quality at the riser outlet as:

$$\bar{\alpha_v} = \frac{\rho_w}{\rho_s - \rho_s}\left(1 - \frac{\rho_s}{(\rho_w - \rho_s)\alpha_r} ln\left(1 + \frac{\rho_w - \rho_s}{\rho_s}\alpha_r\right)\right) \tag{3.4}$$

Differentiating equation (3.4) with respect to pressure and mass fraction results in the following partial derivatives of the steam volume fraction:

$$\frac{\partial \bar{\alpha_v}}{\partial P} = \frac{1}{(\rho_w - \rho_s)^2}\left(\rho_w \frac{\partial \rho_s}{\partial P} - \rho_s \frac{\partial \rho_w}{\partial P}\right)\left(1 + \frac{\rho_w}{\rho_s}\frac{1}{1+\eta} - \frac{\rho_s + \rho_s}{\eta \rho_s} ln(1+\eta)\right)$$

$$\frac{\partial \bar{\alpha_v}}{\partial \alpha_r} = \frac{\rho_w}{\rho_s \eta}\left(\frac{1}{\eta} ln(1+\eta) - \frac{1}{1+\eta}\right) \tag{3.5}$$

where
$\eta = \alpha_r \dfrac{(\rho_w - \rho_s)}{\rho_s}$.

The downcomer flow rate is expressed as:

$$q_{dc}^2 = \frac{2\rho_w A_{dc}(\rho_w - \rho_s) g \bar{\alpha_v} V_r}{\kappa} \tag{3.6}$$

where g is the gravitational force, A_{dc} is the area, and κ is a dimensionless friction coefficient. The volume of water in the drum is:

$$V_{wd} = V_{wt} - V_{dc} - (1 - \bar{\alpha_v}) V_r \tag{3.7}$$

Knowing the steam distribution under the water level and the volume of the water inside the drum, the drum level, l, expressed as the deviation from the centerline is given by:

$$l = \frac{V_{wd} + V_{sd}}{A_d} \tag{3.8}$$

where A_d is the wet surface of the liquid. Notice that the term $\dfrac{V_{wd}}{A_d}$ represents the deviation caused by changes in the amount of water inside the drum and the term $\dfrac{V_{sd}}{A_d}$ represents the deviation caused by changes in the amount of steam inside the drum.

3.2.3 Turbine-generator dynamics

As discussed in 2.2.2, the model of the turbine-generator system is:

$$\tau \frac{dE}{dt} = q_s(h^{sup}(T^{sup}, P_b^{sat}) - h^{ise}(P_{cond}^{sat})) - E \tag{3.9}$$

3.3 Control problem description

The boiler drum level is a significant factor that dictates the quality of the steam produced as well as the safe operation of the steam generator. A deviation above the centerline results in low steam quality and risks the life of the turbine due to entrained water particles. A deviation below the centerline may cause overheating and damaging of the boiler's tubes. A typical acceptable range of deviation is within 2 to 5 cm from the centerline [54].

In the dynamic models presented in section 3.2, the variables in equations (3.2-3.3) can be grouped to make sets of models that are one way coupled. The model (3.2), with state variables P and V_{wt}, describes the boiler pressure and total volume of water inside the boiler. This model can independently illustrate the response of the boiler pressure for changes in the manipulated variables. Adding the dynamics of the state variable α_r, the new model now describes the steam dynamics inside the risers. Finally including the dynamics of the state variable V_{sd}, the overall model (3.2-3.3) captures the dynamics of the steam under the water level in the drum. The overall model, (3.2-3.3), suggests that the successful control of the outputs of the primary group facilitates the control of the following one. Thus the boiler-turbine system now can be divided into two subsystems to be controlled, a subsystem that controls the boiler pressure, taking into consideration the dynamics of the boiler pressure and the total volume of water inside the boiler, and a subsystem that controls the drum level inside the boiler. Based on this

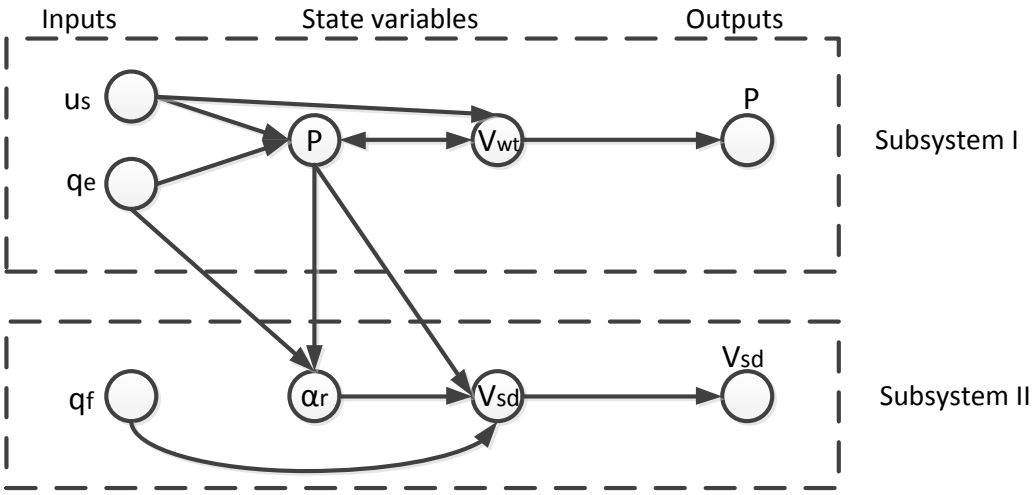

Figure 3.2: Directed graph of the dynamics for the boiler.

partition, it is of interest to have separate manipulated variables for each subsystem to have the first subsystem be completely independent from the second. A way to achieve this objective is to assume different feedwater flow rates for each subsystem. A reasonable assumption is to choose the feedwater flow rate in the first subsystem to be equal to the steam flow rate. This choice arises from the fact that this is the desired feedwater flow rate response for the control of the drum level. The controller of the first subsystem can then be designed based on the assumption that the drum level is well controlled with the turbine valve opening and fuel flow rate as its manipulated variables. The second subsystem can be controlled using the conventional three-element level controller discussed in section 3.1. A directed graph of the subsystems is shown in Figure 3.2.

In this study we study the control of the drum level using the the deadtime compensated nonlinear controller designed in Chapter 2 for the first subsystem, and the three-element level controller for the second subsystem.

As discussed in Chapter 2 a time delay, θ, is added to the fuel flow rate. Substituting the steam flow rate by a function of the turbine steam valve opening as shown in equation (2.3), the system to be controlled becomes:

$$k_{11}\frac{dV_{wt}}{dt} + k_{12}\frac{dP}{dt} = q_f - \frac{kP}{\sqrt{T^{sup}}}u_s$$

$$k_{21}\frac{dV_{wt}}{dt} + k_{22}\frac{dP}{dt} = \eta_b \Delta H q_e(t-\theta) + q_f h_f - \frac{kP}{\sqrt{T^{sup}}}u_s h_s$$

$$k_{32}\frac{dP}{dt} + k_{33}\frac{d\alpha_r}{dt} = \eta_b \Delta H q_e(t-\theta) - \alpha_r h_v q_{dc} \tag{3.10}$$

$$k_{42}\frac{dP}{dt} + k_{43}\frac{d\alpha_r}{dt} + k_{44}\frac{dV_{sd}}{dt} = \frac{\rho_s}{T_d}(V_{sd}^0 - V_{sd}) + \frac{(h_f - h_w)}{h_v}q_f$$

$$\tau\frac{dE}{dt} = \frac{kP}{\sqrt{T^{sup}}}u_s(h^{sup}(T^{sup}, P_b^{sat}) - h^{ise}(P_{cond}^{sat})) - E$$

The parameters of the system above are defined in section 3.2.2, the steam correlations used are the same as the ones presented in section 2.3, and the nominal parameters used for the power plant are in Table 3.1.

Table 3.1: Nominal Parameters for the Steam Power Plant

m_t	300×10^3 kg	m_r	160×10^3kg
m_d	140×10^3kg	τ	0.4 s
ΔH	24 MJ/kg	η_b	0.88
h_f	1030 kJ/kg	η_T	0.725
V_t	89 m^3	V_r	38 m^3
V_{dc}	11 m^3	V_d	40 m^3
β	0.3	A_d	20 m^2
A_{dc}	0.3809 m^2	κ	25
T_d	12	V_{sd}^0	7.793

3.4 Case study

Referring to the power plant model in (3.10), there are three manipulated variables, q_f, q_e and u_s, five state variables, P, V_{wt}, α_r, V_{sd}, and E, and three outputs, P, l, and E. The deadtime appears only in the fuel flow rate. Two controllers are used for the control of the boiler-turbine system. The nonlinear deadtime compensated model state feedback structure described in Chapter 2 is used for the simultaneous control of the boiler pressure and power generation. The design of this controller does not consider the drum level dynamics. A conventional three-element PI controller is used for the control of the drum level.

The MIMO nonlinear decoupling controller used is:

Process Model:

$$\left[V_s\left(\rho_s\frac{\partial h_s}{\partial P_m}\right)+V_{wt}\left(\rho_w\frac{\partial h_w}{\partial P_m}\right)-V_t+m_tC_p\frac{\partial T^{sat}}{\partial P_m}\right]\frac{dP_m}{dt}$$

$$=\frac{kP_m}{\sqrt{T^{sup}}}u_s(h_f-h_s)+\eta_b\Delta Hq_e(t-\theta)$$

$$\tau\frac{dE_m}{dt}=\eta_T\frac{kP_m}{\sqrt{T^{sup}}}u_s(h^{sup}(T^{sup},P_m)-h^{ise}(P^{sat}_{cond}))-E_m$$

where the subscript m denotes a model state.

Static-state feedback:

– Characteristic matrix:

$$C(x) = \begin{bmatrix} \dfrac{\dfrac{kP_m}{\sqrt{T^{sup}}}(h_f - h_s)}{V_s\left(\rho_s\dfrac{\partial h_s}{\partial P_m}\right) + V_w\left(\rho_w\dfrac{\partial h_w}{\partial P_m}\right) - V_t + m_t C_p\dfrac{\partial T^{sat}}{\partial P_m}\dfrac{dP_m}{dt}} & \\ \dfrac{kP_m\eta_T}{\tau\sqrt{T^{sup}}}(h^{sup} - h^{sat}_{cond}) & \dfrac{(\eta_b\Delta H)}{V_s\left(\rho_s\dfrac{\partial h_s}{\partial P_m}\right) + V_w\left(\rho_w\dfrac{\partial h_w}{\partial P_m}\right) - V_t + m_t C_p\dfrac{\partial T^{sat}}{\partial P_m}\dfrac{dP_m}{dt}} \\ 0 & \end{bmatrix}$$

– Control law:

$$u = C(x)^{-1}\begin{bmatrix} \dfrac{v_1 - P_m}{\beta_{11}} \\ \dfrac{v_2 - \left(1 - \dfrac{\beta_{21}}{\tau}\right)E_m}{\beta_{21}} \end{bmatrix}$$

The artificial delay of the steam flow as well as the delay of the model outputs, P_m and E_m, is equal to the deadtime that appears in q_e.

A description of the power plant studied is given in section 2.4. In order to examine the performance of the controller, different scenarios of set point tracking of power demand and disturbance rejection are investigated. The tests conducted for set point tracking are:

- A ramp up of power set point from 80 MW to 160 MW at a rate of 2% per minute.
- A "worst case" scenario of ± 32MW (20% of the Maximum Continuous Rate) step changes in power set point at 20 minute intervals with simultaneous random fluctuations in deadtime associated with the fuel flow [17].

For disturbance rejection, the following tests are conducted:

- A 5% decrease in the heating value of the fuel.
- A 5% decrease in the turbine efficiency of the turbine-generator system.

The power change rate is selected from a range of 2-3% per minute that is a typical range for power plants with drum boilers [51].

The tuning parameters are kept the same for all tests and are summarized in Table 3.2. The subscripts p and s denotes primary and secondary controllers of the three-element level controllers.

Table 3.2: Controller Parameters for the Steam Power Plant

Controller	**Parameter**	
Nonlinear DT compensated	β_{11}	500 s
	β_{21}	200 s
PI-Level controller	k_{cp}	40
	τ_{Ip}	0.05 s
	k_{cs}	200
	τ_{Is}	0.05 s
PI-GMDC	k_{c1}	$1.9 \times 10^{-4} MW^{-1}$
	τ_{I1}	50 s
	k_{c2}	0.01 $\frac{kg/s}{MPa}$
	τ_{I2}	5 s
PI-Level controller	k_{cp}	40
	τ_{Ip}	0.05 s
	k_{cs}	200
	τ_{Is}	0.05 s

The three-element drum level controller is also applied with the PI-GMDC controller introduced in Chapter 2 for comparison purposes with the proposed control strategy.

The results of the controllers' testing are discussed in the next section. For brevity, although the level controllers used with the nonlinear controller and with the PI-GMDC are the same, the terms "nonlinear controller" and "PI-GMDC controller" will be used to indicate the integration of the level controller with each boiler pressure and power generation controller. The tuning parameters of both control structures are tuned to provide a fast and stable response with no oscillations. The rule of thumb of tuning the level controller is that the primary controller should be at least 5 times slower than the secondary controller [55].

3.5 Simulation results

3.5.1 Set point tracking

The drum level response for ramping of the power set point at a rate of 2%/min is shown in Figure 3.3 for the nonlinear and the PI-GMDC controllers. Both level responses initially experience a slight increase then fall and increase again as they approach the set point.

There are three factors that affect directly and indirectly the response of the drum level. The ramping of the power generation prompts the turbine valve opening to ramp up to allow more steam into the turbine (Figure 3.4), consequently, the feedwater flow rate (Figure 3.5) ramps up prior to detecting the disturbance in the drum level. The ramp up of the feedwater flow rate is a result of the feedforward signal of the steam flow rate that corrects the set point of the secondary controller of the three-element level controller. Simultaneously, the fuel flow rate increases to control the pressure and increase steam generation as shown in Figure 3.6. The three manipulated variables concurrently increase for the requested change in the power generation, thus a direct justification on the behavior of the drum level based on these variables is not simple,

instead the behavior of the state variables and other processes inside the drum should be analyzed.

As discussed earlier, the drum level is a result of the changes in the drum water volume and the volume of the steam under the water level of the drum. In the case study utilizing the nonlinear controller, the response of the level controller can be divided into three stages as shown in Figure 3.3. The deviation of the drum level above the centerline as shown at point A is explained as follows. The increase of the fuel flow rate causes the volume of water inside the boiler to slightly decrease (Figure 3.8), the steam quality at the outlet of the risers to increase, and thus the average volume fraction of steam to increase (Figure 3.7). Although the volume of water inside the boiler decreases, the increase in the average volume fraction of steam causes an increase in the drum water volume, V_{wd}, according to equation (3.7), and hence the drum level increases. The drum level response then decreases to point B as shown Figure 3.3. At this stage the effect of increasing the feedwater flow rate becomes more prominent. As the feedwater flow rate increases, the temperature of the water inside the drum drops which decreases the volume of steam under the water level as the steam condenses. Since the density of steam is much lower than the density of water, the condensation of steam will result in a decrease in the drum level. Figure 3.9 shows the volume of steam under the water level as a response to a ramp in the power demand. Following point B, the drum level increases to point C before decreasing back to the centerline of the boiler. This increase is due to the increase in the boiler pressure. As the fuel flow rate increases, the boiler pressure increases as shown in Figure 3.11, which increases the condensation rate of the steam inside the boiler. Upon steam condensation the water volume inside the boiler, V_{wt}, increases, thus increasing the water level inside the drum.

The response of the boiler pressure as shown in Figure 3.11 experiences disturbances as power is changed. The change in pressure results from the changes in steam turbine

valve opening, in fuel flow rate and their interactions with the volume of water inside the boiler. As the fuel flow rate increases, the volume of the water inside the boiler initially decreases as the water vaporizes, increasing the boiler pressure. As the steam turbine valve opening increases, more steam leaves the boiler decreasing its pressure. The pressure then increases and returns back to its set point as the valve opening and fuel flow rate become constant and their effect on the boiler pressure stabilizes it. Although the decoupling between the power generation and boiler pressure is nullified, due to neglecting the dynamics of the water volume inside the boiler in the design of the nonlinear controller, the boiler pressure fluctuates at a very narrow range for the change in the power demand.

In the case study utilizing the PI-GMDC controller, the water level initially experiences a slight increase before declining (point a in Figure 3.3). This increase is due to the swell effect that occurs due to the decrease in boiler pressure as discussed earlier in section 3.1. As the turbine valve opening increases, the boiler pressure decreases, thus decreasing the condensation rate of steam inside the drum as shown in Figure 3.12. In an open loop situation, the vaporization rate of water increases as the boiler pressure decreases, however, in the closed loop situation, the increase in the feedwater flow rate prevent this increase. Consequently, the drum level decreases to point b. The level of the water inside the drum then increases to point c before decreasing back to the centerline of the boiler. At this stage of the drum level increase, the effect of the feedwater flow rate dominates, causing the condensation rate of steam inside the drum to increase, thus increasing the water level.

Comparing the response of the drum level resulting from both controllers shows that the nonlinear controller results in a different control path for the drum level, and thus in different interactions that contribute to the response of the drum level. In addition, the nonlinear controller results in a better performance of the three-element level controller.

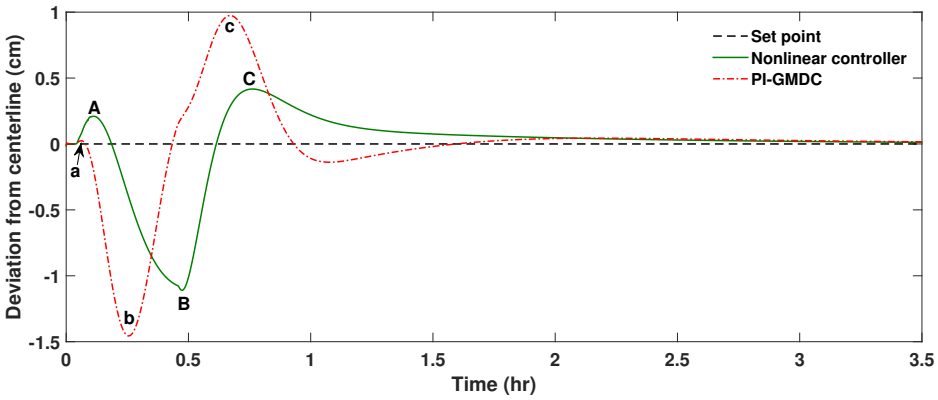

Figure 3.3: Deviation of the water level from the centerline of the boiler drum for a ramp of power set point at a rate of 2%/min.

The power generation resulting from both control structures is illustrated in Figure 3.13. The response of the controllers for power set point tracking is the same as the response presented in Chapter 2, thus the discussion of power generation will not be presented here to avoid repetition.

The drum level response to the "worst case" scenario performance test is presented in Figure 3.14. The drum level is expected to experience disturbances from two sources; changes in power set point and fluctuating deadtimes. In the case study utilizing the nonlinear controller, the drum level response appears to be tightly controlled around the set point despite the changes in deadtime. However, in the case study utilizing the PI-GMDC controller, the disturbances caused by the step changes in the power generation are intensified by the deadtime uncertainty. This is illustrated by comparing the sizes of disturbances in the drum level. For the first step change in the power set point, the deadtime is unchanged and the deviation in the drum level did not exceed 2 cm below the centerline; as the deadtime fluctuated, the deviations increased to around 4 cm from the centerline as shown in Figure 3.14.

The pressure response for the nonlinear controller, illustrated in Figure 3.16, reflects

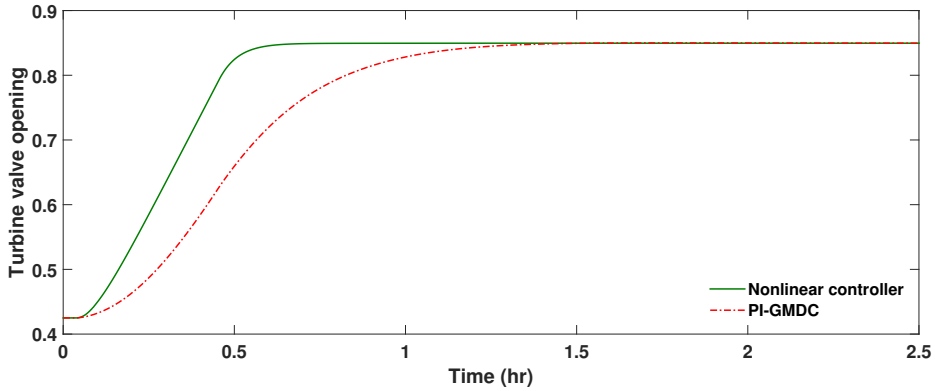

Figure 3.4: Control actions of the turbine valve opening for a ramp of power set point at a rate of 2%/min.

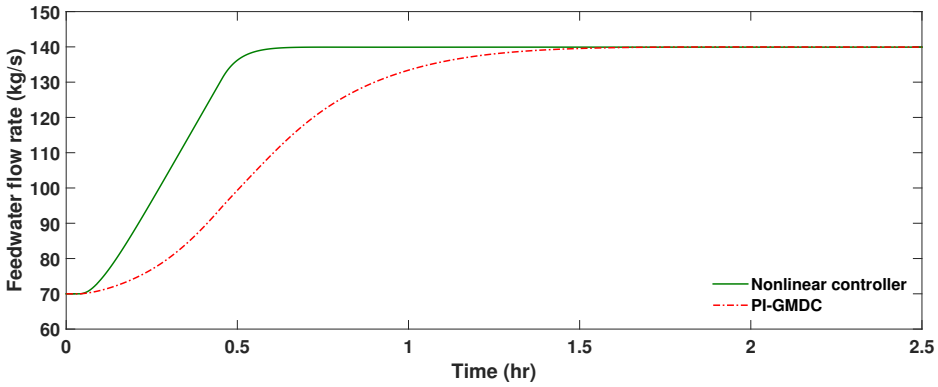

Figure 3.5: Control actions of the feedwater flow rate for a ramp of power set point at a rate of 2%/min.

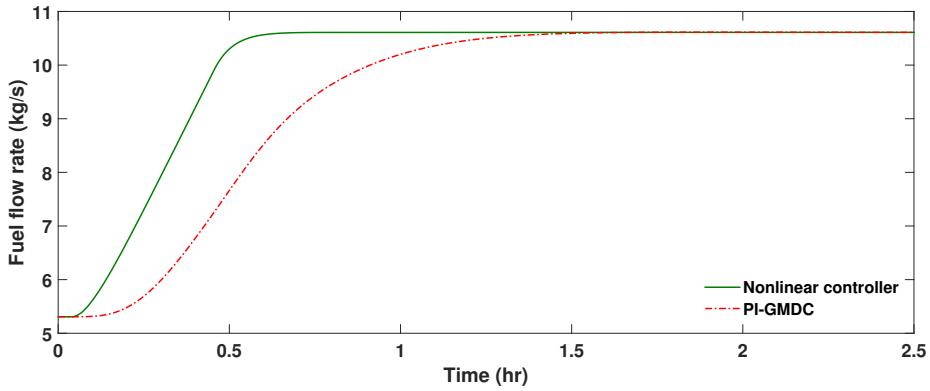

Figure 3.6: Control actions of the fuel flow rate for a ramp of power set point at a rate of 2%/min.

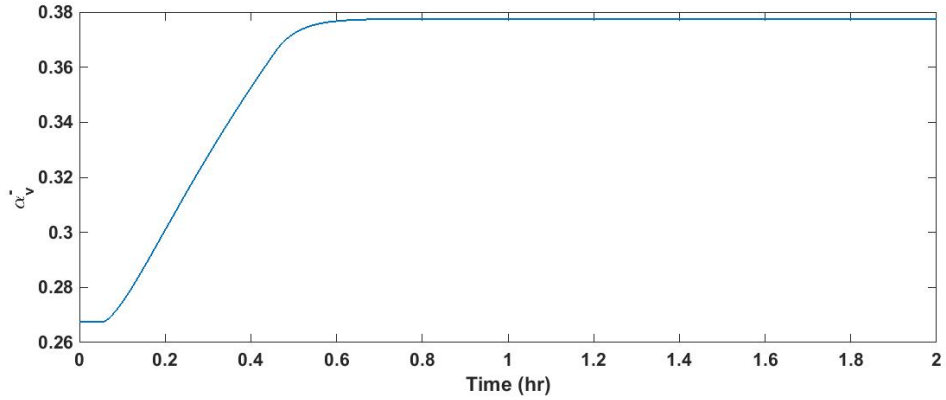

Figure 3.7: Response of the average volume fraction of steam to a ramp of power set point at a rate of 2%/min for the nonlinear controller.

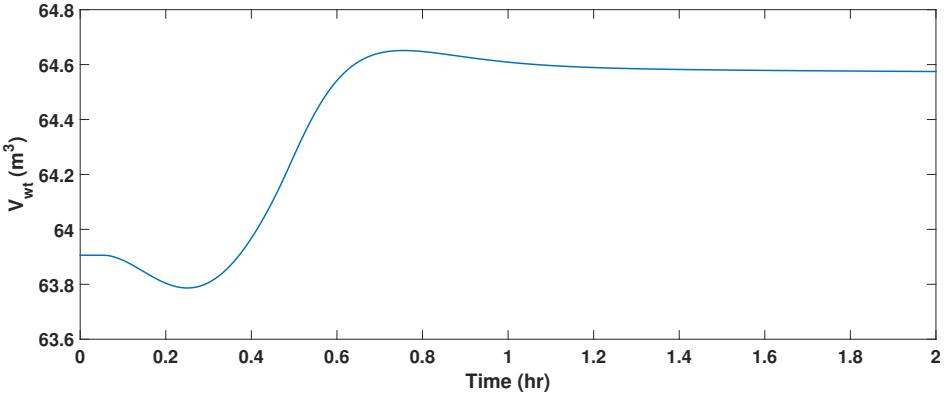

Figure 3.8: Response of the water volume in boiler to a ramp of power set point at a rate of 2%/min for the nonlinear controller.

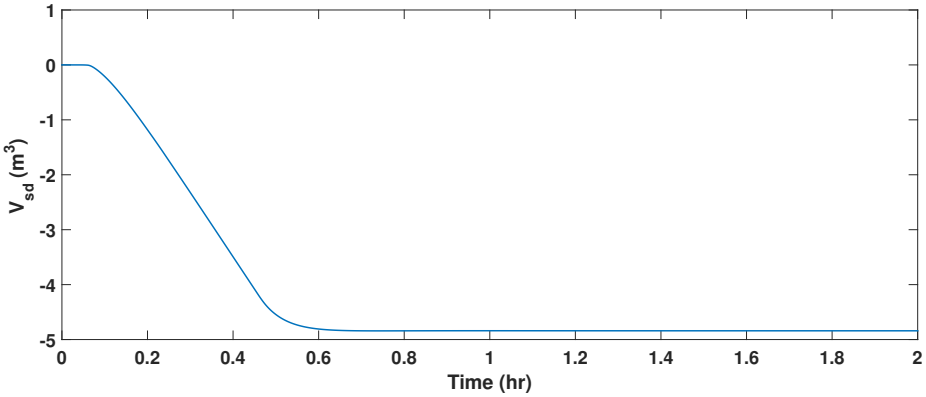

Figure 3.9: Response of the volume of steam under drum level to a ramp of power set point at a rate of 2%/min for the nonlinear controller.

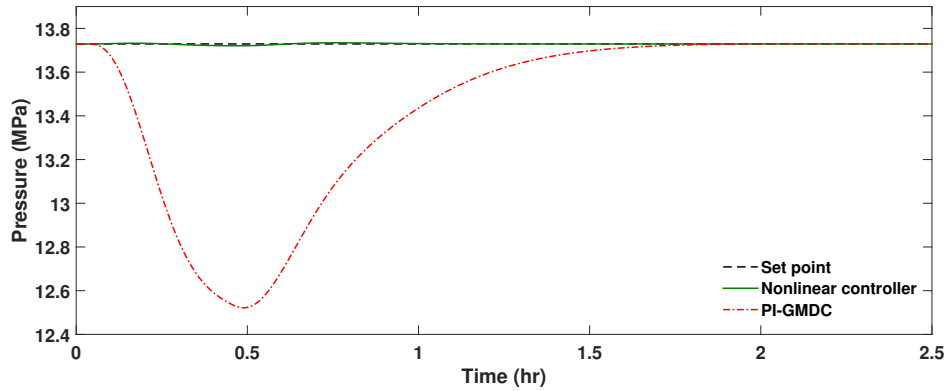

Figure 3.10: Pressure response for a ramp of power set point at a rate of 2%/min.

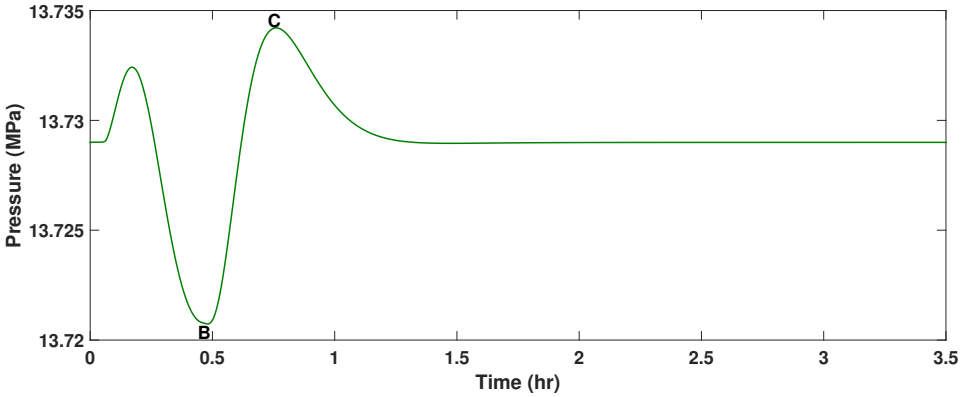

Figure 3.11: Pressure response of nonlinear controller for a ramp of power set point at a rate of 2%/min.

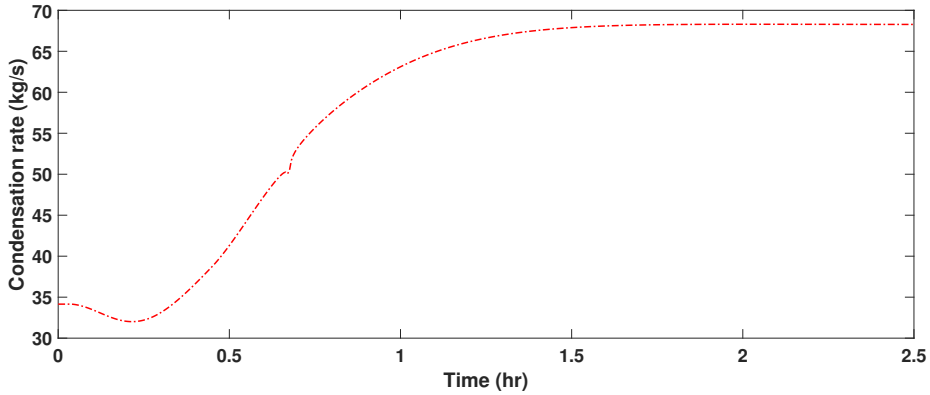

Figure 3.12: Condensation rate of steam inside the boiler drum.

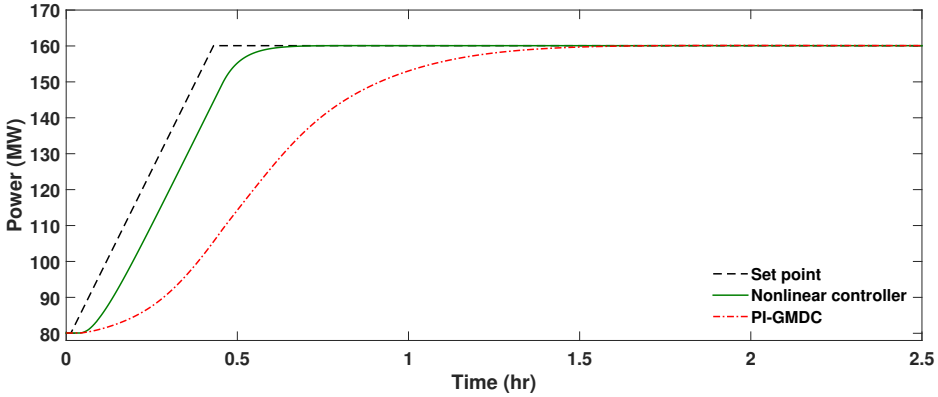

Figure 3.13: Power generation response for a ramp of power set point at rate of 2%/min.

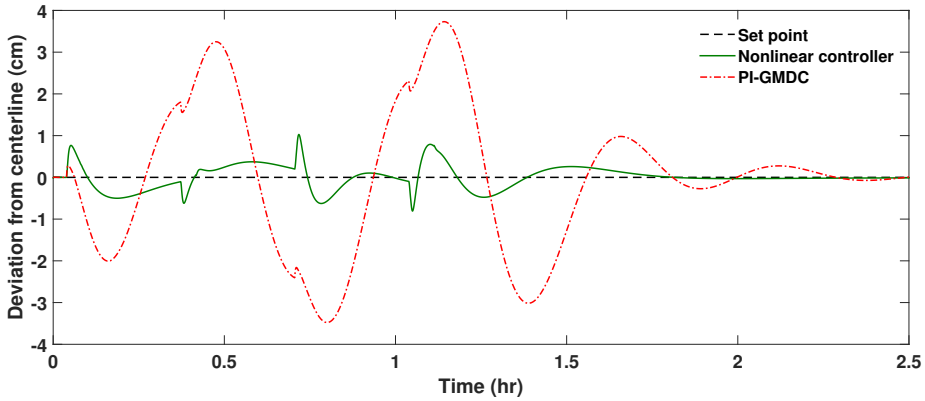

Figure 3.14: Deviation of the water level from the centerline of the boiler drum for a multiple step changes in power set point with deadtime fluctuations.

a disturbance that grows as the deadtime change increases, while power generation tracks the postulated trajectory efficiently as shown in Figure 3.18. Since the nonlinear controller no longer results in a decoupled response another test is performed in order to assess the effect of the dominating disturbance. The test is to apply multiple step changes of ± 32MW in the power set point while keeping the deadtime unchanged. The response of the boiler pressure for this test as illustrated in Figure 3.17 shows that the pressure slightly fluctuates due to the change in power demand, hence, the dominating effect of the disturbances shown in Figure 3.16 is due to the fluctuating deadtime. These results are in agreement with the results described in Chapter 2 where disturbances appear in the pressure response despite the decoupling achieved by the nonlinear controller.

3.5.2 Disturbance rejection

The effect of a 5% decrease in the heating value of coal on the drum level is shown in Figure 3.19. In the case study utilizing the nonlinear controller, the drum level response 1) falls below the centerline, then 2) increases to above the centerline, 3) then

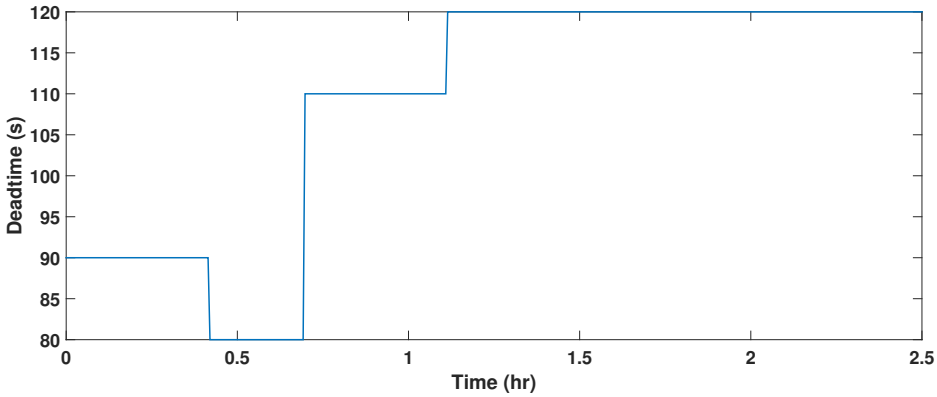

Figure 3.15: Applied deadtime values.

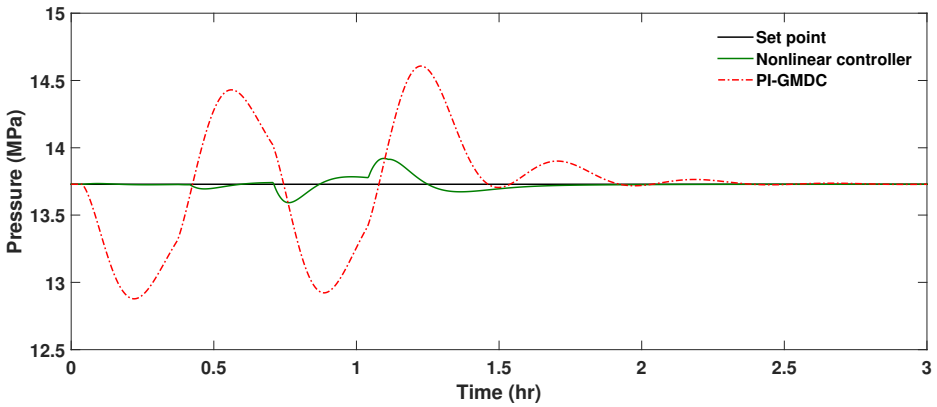

Figure 3.16: Pressure response for a multiple step changes in power set point with deadtime fluctuations.

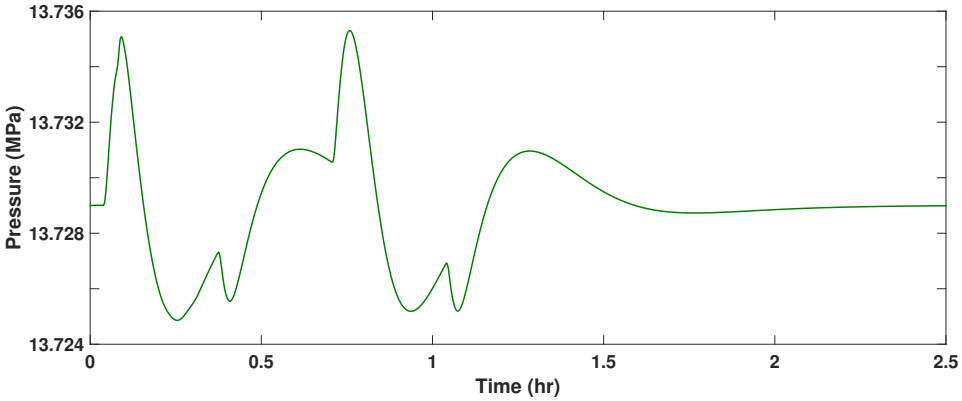

Figure 3.17: Pressure response for a multiple step changes in power set point with deadtime fluctuations.

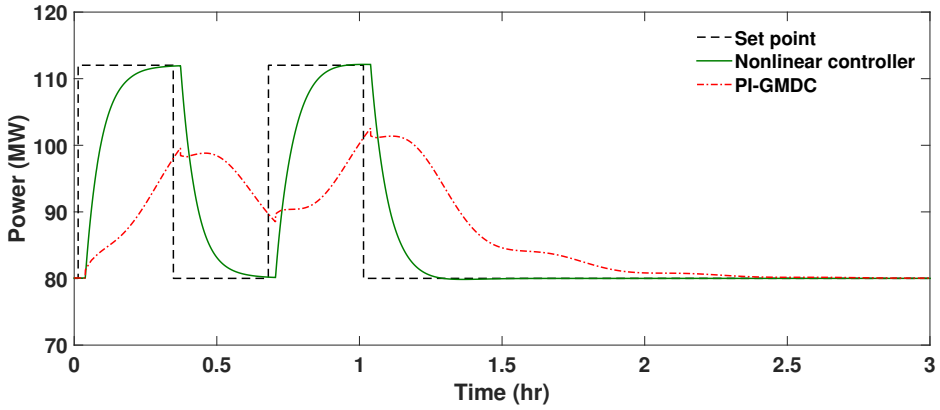

Figure 3.18: Power generation response for a multiple step changes in power set point with deadtime fluctuations.

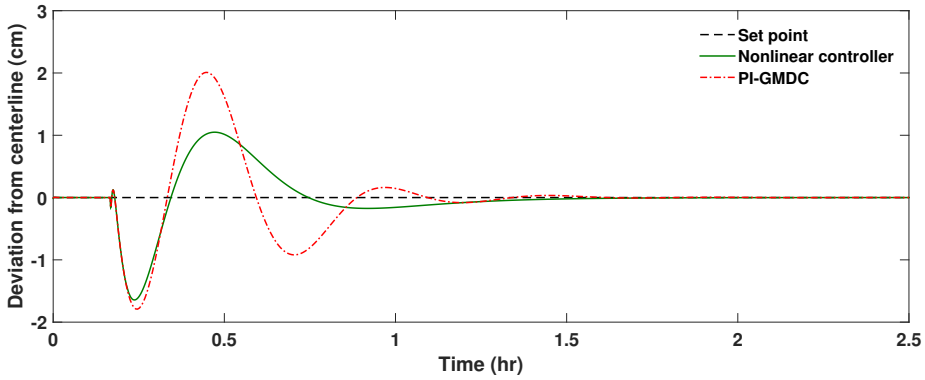

Figure 3.19: Deviation of the water level from the centerline of the boiler drum for a 5% decrease in the heating value of the fuel.

approaches its set point. The initial response of the drum level can be explained by the response of the boiler pressure as shown in Figure 3.20. The decrease in the heating value of coal results in a decrease in the boiler pressure, which according to equation (2.3) decreases the amount of steam passing through the turbine valve opening. Because of the feedforward signal of the steam flow rate to the level controller, the feedwater flow rate decreases (Figure 3.21), decreasing the water level inside the drum. A lower boiler pressure indicates a higher latent heat for steam production, thus the vaporization rate of saturated water decreases, causing an increase in the water level inside the drum. Finally the increase in fuel flow rate, illustrated in Figure 3.22, increases the boiler pressure and steam production, and hence the level drum decreases back to its set point. The power generation response to the 5% decrease in heating value of fuel is shown in Figure 3.23. The performance of the level controller in the case study utilizing the PI-GMDC is similar to that of the nonlinear controller, however the disturbance results in oscillatory responses unlike those of the nonlinear controller.

The drum level response to a 5% decrease in turbine efficiency is presented in Figure 3.24. The response of the drum level in the case study utilizing the nonlinear controller

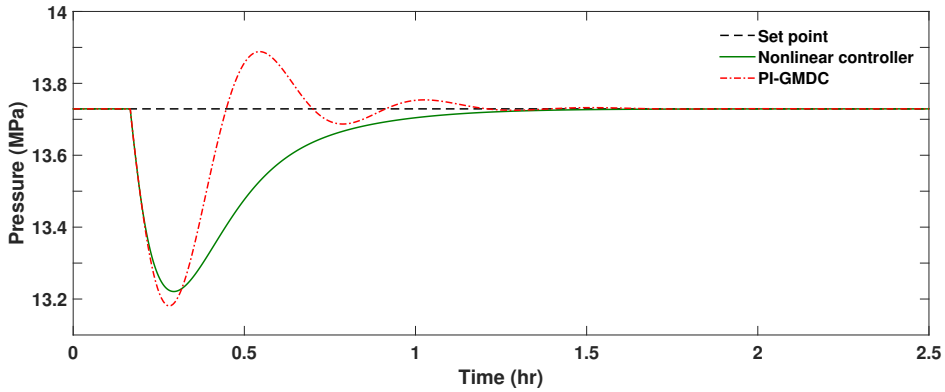

Figure 3.20: Pressure response to a 5% decrease in the heating value of the fuel.

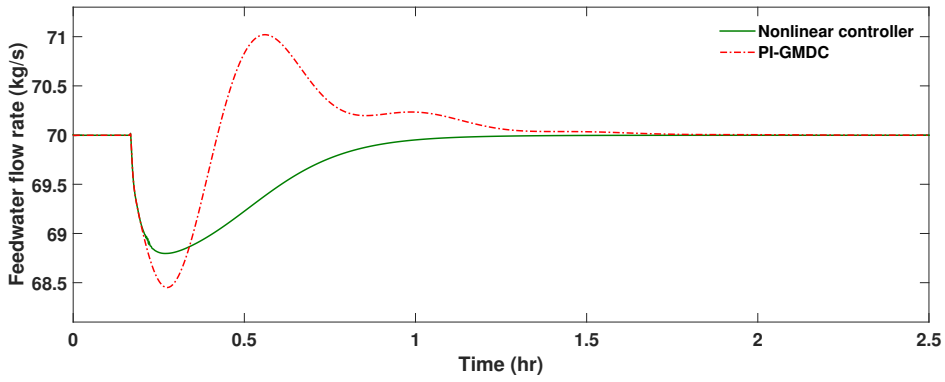

Figure 3.21: Feedwater flow rate control actions for a 5% decrease in the heating value of the fuel.

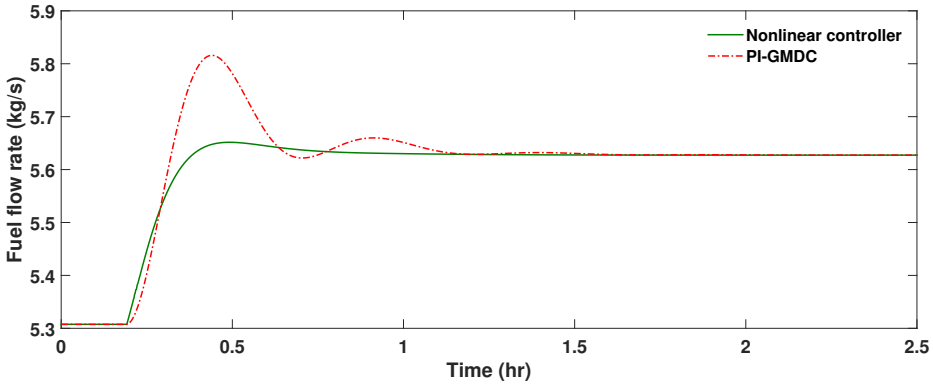

Figure 3.22: Fuel flow rate control actions for a 5% decrease in the heating value of the fuel.

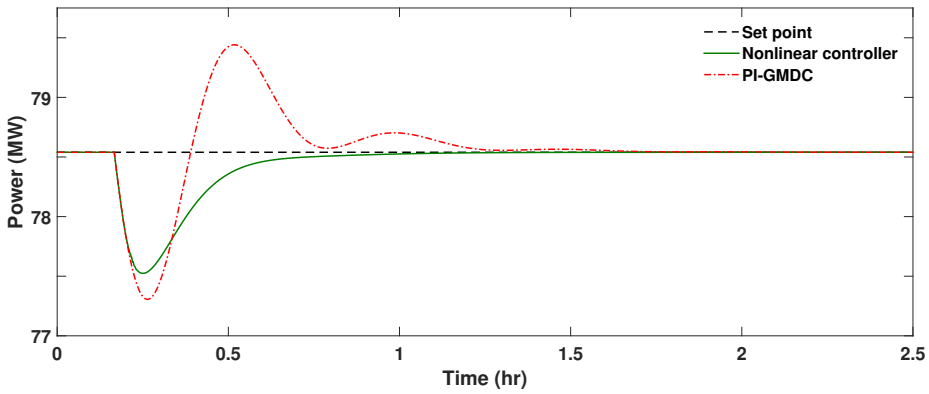

Figure 3.23: Power generation response to a 5% decrease in the heating value of the fuel.

is driven by the same drum level control path that is discussed for ramping the power set point. The disturbance initially affects the power generation as shown in Figure 3.26. The fuel flow rate and the turbine valve opening changes after the actual fuel flow deadtime and artificial turbine valve opening deadtime elapses. Both manipulated variables increase as a result of the 5% decrease in the turbine efficiency to increase the flow of steam into the turbine. Figure 3.27 illustrates the response of the fuel flow rate. The feedwater flow rate also increases as a result of the steam flow feedforward signal to the level controller. Similar to the drum level control path of ramping set point, the increase in the manipulated variables causes the volume of water inside the boiler to slightly decrease, the steam quality at the outlet of the risers to increase, the average volume fraction of steam to increase, and thus the volume of water inside the drum to increase. Consequently, the drum level experiences an initial increase. As the feedwater flow rate increases, the temperature of the water inside the drum and the volume of steam under the water level decreases as the steam condenses. Because of the density difference between steam and water, the condensation of steam will result in a decrease in the drum level. The drum level then stabilizes at the centerline as the effect of changing the manipulated variables stabilizes the boiler pressure and power generation.

The responses of the PI-GMDC case study also follows that of ramping the power set point. The water level initially experiences a "swell" due to the decrease in boiler pressure as discussed earlier in section 3.1. Then due to the pressure drop and the effect of the feedwater flow rate increase, the condensation rate of steam fluctuates causing the drum level to oscillate before stabilizing at the centerline.

Comparing the response of the drum level resulting from both controllers reveals that the nonlinear controller results in a better performance of the three-element level controller, where the response of the drum level is less oscillatory compared to that

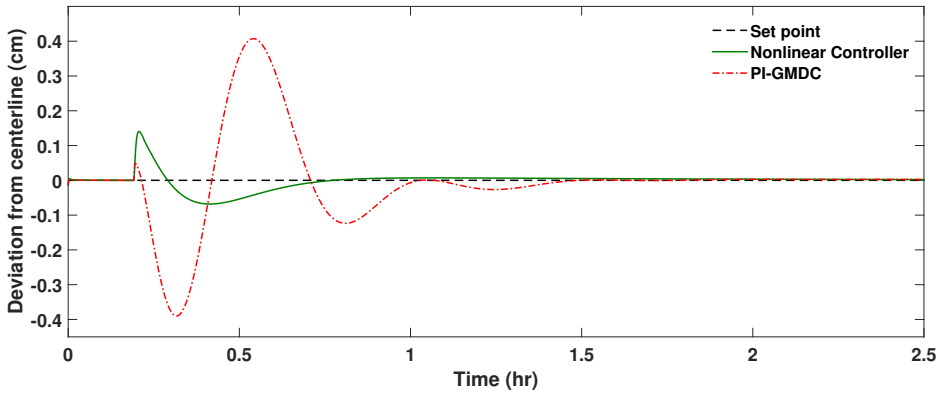

Figure 3.24: Deviation of the water level from the centerline of the boiler drum for a 5% decrease in the turbine efficiency of the turbine-generator system.

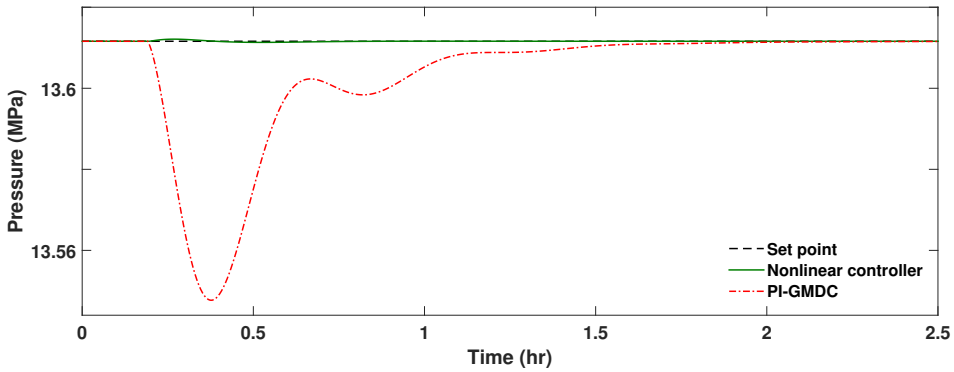

Figure 3.25: Boiler pressure response to a 5% decrease in the turbine efficiency of the turbine-generator system.

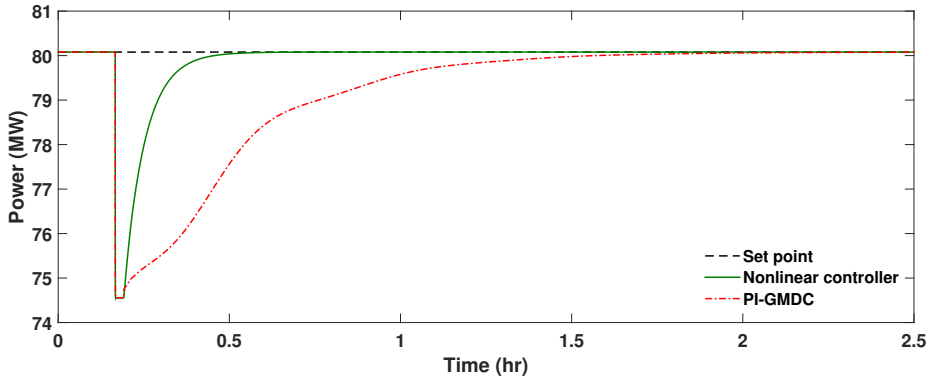

Figure 3.26: Power generation response to a 5% decrease in the turbine efficiency of the turbine-generator system.

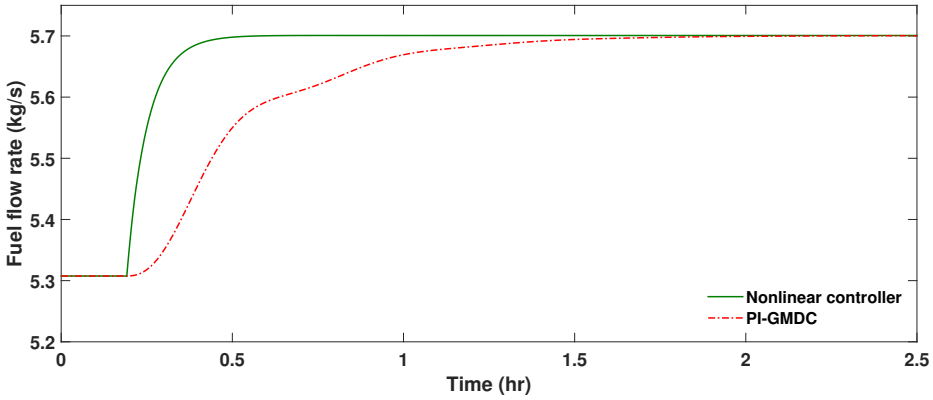

Figure 3.27: Fuel flow rate control actions to a 5% decrease in the turbine efficiency of the turbine-generator system.

resulted from the PI-GMDC controller. Moreover, the results of the PI-GMDC case study shows that the drum level approaches the upper limit of the acceptable range for the deviation from the set point.

3.6 Conclusions

Water level inside the boiler drum is a critical factor that determines the safety of the boiler and the quality of steam traveling to the steam turbine. In this chapter, the control of the drum level was taken into consideration in addition to the control of the boiler pressure and power generation. The level dynamics included the volume of steam under the water level, the volume of water inside the drum, and the quality of steam leaving the risers. The manipulated variable used for controlling the drum level is the feedwater flow rate. A three-element conventional PI level controller is used together with the model state feedback controller designed in the Chapter 2. The power plant performance was then tested for wide range power set point tracking, disturbance rejection, and deadtime uncertainty. The results showed that using the nonlinear controller along with the conventional level controller resulted in a different control path for the drum level than for the case using linear controllers, and an efficient regulation of the drum level is illustrated for each case studied. The results also showed that changes in the feedwater flow rate did not have an apparent effect on the power set point tracking capability of the nonlinear controller.

Chapter 4

Temperature control in power plants

4.1 Introduction

The efficiency of power generation depends on the heat content of the steam and the amount of heat expanded in the steam turbines. The higher the pressure and temperature of steam the higher is its heat content. Thus the more superheated the steam is, the more efficient is power generation.

Production of superheated steam for power generation is achieved at different stages. Depending on the stage of superheating the location of the superheater in the steam generator is selected. Primary stages of superheating that produces low temperature superheated steam are located downstream of the steam generator back pass section, where the flue gas temperature is low compared to its temperature at the exit of the furnace. The greater the degree of superheating, the closer the superheater is to the furnace. Hence final stages of superheating that produces high temperature superheated steam are located inside the furnace or at the entrance of the back pass where the flue

gas temperature is the highest.

Superheaters in the steam generator can be of different types. Convection-type superheaters are superheaters that transfer energy mainly by convection. In the steam generator, they are located in the back pass section, utilizing flue gas as the heating medium. Platen or radiant-type superheaters are located in the furnace or at the exit of the furnace where they receive thermal radiation from the flue gas and the burning fuel.

To increase the efficiency of power generation the superheated steam may undergo partial expansion in different steam turbines. In the first turbine, called high pressure (HP) turbine, the high pressure superheated steam is partially expanded to typically one fifth of the boiler pressure [51] as it produces power. The expanded superheated steam then returns to the steam generator and is heated in a reheater to the temperature of the high pressure superheated steam. Next, the reheated steam is sent to a low pressure (LP) turbine for further power generation. The reheated steam contains higher heat content than the superheated steam due to its lower pressure. Thus power generation in the LP turbine is greater than the generation in the HP turbine. Depending on the scale of power generation and the design of the power plant, intermediate pressure turbines may also be used.

Controlling superheated and reheated steam temperatures is important for the safety of the tubings and for a uniform generation of power. Typically the operation range at which steam temperature must be controlled is 60%-100% of the maximum continuous rating (MCR) of the power plant [6, 56]. The temperatures of the superheated and reheated steam are desired to be maintained within $\pm 6^{o}C$ of their set points [57, 58].

Superheated steam temperatures are controlled by spraying feed water into the superheated steam exiting the primary and secondary superheaters. Spraying feed water

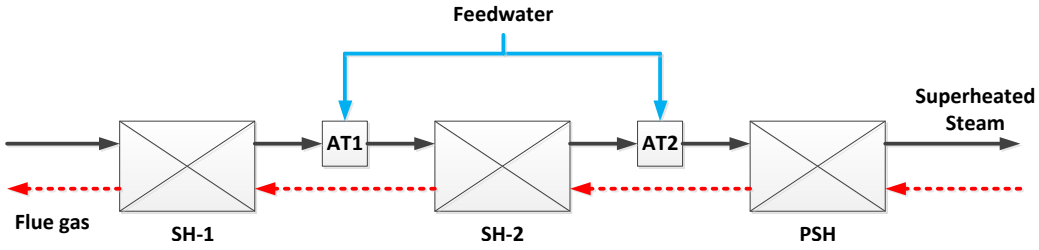

Figure 4.1: A schematic of the attemperation process. SH-superheater, PSH-platen(radiant)superheater, AT-attemperator.

decreases the enthalpy of the steam and thus decreases its temperature prior to entering the next stage of heating; this process is called attemperation or desuperheating. Spraying feed water in these locations avoids overheating of steam and over heating of the heat exchanger tube walls, protecting it from damage [6]. An illustration of the attemperation process is shown in Figure 4.1.

The conventional control strategy for superheated steam temperatures is a PI cascade type control. The outer loop controller measures the final superheater temperature and compares it to the desired set point. The produced control action serves as a set point for the inner loop controller which controls the temperature of the steam leaving the attemperator that is located before the final superheater. Thus the inner loop varies the attemperator feedwater flow rate to adjust the de-superheated steam temperature [59].

Considering the use of a reheater in power generation can be profitable. Reheating steam results in power generation higher than that generated from an equal amount of steam without reheat. Thus, smaller plant components may be installed which, in turn, may reduce initial plant costs [60]. However, the use of a reheater is viable for power generation over 100 MW [56].

The reheated steam temperature is controlled by different techniques. One of these

techniques is the bypass dampers positioning which varies the amount of energy the reheater receives from the flue gas. Flue gas leaving the furnace enters the back pass section that encloses the convection-type heat exchangers. The back pass is divided into two sections with primary and secondary superheaters stacked in one section, and the reheater is located in the second one. Below the reheater are bypass dampers, which changes position depending on the amount of energy required by the partially expanded steam to be reheated to the desired set point. Thus, if the temperature of the partially expanded steam is low, the bypass dampers will adjust to allow more gas to enter the reheater section. This positioning however, should not be reducing the heat transferred to the superheaters to the extent that both attemperators be fully closed [6]. A schematic of the bypass dampers and the back pass section is illustrated in 4.2

In this chapter, we propose a nonlinear control strategy for steam generator-turbine system that aims to control the boiler pressure, superheated steam temperatures, reheated steam temperature, and power generation. The strategy decomposes the overall plant into three separate subsystems with minimum interactions among them and applies nonlinear decoupling feedback controllers with deadtime compensation for each one of them. In the following sections, the modeling of the steam generator-turbine system is presented, the considered control problem is described, the proposed controller is implemented and tested for different scenarios, and the results are discussed.

4.2 Modeling of steam power plant

The units of the steam generator-turbine system to be modeled are the boiler, superheaters, reheater, and the turbine-generator systems. The model of the boiler is the same as that presented in Chapter 2 and thus will not be repeated in this section.

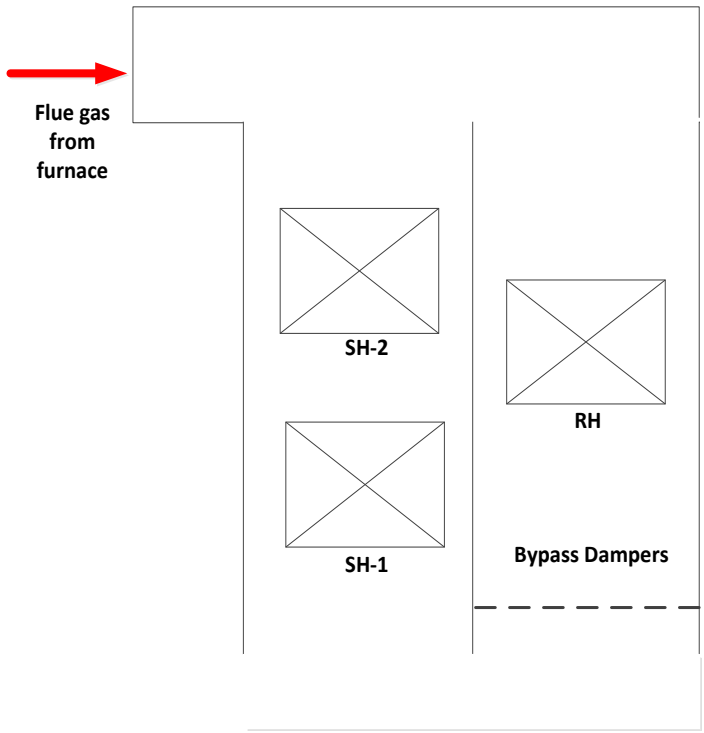

Figure 4.2: A schematic of the back pass section and bypass dampers. SH-superheater, RH-reheater.

4.2.1 Superheaters and reheater

Superheaters can be of convection-type, radiant-type or a combination of both. In the current study, a radiant-type superheater is used as a final stage of superheating preceded by two convection-type superheaters; primary and secondary superheaters respectively. The reheater is a convection-type one. The superheaters are modeled as shell and tube heat exchangers [61, 62], where steam flowing inside the tubes is being heated by the temperature increase of the metal walls that are heated by the flue gas flowing through the shell. The radiant-type heat exchanger is placed at the end of the furnace before the convection pass. In order to model the dynamics of the heat exchangers the following assumptions are made:

- The temperature inside the furnace is constant.
- The temperature of the flue gas is constant but different at each location of the gas path.
- In the radiant-type superheater, the heat between the gas and the metal wall is transferred by radiation, while the heat between the metal walls and steam is transferred by convection.
- Mass transfer dynamics is much faster with respect to energy transfer dynamics and therefore it is not considered.
- The expansion of steam in the turbines is isentropic.
- $\Delta P = 0$ across all superheaters.

Energy balance

The energy balance for the superheaters and reheater is modeled as follows:

- Primary Superheater

  Tube walls side:

$$\frac{dT_{w_{SH1}}}{dt} = \frac{\bar{h}_w^{SH1} q_{fg-SH1}^{0.6}(T_{g_{SH1}} - T_{w_{SH1}}) - \bar{h}^{SH1} q_{in_{SH1}}^{0.8}(T_{w_{SH1}} - T_{SH1})}{\rho_{w_{SH1}} V_{w_{SH1}} c_{p_{w_{SH1}}}} \tag{4.1}$$

  Steam side:

$$\frac{dh_{SH1}}{dt} = \frac{\bar{h}^{SH1} q_{in_{SH1}}^{0.8}(T_{w_{SH1}} - T_{SH1}) - q_{in_{SH1}}(h_{SH1} - h_{SH1}^{in})}{\rho_{SH1} V_{SH1}} \tag{4.2}$$

  Steam flow rate:

$$q_{in_{SH1}} = \frac{kP}{\sqrt{T_{PSH}}} u_s \tag{4.3}$$

- Secondary Superheater

  Tube walls side:

$$\frac{dT_{w_{SH2}}}{dt} = \frac{\bar{h}_w^{SH2} q_{fg-SH2}^{0.6}(T_{g_{SH2}} - T_{w_{SH2}}) - \bar{h}^{SH2}(q_{in_{SH1}} + q_{at_1})^{0.8}(T_{w_{SH2}} - T_{SH2})}{\rho_{w_{SH2}} V_{w_{SH2}} c_{p_{w_{SH2}}}} \tag{4.4}$$

  Steam side:

$$\frac{dh_{SH2}}{dt} = \frac{\bar{h}^{SH2}(q_{in_{SH1}} + q_{at_1})^{0.8}(T_{w_{SH2}} - T_{SH2}) - (q_{in_{SH1}} + q_{at_1})(h_{SH2} - h_{SH2}^{in})}{\rho_{SH2} V_{SH2}} \tag{4.5}$$

Enthalpy of steam at inlet condition:

$$h_{SH2}^{in} = \frac{q_{in_{SH1}} h_{SH1} + q_{at_1} h_{at_1}}{q_{in_{SH1}} + q_{at_1}} \tag{4.6}$$

- Platen (Radiant) Superheater

  Tube walls side:

$$\frac{dT_{w_{PSH}}}{dt} = \frac{A\sigma\epsilon(T_{g_{PSH}}^4 - T_{w_{PSH}}^4) - \bar{h}^{PSH}(q_{in_{SH1}} + q_{at_1} + q_{at_2})^{0.8}(T_{w_{PSH}} - T_{PSH})}{\rho_{w_{PSH}} V_{w_{PSH}} c_{p_{w_{PSH}}}} \tag{4.7}$$

  Steam side:

$$\frac{dh_{PSH}}{dt} = \frac{\bar{h}^{PSH}(q_{in_{SH1}} + q_{at_1} + q_{at_2})^{0.8}(T_{w_{PSH}} - T_{PSH}) - (q_{in_{SH1}} + q_{at_1} + q_{at_2})(h_{PSH} - h_{PSH}^{in})}{\rho_{PSH} V_{PSH}} \tag{4.8}$$

  Enthalpy of steam at inlet condition:

$$h_{PSH}^{in} = \frac{(q_{in_{SH1}} + q_{at_1}) h_{SH2} + q_{at_2} h_{at_2}}{q_{in_{SH1}} + q_{at_1} + q_{at_2}} \tag{4.9}$$

- Reheater

  Tube walls side:

$$\frac{dT_{w_{RH}}}{dt} = \frac{\bar{h}_w^{RH} q_{fg-RH}^{0.6}(T_{g_{RH}} - T_{w_{RH}}) - \bar{h}^{RH}(q_{in_{SH1}} + q_{at_1} + q_{at_2})^{0.8}(T_{w_{RH}} - T_{RH})}{\rho_{w_{RH}} V_{w_{RH}} c_{p_{w_{RH}}}} \tag{4.10}$$

Steam side:

$$\frac{dh_{RH}}{dt} = \frac{\bar{h}^{RH}(q_{in_{SH1}} + q_{at_1} + q_{at_2})^{0.8}(T_{w_{RH}} - T_{RH}) - (q_{in_{SH1}} + q_{at_1} + q_{at_2})(h_{RH} - h_{RH}^{in})}{\rho_{RH} V_{RH}} \tag{4.11}$$

Enthalpy of steam at inlet condition:

$$h_{RH}^{in} = \eta_T(h_{HP}^{is,th} - h_{PSH}) + h_{PSH} \tag{4.12}$$

where h denotes the specific enthalpy of the steam leaving the heat exchanger, q_{in} denotes the flow rate of steam entering, h^{in} denotes the enthalpy of steam entering the heat exchanger, ρ denotes the average density of steam, V denotes the volume of steam, T_w is the temperature of the tube walls, ρ_w is the density of the tube walls, V_w is the volume of the tube walls, cp_w is heat capacity of the tube walls, $\bar{h}$ is the tube walls to steam heat transfer coefficient, T is the average temperature of steam, $\bar{h_w}$ is the gas to tube walls heat transfer coefficient, q_{fg} is the flue gas mass flow rate, T_g is the flue gas temperature, q_{at} is the attemperator flow rate, A is the heat transfer area, σ is the Stefan-Boltzmann constant, ϵ is the surface emissivity of the tube walls, η_T is the isentropic efficiency, and $h_{HP}^{is,th}$ is the isentropic enthalpy at the outlet pressure of the turbine for η_T=100%. Superheated steam properties are calculated using the standard formulas given by the International Association for the Properties of Water IAPWS-IF97 using a MATLAB coded file [49].

4.2.2 Spray water attemperators

The dynamics of the attemperators does not significantly affect the performance of the steam generator, therefore the mass and energy balances are assumed at steady state as follows:

$$q_{out} = q_{in} + q_{at} \tag{4.13}$$

$$q_{out}h_{out} = q_{in}h_{in} + q_{at}h_{at} \tag{4.14}$$

4.2.3 Turbine-generator model

HP turbine partially expands superheated steam to one fifth its original pressure. The exiting low pressure steam passes through the reheater and enters a LP turbine where most of the power is being generated.

The system of turbines and generator is modeled as a single lumped system in order to avoid the complications present in generator modeling. A dynamic model of the turbine-generator system can be represented by a first order differential equation as a function of the enthalpy change in the turbine, thus the model of the HP and LP turbines becomes:

$$\tau_i \frac{dE_i}{dt} = q_{in}(h_i(T_i, P_i) - h_i^{ise}(P_{out_i})) - E_i \tag{4.15}$$

where τ_i denotes the time constant for the turbine-generator system, E_i is the power generated, h_i^{ise} is the actual isentropic enthalpy at the outlet pressure of the turbine, P_i is the boiler pressure at the turbine inlet, and P_{out_i} is the pressure at outlet of the turbine. The subscript i is replaced by HP for the high pressure turbine and LP for the low pressure turbine.

4.3 Proposed control structure

4.3.1 Control problem description and strategy

The dynamics of the power plant and the resulting interactions render the control problem a complicated one. A source of complexity is the interconnection of the different parts of the power plant; the dynamics of the superheaters, reheater, and turbines are coupled with the dynamics of the boiler pressure, while the boiler pressure dynamics is coupled with that of the final superheater's outlet temperature, which is also coupled with the dynamics of the power generation. In an open loop simulation, if the turbine steam valve opening increases, the boiler pressure decreases, however, the outlet temperatures of the superheaters initially decrease due to the increase in steam flow and then they increase. This inverse response is due to the lowered heating requirements resulting from the pressure decrease while the fuel flow is kept constant.

Based on standard practice of superheated and reheated steam temperature control, the superheaters and reheater system is decomposed into two subsystems for controller design; the first subsystem constitutes the first, second, and platen superheaters. The outputs of the subsystem are the outlet superheated steam temperatures of the second and platen superheaters and its inputs are the flow rate of the attemperators. The second subsystem is the reheater with the outlet reheated steam temperature as its output and the bypass dampers opening as its input. A third subsystem including the dynamics of the boiler pressure and turbines is also considered. The outputs of this subsystem are the boiler pressure and the power generated by the HP and LP turbines, and the inputs are the turbine valve opening and fuel flow.

The control strategy to be implemented is the decoupling feedback linearization technique with deadtime compensation discussed in Chapter 2. Prior to implementing the discussed control strategy, the complication due to the presence of the inverse response

and the nonlinearity of the manipulated variables should be addressed, along with additional decoupling compensation between the plant's subsystems. The temperature of the superheaters exhibits an inverse response to a change in the turbine valve position. The presence of the inverse response is associated with non-minimum phase behavior (unstable zero dynamics) and therefore precludes the direct application of feedback linearization based controllers. In order to overcome this problem, the following steps are taken:

1. The open-loop dynamics of the superheaters temperatures suggest that if the pressure is well controlled at its set point, increasing the turbine valve opening will cause the superheated steam temperature to decrease and the inverse response will be eliminated. Therefore an efficient independent controller for the boiler pressure is required to ensure that the boiler pressure is controlled. A starting point to control pressure is the use of a deadtime compensated model state feedback linearization controller designed in Chapter 2.

2. Controlling the pressure then allows the temperature observers to be designed according to the new minimum phase temperature dynamics by assuming constant boiler pressure.

Since the boiler pressure depends on the steam flow, which itself depends on the superheated temperature as shown in (4.3), a decoupler that decouples the dynamics of the boiler pressure from the superheater temperature is designed so that the controller in Chapter 2 be applicable. Knowing that the temperature of the final superheater, T_{PSH}, is a measured variable, if the following compensator is applied to the turbine valve position signal produced by the"boiler pressure-power" controller,

$$\alpha = u_s \frac{\sqrt{T_{PSH}}}{\sqrt{T_{PSH}^{sp}}} \tag{4.16}$$

then substituting α instead of u_s in (4.3) gives:

$$q_{in_{SH1}} = \frac{kP}{\sqrt{T_{PSH}^{sp}}} u_s \tag{4.17}$$

resulting in a decoupled dynamics between the boiler pressure and the superheater temperature. T_{PSH}^{sp} is the desired set point of the steam temperature leaving the final superheater. A block diagram of the complete power plant control structure is shown in Figure 4.3.

For the controller design the system to be controlled should be affine in the inputs. However, the models for the superheaters and reheater temperature dynamics are non-affine with respect to the attemperator flow rates and the flue gas flow adding more complexity to the controllers design. Thus, an adjustment is necessary to convert the inputs to affine ones. For the superheaters, the manipulated variables, q_{at_1}, q_{at_2} are modified by the use of the binomial theorem as follows:

$$(q_{in_{SH1}} + q_{at_1} + q_{at_2})^{0.8} = q_{in_{SH1}}^{0.8} + 0.8 q_{in_{SH1}}^{-0.2} (q_{at_1} + q_{at_2}) \tag{4.18}$$

As for the reheater, the temperature is controlled by the amount of flue gas to be bypassed to the reheater, which is achieved by the use of bypass dampers located at the exit of the bypass section; thus the flue gas flow is expressed as:

$$q_{fg-_i}^{0.6} = q_{fg}^{0.6} \gamma_i^{0.6} \tag{4.19}$$

The manipulated variable, γ_i, the fraction of the opening of the damper in the side of the reheater, can then be converted to an affine variable using:

$$\gamma_i^{0.6} = \lambda_i \tag{4.20}$$

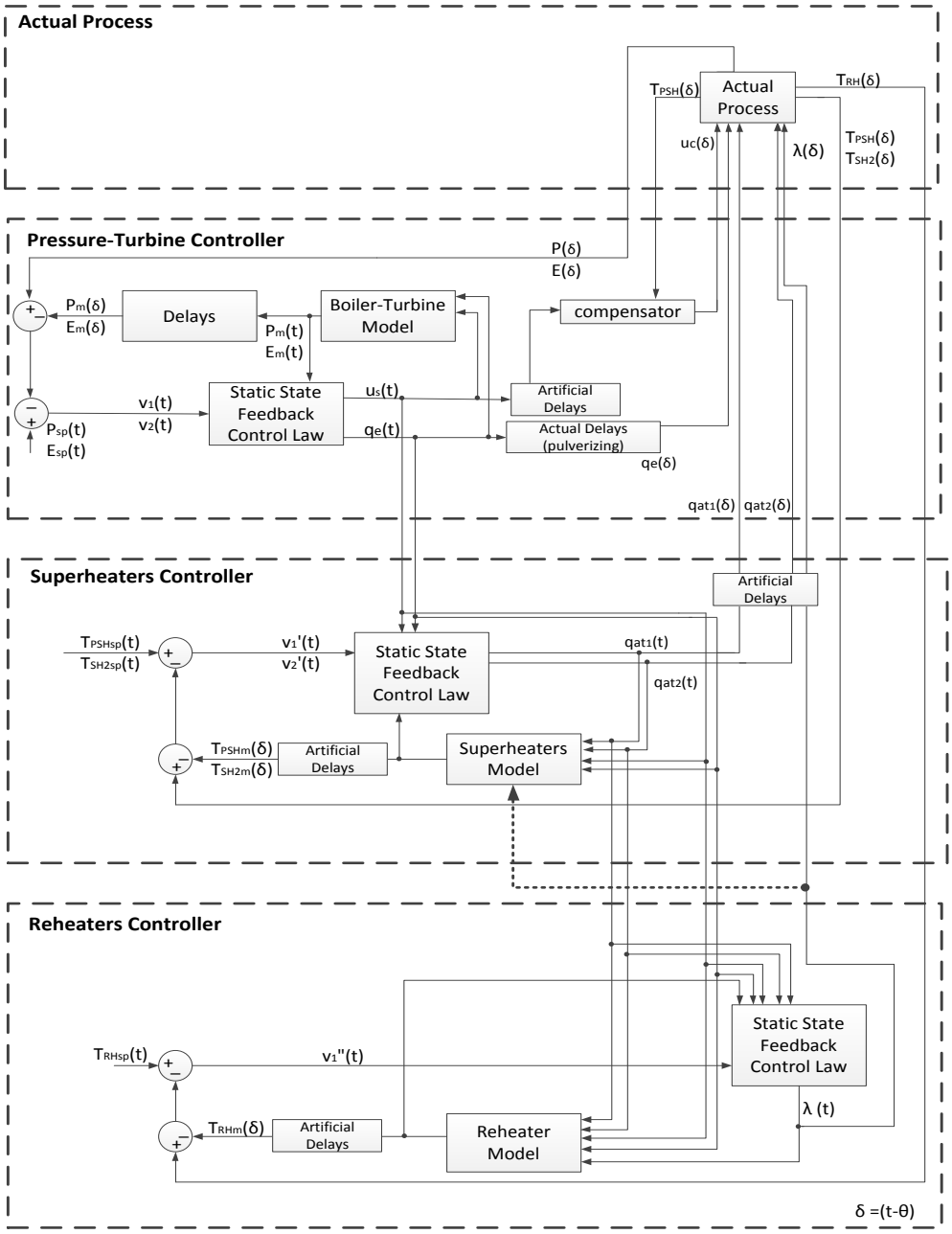

Figure 4.3: Block diagram of the proposed control structure

4.3.2 Controller design

Boiler pressure-power control

The boiler pressure and the turbines are controlled through an independent model state feedback linearization which was designed in Chapter 2. However a slight adjustment must be made to account for the HP and LP turbines individually since they were assumed to be a single lumped system. Referring to the boiler pressure and turbines models in (2.5) and (4.15), there are two manipulated variables, q_e and u_s, three state variables, P, E_{HP}, and E_{LP}, and two outputs, P, $E = E_{HP} + E_{LP}$. The deadtime appears only in the fuel flow rate. The T^{sup} is the nominal value of the superheated steam. The following MIMO nonlinear decoupling controller was designed:

Process Model:

$$\left[V_s\left(\rho_s\frac{\partial h_s}{\partial P_m}\right)+V_{wt}\left(\rho_w\frac{\partial h_w}{\partial P_m}\right)-V_t+m_t c_p\frac{\partial T^{sat}}{\partial P_m}\right]\frac{dP_m}{dt}$$

$$=\frac{kP_m}{\sqrt{T^{sup}}}u_s(h_f-h_s)+\eta_b\Delta H q_e(t-\theta)$$

$$\tau_{HP}\frac{dE_{HP_m}}{dt}=q_{in}(h_{PSH}-h_{RH}^{in})-E_{HP_m}$$

$$\tau_{LP}\frac{dE_{LP_m}}{dt}=q_{in}(h_{RH}-h_{LP}^{ise}(P_{out_{LP}}))-E_{LP_m}$$

$$\mathbf{y_m}=\begin{bmatrix} P_m \\ \\ E_{HP_m}+E_{LP_m} \end{bmatrix}$$

where the subscript m denotes a model state.

Static-state feedback:

- Characteristic matrix:

$$\mathbf{C}(\mathbf{x}) = \begin{bmatrix} \dfrac{\frac{kP_m}{\sqrt{T^{sup}}}(h_f - h_s)}{V_s\left(\rho_s\frac{\partial h_s}{\partial P_m}\right) + V_{wt}\left(\rho_w\frac{\partial h_w}{\partial P_m}\right) - V_t + m_t c_p\frac{\partial T^{sat}}{\partial P_m}\frac{dP_m}{dt}} \\ \dfrac{kP_m}{\tau_{HP}\sqrt{T^{sup}}}(h_{PSH} - h_{RH}^{in}) + \dfrac{k_{RH}P_{out_{HP}-m}}{\tau_{LP}\sqrt{T^{RH}}}(h_{RH} - h_{LP}^{ise}) \\ 0 \end{bmatrix}$$

$$\dfrac{(\eta_b \Delta H)}{V_s\left(\rho_s\frac{\partial h_s}{\partial P_m}\right) + V_{wt}\left(\rho_w\frac{\partial h_w}{\partial P_m}\right) - V_t + m_t c_p\frac{\partial T^{sat}}{\partial P_m}\frac{dP_m}{dt}}$$

- Control law:

$$\mathbf{u} = \mathbf{C}(\mathbf{x})^{-1}\begin{bmatrix} \dfrac{v_1 - P_m}{\beta_{11}} \\ \dfrac{v_2 - E_m - \beta_{21}\left(\dfrac{(h_{PSH} - h_{RH}^{in})(q_{at_1 s} + q_{at_2 s}) - E_{HP_m} + }{\tau_{HP}}\right.}{\beta_{21}} \\ \left.\dfrac{\dfrac{(h_{RH} - h_{LP}^{ise})(q_{at_1 s} + q_{at_2 s}) - E_{LP_m}}{\tau_{LP}}\right)}{\beta_{21}} \end{bmatrix}$$

$q_{at_1 s}, q_{at_2 s}$ are the values of attemperator flows at steady state. The artificial delay of

the steam flow as well as the delay of the model outputs, P_m and E_m, are equal to the deadtime that appears in q_e. Therefore the corrected set points are:

$$v_1(t) = P_{sp}(t) - P(t-\theta) + P_m(t-\theta)$$

$$v_2(t) = E_{sp}(t) - E(t-\theta) + E_m(t-\theta)$$

and the closed-loop system under nominal conditions is fully linearized and has the form:

$$P(t) + \beta_{11}\frac{dP(t)}{dt} = P_{sp}(t-\theta)$$

$$E(t) + \beta_{21}\frac{dE(t)}{dt} = E_{sp}(t-\theta)$$

Choosing the parameters β_{11} and β_{21} to place the poles of the above responses in the left hand side of the complex plane results in a stable closed loop system.

Temperature control

The temperatures to be controlled are the outlet temperatures of the second convection type superheater T_{SH2}, the final radiant type superheater T_{PSH}, and the reheater T_{RH}, the corresponding manipulated variables are the flow rate of the attemperators, q_{at_1}, q_{at_2}, and the opening of the damper, γ_{RH} respectively. The temperatures are controlled by nonlinear decoupling controller designed by the model state feedback procedure described earlier. A 2 x 2 controller for the control of the superheaters outlet temperature, and a separate controller for the control of the reheater outlet temperature are used. To synchronize all manipulated variables applied to the power plant, the signals of the flow rate of the attemperators and the opening of the dampers were artificially delayed by θ. Consequently, the predicted model outputs of the temperatures were also artificially delayed by θ to eliminate deadtime form the feedback loop when

there are no modeling errors [5, 41].

Control design for superheaters outlet temperatures

Referring to the superheaters models (4.1-4.9), there are two manipulated variables, the attemperator flows, q_{at_1} and q_{at_2}, six state variables, $T_{w_{SH1}}$, h_{SH1}, $T_{w_{SH2}}$,h_{SH2}, $T_{w_{PSH}}$,h_{PSH}, and two outputs, T_{SH2}, T_{PSH}. In addition, the values of u_s, and q_e are cascaded from the boiler pressure-turbine controller. To account for interactions with the reheater controller, the control actions of the bypass dampers opening are utilized in the model of the superheaters. The following MIMO nonlinear controller is designed:

Process Model:

$$\frac{dT^m_{w_{SH1}}}{dt} = \frac{\bar{h}^{SH1}_w q^{0.6}_{fg_{-SH1}}(1-\gamma_{RH})^{0.6}(T_{g_{SH1}} - T^m_{w_{SH1}}) - \bar{h}^{SH1} q^{0.8}_{in_{SH1}}(T^m_{w_{SH1}} - T_{SH1})}{\rho_{w_{SH1}} V_{w_{SH1}} c_{p_{w_{SH1}}}}$$

$$\frac{dh^m_{SH1}}{dt} = \frac{\bar{h}^{SH1} q^{0.8}_{in_{SH1}}(T^m_{w_{SH1}} - T^m_{SH1}) - q_{in_{SH1}}(h^m_{SH1} - h^{in_m}_{SH1})}{\rho_{SH1} V_{SH1}}$$

$$\frac{dT^m_{w_{SH2}}}{dt} = \frac{\bar{h}^{SH2}_w q^{0.6}_{fg_{-SH2}}(1-\gamma_{RH})^{0.6}(T_{g_{SH2}} - T^m_{w_{SH2}}) - \bar{h}^{SH2}(q_{in_{SH1}} + q_{at_1})^{0.8}(T^m_{w_{SH2}} - T^m_{SH2})}{\rho_{w_{SH2}} V_{w_{SH2}} c_{p_{w_{SH2}}}}$$

$$\frac{dh^m_{SH2}}{dt} = \frac{\bar{h}^{SH2}(q_{in_{SH1}} + q_{at_1})^{0.8}(T^m_{w_{SH2}} - T^m_{SH2}) - (q_{in_{SH1}} + q_{at_1})(h^m_{SH2} - h^{in_m}_{SH2})}{\rho_{SH2} V_{SH2}}$$

$$\frac{dT^m_{w_{PSH}}}{dt} = \frac{A\sigma\epsilon(T^4_{g_PSH} - T^{4m}_{w_PSH}) - \bar{h}^{PSH}(q_{in_{SH1}} + q_{at_1} + q_{at_2})^{0.8}(T^m_{w_{PSH}} - T^m_{PSH})}{\rho_{w_{PSH}} V_{w_{PSH}} c_{p_{w_{PSH}}}}$$

$$\frac{dh^m_{PSH}}{dt} = \frac{\bar{h}^{PSH}(q_{in_{SH1}} + q_{at_1} + q_{at_2})^{0.8}(T^m_{w_{PSH}} - T^m_{PSH}) - (q_{in_{SH1}} + q_{at_1} + q_{at_2})(h^m_{PSH} - h^{in_m}_{PSH})}{\rho_{PSH} V_{PSH}}$$

$$\mathbf{y_m} = \begin{bmatrix} T^m_{SH2} \\ \\ T^m_{PSH} \end{bmatrix}$$

where the subscript m denotes a model state.

Static-state feedback:

- Characteristic matrix:

$$\mathbf{C}(\mathbf{x}) = \begin{bmatrix} \frac{0.8\bar{h}^{SH2} q^{-0.2}_{in_{SH1}}(T^m_{w_{SH2}} - T^m_{SH2}) - (h^m_{SH2} - h^{at}_{SH2})}{\rho_{SH2} V_{SH2}} & 0 \\ \\ \frac{0.8\bar{h}^{PSH} q^{-0.2}_{in_{SH1}}(T^m_{w_{PSH}} - T^m_{PSH}) - (h^m_{PSH} - h^{at}_{PSH})}{\rho_{PSH} V_{PSH}} & \frac{0.8\bar{h}^{PSH} q^{-0.2}_{in_{SH1}}(T^m_{w_{PSH}} - T^m_{PSH}) - (h^m_{PSH} - h^{at}_{PSH})}{\rho_{PSH} V_{PSH}} \end{bmatrix}$$

where h_i^{at} is the enthalpy of the feedwater.

- Control law:

$$\mathbf{u} = \mathbf{C}(\mathbf{x})^{-1} \begin{bmatrix} \dfrac{v_1' - h_{SH2} - \frac{\sigma_{11}}{\rho_{SH2} V_{SH2}} \left(\bar{h}^{SH2} q_{in_{SH1}}^{0.8} (T_{w_{SH2}}^m - T_{SH2}^m) - q_{in_{SH1}} (h_{SH2}^m - h_{SH1}^m) \right)}{\sigma_{11}} \\ \dfrac{v_2' - h_{PSH} - \frac{\sigma_{21}}{\rho_{PSH} V_{PSH}} \left(\bar{h}^{PSH} q_{in_{SH1}}^{0.8} (T_{w_{PSH}}^m - T_{PSH}^m) - q_{in_{SH1}} (h_{PSH}^m - h_{SH2}^m) \right)}{\sigma_{21}} \end{bmatrix}$$

- The corrected set points are:

$$v_1'(t) = h_{SH2}^{sp}(t) - h_{SH2}(t) + h_{SH2}^m(t)$$

$$v_2'(t) = h_{PSH}^{sp}(t) - h_{PSH}(t) + h_{PSH}^m(t))$$

Control design for reheater outlet temperature

Referring to the reheater models (4.10-4.12), there is one manipulated variable, the opening of the damper, γ_{RH}, two state variables, $T_{w_{RH}}$, h_{RH}, and one output, T_{RH}. The values of u_s, and q_e are cascaded from the boiler pressure-turbine controller, and the values of q_{at_1} and q_{at_2} are cascaded from the superheaters controller. The following MIMO nonlinear controller is designed:

Process Model:

$$\frac{dT^m_{wRH}}{dt} = \frac{\bar{h}^{RH}_w q^{0.6}_{fg_{-RH}} \lambda_{RH}(T_{gRH} - T^m_{wRH}) - \bar{h}^{RH}(q_{in_{SH1}} + q_{at_1} + q_{at_2})^{0.8}(T^m_{wRH} - T^m_{RH})}{\rho_{w_{RH}} V_{w_{RH}} c_{p_{w_{RH}}}}$$

$$\frac{dh^m_{RH}}{dt} = \frac{\bar{h}^{RH}(q_{in_{SH1}} + q_{at_1} + q_{at_2})^{0.8}(T^m_{wRH} - T^m_{RH}) - (q_{in_{SH1}} + q_{at_1} + q_{at_2})(h^m_{RH} - h^{in_m}_{RH})}{\rho_{RH} V_{RH}}$$

$$y_m = T^m_{RH}$$

Static-state feedback:

- Control law:

$$\lambda = \frac{v'' - h_{RH} - \left(\frac{\sigma_{31}}{\rho_{RH} V_{RH}} \bar{h}^{RH}(q_{in_{SH1}} + q_{at_1} + q_{at_2})^{0.8}(T^m_{wRH} - T^m_{RH}) \right.}{\sigma_{32} m_1}$$

$$\left. \frac{-(q_{in_{SH1}} + q_{at_1} + q_{at_2})(h^m_{RH} - h^{in_m}_{RH})\right)}{\sigma_{32} m_1} + \frac{1}{\sigma_{32}} \frac{\sigma_{32} m_0}{m_1}$$

where

$$m_0 = \frac{\bar{h}^{RH}(q_{in_{SH1}} + q_{at_1} + q_{at_2})^{0.8}}{\rho_{RH} V_{RH}} \left(\frac{-\bar{h}^{RH}(q_{in_{SH1}} + q_{at_1} + q_{at_2})^{0.8}(T^m_{wRH} - T^m_{RH})}{\rho_{w_{RH}} V_{w_{RH}} c_{p_{w_{RH}}}} \right) +$$

$$\left(\frac{\frac{\bar{h}^{RH}}{2}(q_{in_{SH1}} + q_{at_1} + q_{at_2})^{0.8} \frac{dT_{RH}}{dh_{RH}} - (q_{in_{SH1}} + q_{at_1} + q_{at_2})^{0.8}}{\rho_{RH} V_{RH}} \right.$$

$$+\frac{1}{2V_{RH}}\frac{dV_{RH}}{dh_{RH}}\left(\bar{h}^{RH}(q_{in_{SH1}}+q_{at_1}+q_{at_2})^{0.8}(T^m_{w_{RH}}-T^m_{RH})-(q_{in_{SH1}}+q_{at_1}+q_{at_2})(h^m_{RH}-h^{in_m}_{RH})\right)\left(\frac{\bar{h}^{RH}(q_{in_{SH1}}+q_{at_1}+q_{at_2})^{0.8}(T^m_{w_{RH}}-T^m_{RH})-(q_{in_{SH1}}+q_{at_1}+q_{at_2})(h^m_{RH}-h^{in_m}_{RH})}{\rho_{RH}V_{RH}}\right)$$

$$m_1=\frac{\bar{h}^{RH}(q_{in_{SH1}}+q_{at_1}+q_{at_2})^{0.8}}{\rho_{RH}V_{RH}}\left(\frac{\bar{h}^{RH}_w q^{0.6}_{fg_{-RH}}(T_{g_{RH}}-T^m_{w_{RH}})}{\rho_{w_{RH}}V_{w_{RH}}c_{p_{w_{RH}}}}\right)$$

- The corrected set points are:

$$v_1''(t)=h^{sp}_{RH}(t)-h_{RH}(t)+h^m_{RH}(t)$$

4.4 Controller testing

The performance of the controller is investigated for different scenarios of set point tracking of power demand and disturbance rejection. The tests conducted for set point tracking are:

- A ramp down of power set point from 160 MW to 115 MW at a rate of 2% per minute.
- ± 32MW (20% of the Maximum Continuous Rate) step changes in power set point at 25 minute intervals with simultaneous random fluctuations in deadtime associated with the fuel flow.

For disturbance rejection, the following tests are conducted:

- 3% decrease in the heating value of the fuel.
- 18% decrease in the value of the steam heat transfer coefficient of the second superheater.

Table 4.1: Controller tuning parameters, artificial deadtime, and set points

β_{11}	530	P_{sp}	13.713 MPa
β_{21}	210	T^{sp}_{SH2}	718 K
σ_{11}	1	T^{sp}_{PSH}	808 K
σ_{21}	1	T^{sp}_{RH}	808 K
σ_{31}	80	σ_{32}	70
θ	90 s		

- 14% decrease in the value of the steam heat transfer coefficient of the reheater.

The tuning parameters are kept the same for all tests and are summarized in Table 4.1 along with the set points of boiler pressure, secondary superheater outlet temperature, platen superheater outlet temperature, reheater outlet temperature, and the artificial deadtime.

4.5 Simulation results

4.5.1 Setpoint tracking

The results of the 2% per minute ramping down of power set point are shown in Figures 4.4-4.7. The boiler pressure (Figure 4.4) is unaffected by the change of the power set point. The power generation (Figure 4.5) tracks smoothly the postulated trajectory of the power set point however delayed by the artificial θ seconds applied to the manipulated variables signal. Figure 4.6 illustrates the response of the temperature controllers. Due to the change in power set point, the fuel flow rate and turbine valve opening will change resulting in disturbances in the temperatures of the superheaters and reheater. The temperature controllers regulate the flow rate of the attemperators and the bypass dampers opening, resulting in the superheaters and reheater temperatures kept well within the desired range of $\pm$ 6 ^oC. Figure 4.7 illustrates the response of the

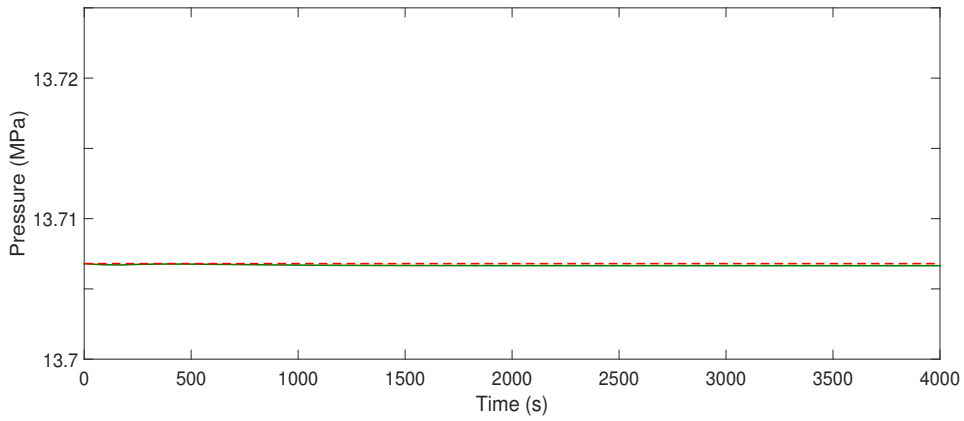

Figure 4.4: Response of boiler pressure to a -2%/min ramp of power setpoint.

attemperator flow rates and bypass dampers opening. These results show the enforced decoupling between boiler pressure and power generation and the successful set point tracking performance despite the disturbance in the temperatures of the superheated steam. Thus they show the applicability of using an independent decoupling controller integrated with the decoupling compensator for the boiler and turbines. The controllers are tuned to give a fast and stable response with no oscillations. The dashed line in the figures indicates the value of the set points.

The robustness of the controllers is then tested by a worst case scenario performance test. Large step changes of ± 32MW in power set point at 25 minute intervals are applied with simultaneous fluctuations in deadtime associated with the fuel flow at the range of 80-120 seconds. A similar test is performed in a power plant in UK to test new controllers before real-time implementation [17]. The response of the controllers as shown in Figures 4.8-4.10 reflects their ability to track the power set point in the presence of deadtime uncertainty. The pressure and temperatures responses show that the fluctuation in deadtime causes a small disturbance that propagates as the error in deadtime increases. The applied random fluctuations are shown in Figure 4.11.

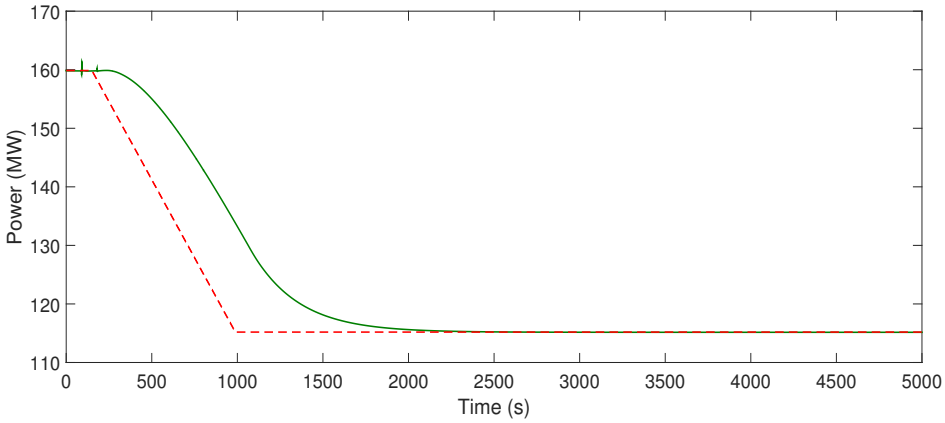

Figure 4.5: Response of power generation to a -2%/min ramp of power setpoint.

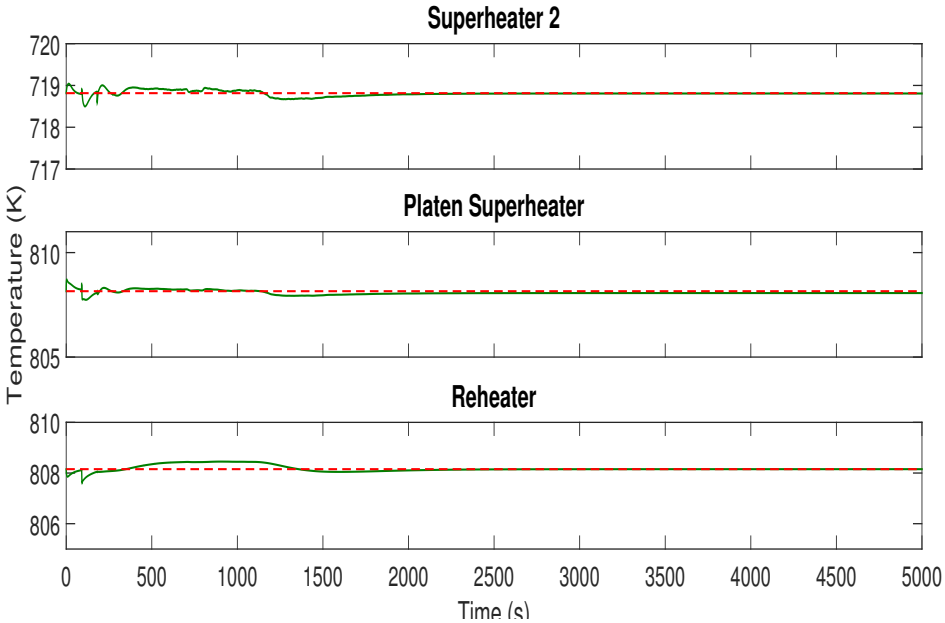

Figure 4.6: Response of outlet superheaters and reheater temperatures to a -2%/min ramp of power setpoint.

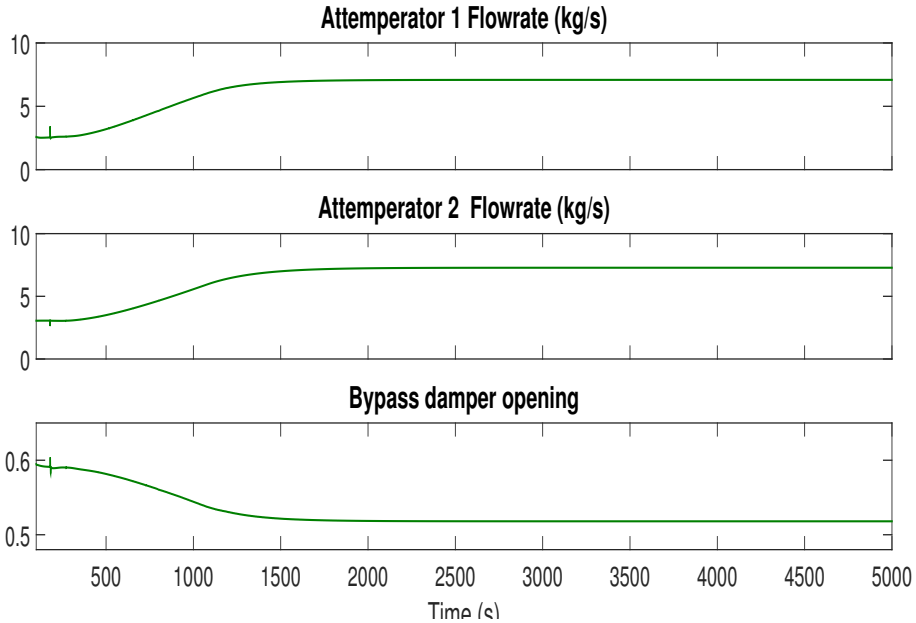

Figure 4.7: Control actions of attemperator flow rates and bypass damper opening to a -2%/min ramp of power setpoint.

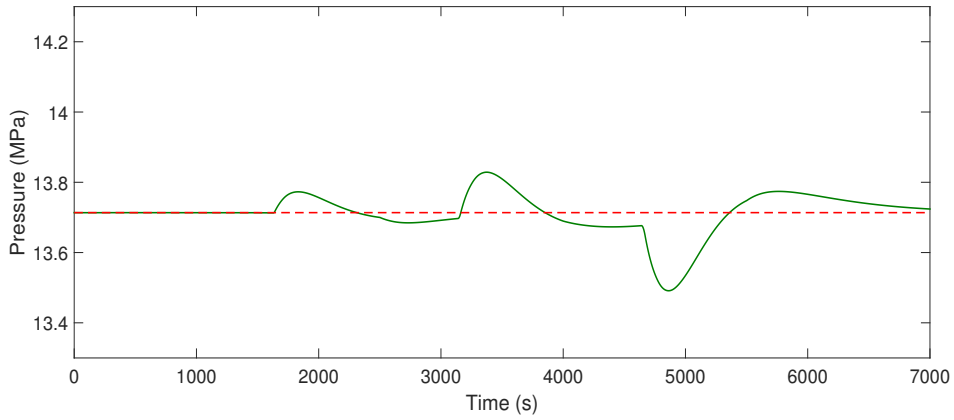

Figure 4.8: Response of boiler pressure to a multi step changes in power setpoint and fluctuations in deadtime associated with the fuel flow rate.

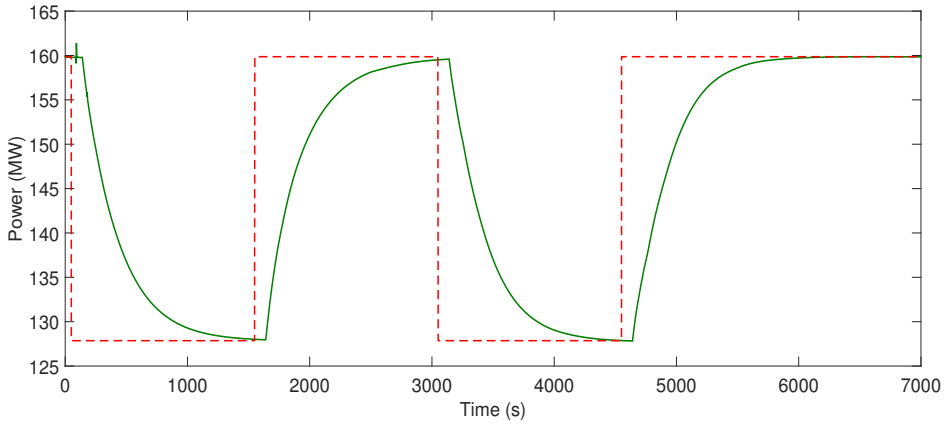

Figure 4.9: Response of power generation to a multi step changes in power setpoint and fluctuations in deadtime associated with the fuel flow rate.

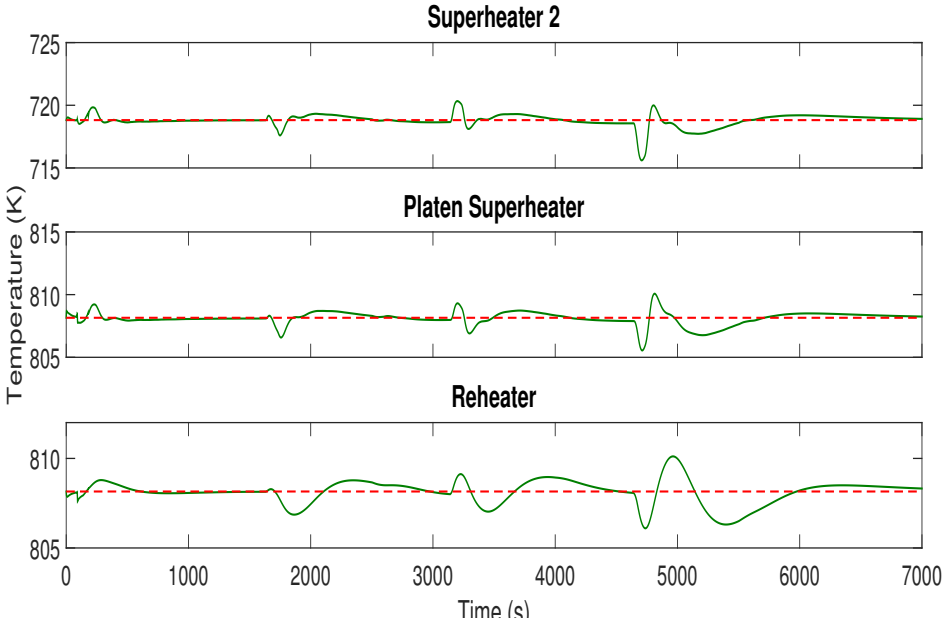

Figure 4.10: Response of the outlet superheaters and reheater temperatures to a multi step changes in power setpoint and fluctuations in deadtime associated with the fuel flow rate.

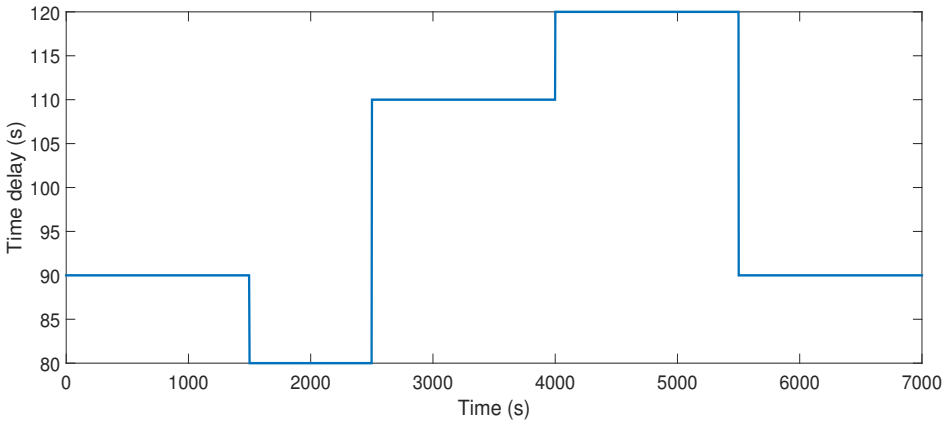

Figure 4.11: Applied random deadtime to the fuel flow rate.

4.5.2 Disturbance rejection

The disturbance rejection capability of the controllers is tested for an unmeasured 3% decrease in the heating value of the fuel. Figures 4.12-4.13 illustrate the performance of the boiler pressure and turbine controller. Both figures reflect a smooth and zero offset rejection indicating the ability of accommodating problems of unsteady heating value of coal, or using another type of solid fuel. Figure 4.14 illustrates the responses of the compensated turbine valve opening and the fuel flow. The valve opening initially increases admitting more steam to the turbine to reject the decrease in power generation, then it decreases as the fuel flow increases to restore the boiler pressure. The performance of the temperature controllers is shown in Figure 4.15. Both controllers reject the effect of the disturbances on the superheated and reheated steam and is maintained within $\pm$ 6 ^oC in less than 500 seconds. The blue dash-dot line shows the predicted temperature profile using the model observer. The profile shows the absence of an inverse response for the disturbance in the boiler pressure, which validates the assumption made of constant boiler pressure in designing the temperature controllers. Figure 4.16 illustrates the response of the attemperator flow rates and bypass dampers opening.

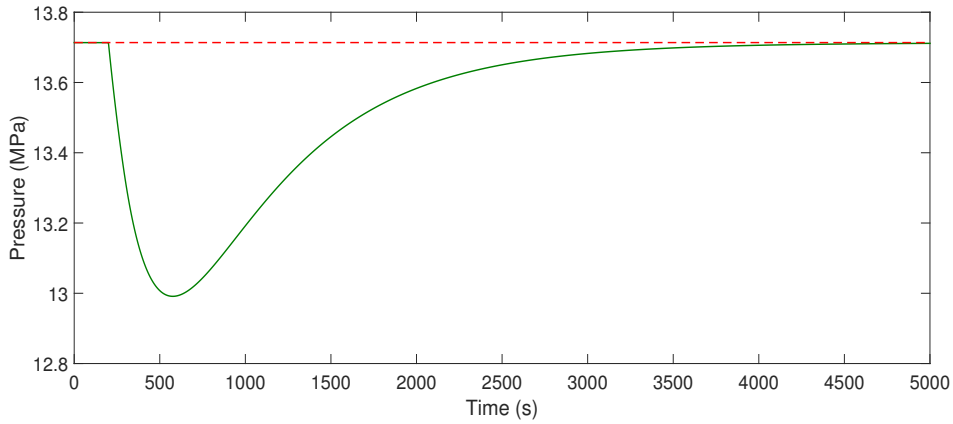

Figure 4.12: Response of boiler pressure to a -3% disturbance in boiler efficiency.

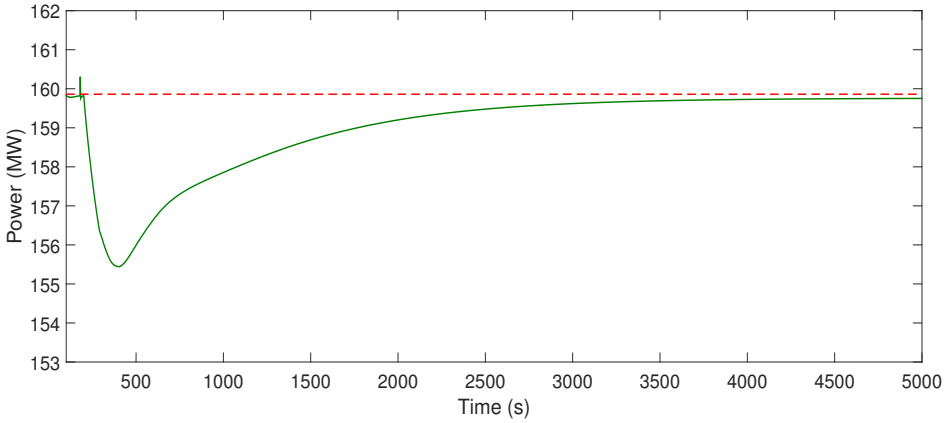

Figure 4.13: Response of power generation to a -3% disturbance in boiler efficiency.

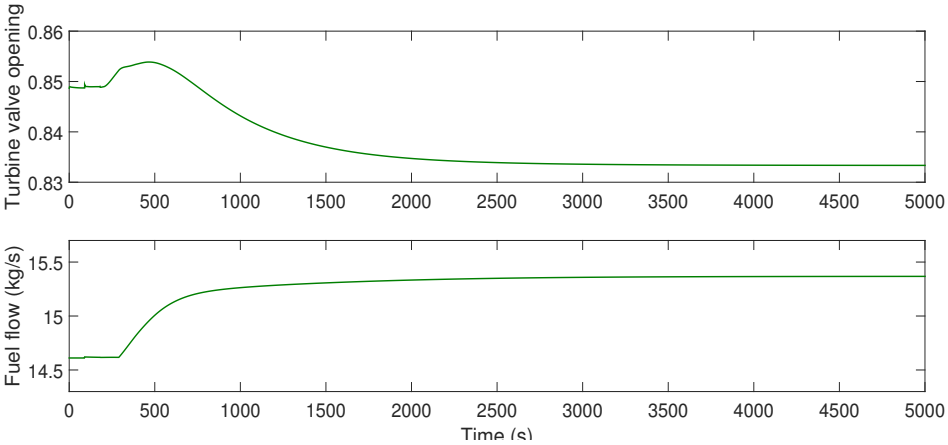

Figure 4.14: Control actions of turbine valve opening and fuel flow rate to a -3% disturbance in boiler efficiency.

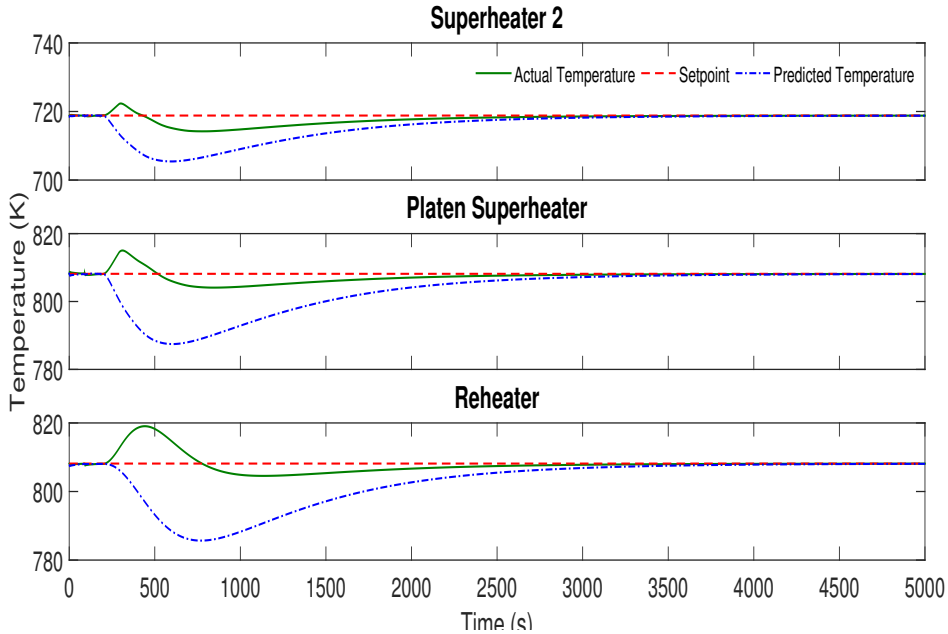

Figure 4.15: Response of outlet superheaters and reheater temperatures to a -3% disturbance in boiler efficiency.

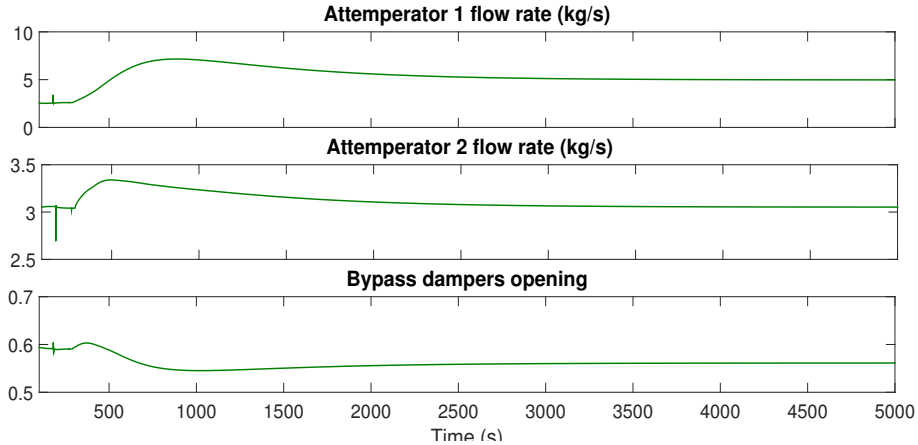

Figure 4.16: Control actions of attemperator flow rates and bypass dampers opening to a -3% disturbance in boiler efficiency.

To assess the performance of the temperature controllers in the presence of modeling errors, a change in the heat transfer coefficient of the steam for the second superheater is applied. Figure 4.17 shows the superheated temperature profiles. The change is implemented at t=250 s. The results show that the mismatch between the heat transfer coefficients did not affect the performance of the controller and the resulted disturbance was rejected. The responses of the attemperator flow rates and bypass dampers opening are shown in Figure 4.18. Figures 4.19 and 4.20 show the boiler pressure and power generation responses. Since power generation depends mainly on the pressure and enthalpy of the superheated steam, a decrease in the steam heat transfer coefficient results in a decrease in the power generation.

The effect of changing the steam heat transfer coefficient in the reheater is similar to that of changing it in the second superheater; the mismatch between the heat transfer coefficients did not affect the performance of the controllers and the resulted disturbances are rejected. The temperature responses and that of the attemperator flow rates and bypass dampers opening are shown in Figures 4.21-4.22. To overcome the decrease in the reheated steam temperature the bypass dampers opening increased to allow more

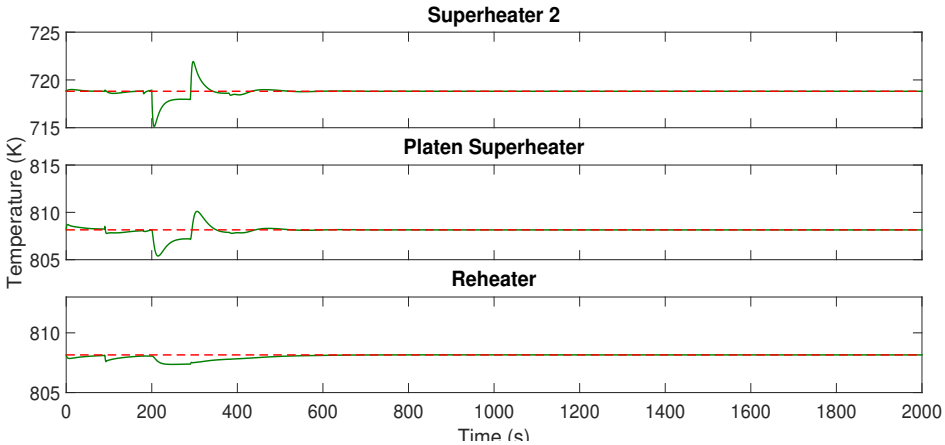

Figure 4.17: Response of outlet superheaters and reheater temperatures to a -18% disturbance in steam heat transfer coefficient of secondary superheater.

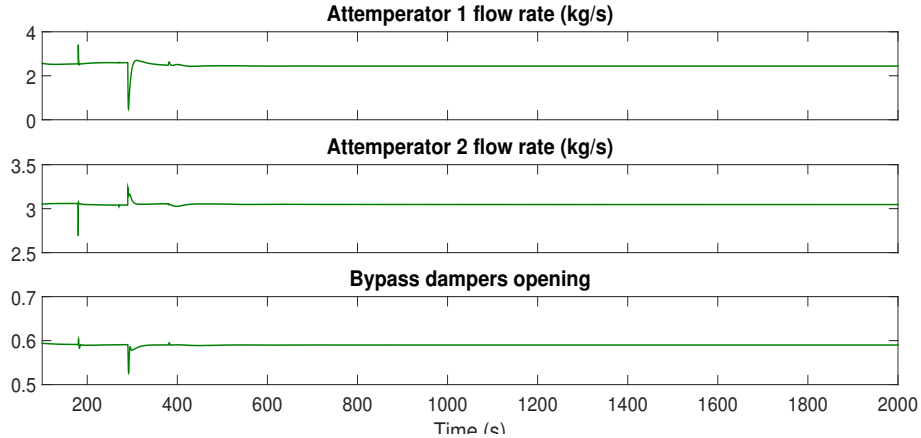

Figure 4.18: Control actions of attemperator flow rates and bypass dampers opening to a -18% disturbance in steam heat transfer coefficient of secondary superheater.

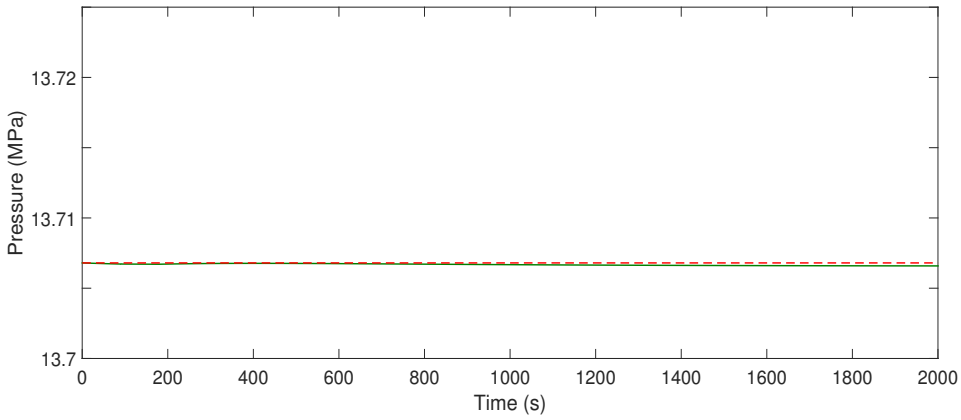

Figure 4.19: Response of boiler pressure to a -18% disturbance in steam heat transfer coefficient of secondary superheater.

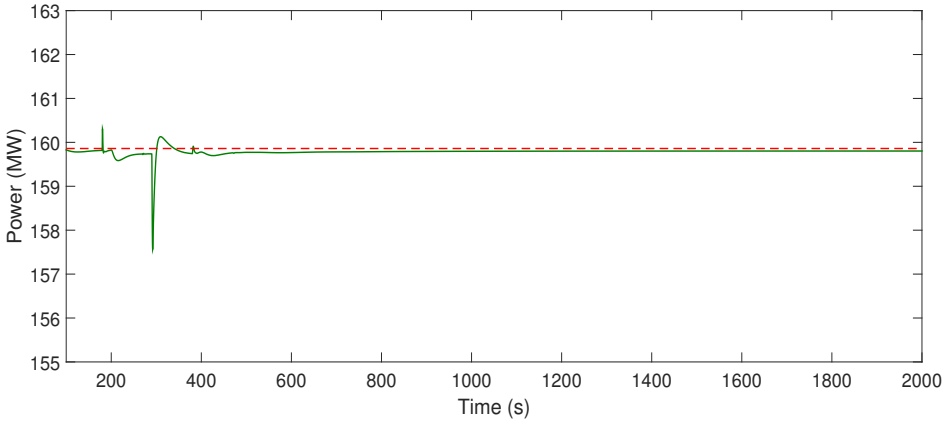

Figure 4.20: Response of power generation to a -18% disturbance in steam heat transfer coefficient of secondary superheater.

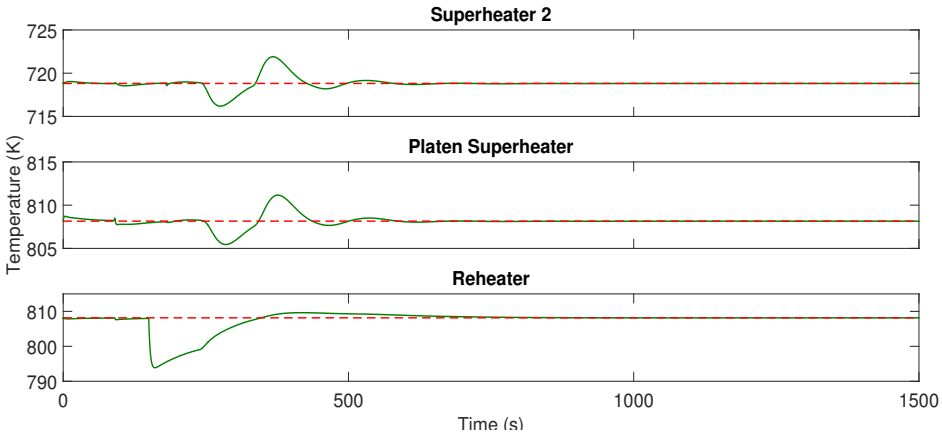

Figure 4.21: Response of the outlet superheaters and reheater temperatures to a -14% disturbance in steam heat transfer coefficient of reheater.

flue gas to pass to the reheater. As a result, the flow rate of attemperator 1 decreased to reject the decrease in the superheated steam temperature caused by the decrease in the flue gas flow rate passing it. The response of the power generation is shown in Figure 4.23. The effect on the power generation is more significant in this case compared to the previous case. This is because as discussed previously, most of the power generation is due to the LP turbine which receives the reheated steam. The boiler pressure response is shown in Figure 4.24.

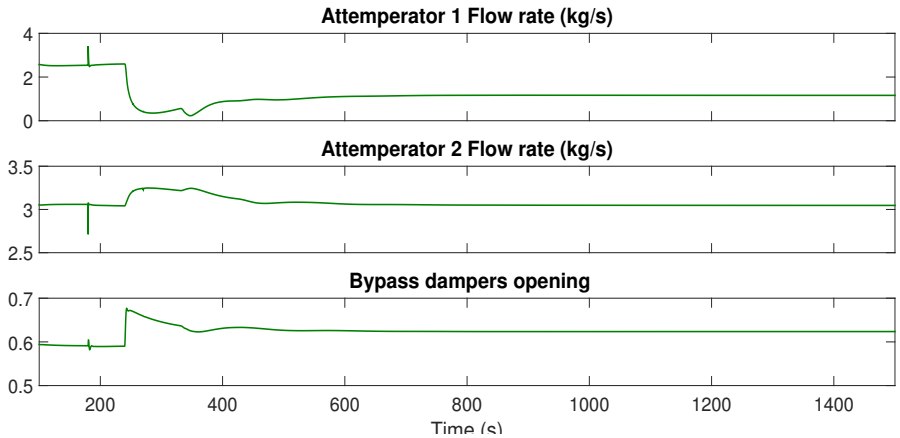

Figure 4.22: Control actions of attemperator flow rates and bypass dampers opening to a to a -14% disturbance in steam heat transfer coefficient of reheater.

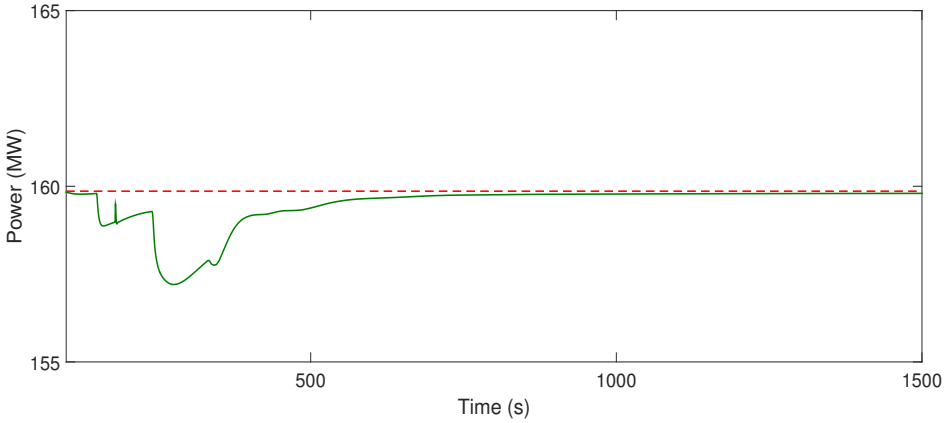

Figure 4.23: Response of power generation to a -14% disturbance in steam heat transfer coefficient of reheater.

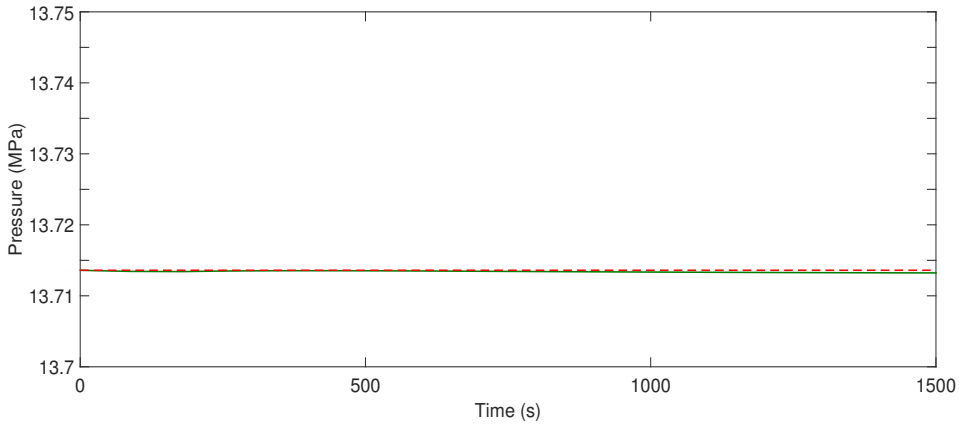

Figure 4.24: Response of boiler pressure to a -14% disturbance in steam heat transfer coefficient of reheater.

4.6 Conclusions

This chapter has developed a practically implementable nonlinear control strategy for control of power plants subject to frequent changes in operating conditions. The proposed strategy decomposes the overall plant into three subsystems, minimizes the interactions between them, and implements nonlinear decoupling with deadtime compensation for each of them. Effective control of power generated, boiler pressure, and superheater and reheater temperatures is documented for several realistic set point and disturbance rejection scenarios, including unknown deadtimes and other modeling errors.

Chapter 5

Summary and future research

5.1 Thesis summary

Although power generation from fossil fuels has been common practice for many decades, the operation of power generation continuous to face new challenges. One of these challenges is the integration of power generated from renewable sources into the electric grid. Due to the intermittency of renewable sources, the power demanded from conventional power plants is expected to change frequently. Thus fossil fueled power plants will be required to accommodate a wide range operation of power production. This imposes strong limitations on the performance of existing linear control methods applied in power plants. Motivated by this, a nonlinear control strategy based on feedback linearization for controlling coal-fired conventional steam power plants was developed. The control design focused on the ability of the controller to mitigate the strong nonlinear interactions between the different units of the power plant, and on the ability to generate power under wide variations in power set point and under various types of disturbances.

Due to the complexity of the power plants dynamics, the control structure was built

on different stages, each stage considering a different control aspect of the power plant. In the first part of the thesis, the boiler-turbine system was considered for the regulation of the boiler pressure and set point tracking of power generation. The manipulated variables were the steam turbine valve opening and the fuel flow rate, with a deadtime associated with the fuel flow rate taking into account upstream handling and pulverizing of coal.

The application of a deadtime compensated model state feedback structure based on feedback linearization resulted in complete decoupling of the boiler pressure and power generated. The advantage of the complete decoupling is mainly the elimination of fluctuating thermal stresses in the boiler which maintains the lifetime of the boiler, and production of steam at constant pressure which improves the stability of power generation. Different scenarios were tested to cover narrow and wide range power set point tracking, and disturbance rejection. The results showed a stable and efficient operation under narrow and wide range changes in power demand. In addition, sensitivity analysis results showed robustness of the power plant performance utilizing the applied controller.

Water level inside the boiler drum is a critical factor that determines the safety of the boiler and the quality of steam traveling to the steam turbine. In the second part of the thesis, the control of the drum level was taken into consideration in addition to the boiler pressure and power generation. The level dynamics were included in the model by accounting for the volume of steam under the water level, the volume of water inside the drum, and the quality of steam leaving the risers. The manipulated variable used for controlling the drum level was the feedwater flow rate. A three-element conventional PI level controller was used together with the model state feedback controller designed in the first part. The power plant performance was then tested for wide range power set point tracking, disturbance rejection, and deadtime uncertainty. The results showed

that using the nonlinear controller along with the conventional level controller resulted in a different control path for the drum level than for the case using linear controllers and an efficient regulation of the drum level is illustrated for each case studied. The results also showed that changes in the feedwater flow rate did not have an apparent effect on the power set point tracking capability of the nonlinear controller.

In the last part of the thesis, the control of superheated steam was considered along with the control of the boiler pressure and power generation. The proposed control structure decomposed the overall plant into three subsystems, namely the boiler-turbine subsystem, the superheaters subsystem, and the reheater subsystem. The decomposition made minimized the interactions between the different subsystems and allowed the implementation of a nonlinear decoupling control with deadtime compensation for each of them. In the first subsystem, the controlled variables were the boiler pressure and power generation, and the manipulated variables were the steam turbine valve opening and fuel flow rate. In the second subsystem the controlled variables were the outlet steam temperatures from the second and radiant superheaters, and the manipulated variables were the first and second attemperators flow rate. In the third subsystem, the controlled variable was the reheater outlet steam temperature, and the manipulated variable was the opening of the bypass dampers. The performance of the control structure was tested for its capability of tracking power set point while regulating the rest of the controlled variables. Effective control of power generated, boiler pressure, and superheater and reheater temperatures was documented.

5.2 Future research directions

In the power plant models utilized in this thesis the power generated is assumed to be the same as the mechanical power generated by the steam turbines. However, an actual

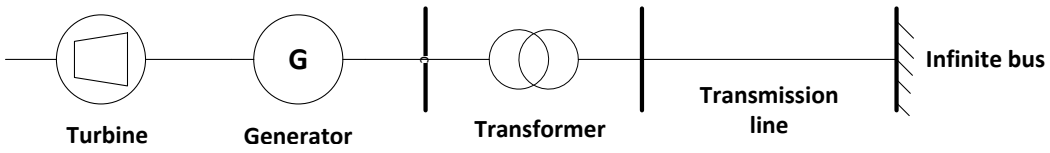

Figure 5.1: A single machine infinite bus power system. *Reproduced from [64] with a slight modification.*

steam turbine-generator system transforms mechanical power generated in the turbine into electrical power. The shaft rotating in the turbine extends to the generator. The shaft in the generator, called generator rotor, rotates a set of magnetic poles inside a stator winding producing electric current. To generate power, the electrical power demand is first expressed in the form of a rotor angle, which is the angle between the magnetic fields of the rotor and stator in the generator. The rotor angle is then translated into an additional (or a lower) torque that steam is required to apply to the turbine shaft. According to the required torque, the turbine valve opening will be adjusted. Having the shaft of the turbine rotate at a constant speed, the change in torque changes the mechanical power, hence the electrical power is changed. Since the turbine and generator operate on the same shaft, there are strong interactions between the dynamics of the generator and that of the turbine [63].

Control studies considering the boiler-turbine-generator system are scarce due to the complexity of the turbine-generator dynamics, however they are essential [30]. The turbine model used throughout the thesis can be extended to account for the generation of electric power. The advantage of this model extension is to have a model that represents the actual desired output, thus interactions of the different parts of the power plant with the actual output can be studied.

The second advantage is the ability to extend the studies to systems beyond the power plant. The modeling of the generator serves as a connection between the power

plant and the grid. The electric power produced by the generator is transferred to the grid through a transformer followed by transmission lines. A single turbine-generator-transformer-grid power system as illustrated in Figure 5.1 is called a single machine infinite bus (SMIB). When the generator is connected to the grid, transient stability of the power system becomes a concern and thus appropriate control strategies are required. Another direction for research is to integrate the dynamics of the power plant to that of the power system and design a nonlinear control structure that can provide a stable transient phase when connecting the generator to the power system. The current researches on this subject are limited to an empirical model of the boiler pressure and neglected superheated steam temperature dynamics [30, 34].

Bibliography

[1] *International Energy Outlook 2013 report*, U.S. Energy Information Administration, 2013.

[2] *International Energy Outlook 2015 report*, U.S. Energy Information Administration, 2015.

[3] E. B. Woodruff, H. B. Lammers, T. F. Lammers, *Steam power operation*, 9th Ed., 2012.

[4] X. Wu, J. Shen, Y. Li, K. Lee, "Fuzzy modeling and stable model predictive tracking control of large-scale power plants", *Journal of Process Control*, vol. 24, pp.1609-1626, 2014.

[5] N. Alamoodi, P. Daoutidis, "Nonlinear Decoupling Control with Deadtime Compensation for Multi-Range Operation of Steam Power Plants", *IEEE Trans. Control System Technology*, vol. 24, No. 1, pp.341-348, 2016.

[6] L. Drbal, P. Boston, K. Westra, R. Erickson, "Power plant engineering by black and veatch", Chapman and Hall, 1996.

[7] P. Chattopadhyay, *Boiler operation engineering: questions and answers*, 3rd Ed., 2013.

[8] A. Penninger, L. Karpati, "Effect of power plant steam boilers' control system on the stability of the fuelling", *Periodica polytechnica ser. mech. eng*, vol. 40, No. 5, pp.69-76, 1995.

[9] D. Kalix, "Steam drum water level measurement", Fossil Power Systems Inc, 2011.

[10] G. Hahn, "Boiler efficiency and steam quality: The challenge of creating quality steam using existing boiler efficiencies", *National Board Classic Series*, 1998.

[11] M. Xu, S. Li, W. Cai, "Cascade generalized predictive control strategy for boiler drum level", *ISA Transactions*, vol. 44, pp.399-411, 2005.

[12] H. Liu, S. Li, T. C, "Intelligent decoupling control of power plant main steam pressure and power output", *Int. J. Elec. Power*, vol. 25, pp.809-819, 2003.

[13] S. Li, H. Lui, W. Cai, Y. Soh, L. Xie, "A New Coordinated Control Strategy for Boiler-Turbine System of Coal-Fired Power Plant", *Int. J. Elec. Power*, vol. 25, pp.809-819, 2003.

[14] J. M. Blaazer, "Advanced process control for power plants: Improving overall performance through control of internal process variables", M.S. thesis, 3mE, TUDelft, Netherlands, 2010.

[15] G. Lausterer, "Improved maneuverability of power plants for better grid stability", *Control Eng. Pract.*, vol. 6, pp. 1549-1557, 1998.

[16] X. Liu, P. Guan, C. Chan, "Nonlinear Multivariable Power Plant Coordinated Control by Constrained Predictive Scheme", *IEEE Trans. Control System Technology*, vol. 18, pp. 1116-1125, 2010.

[17] G. Prasad, G. Irwin, E. Swidenbank, B. Hogg, "Plant-wide predictive control for a thermal power plant based on a physical plant model" *IEE Proc-Control Theory Appl.*, vol. 147, 2000.

[18] X. Liu, X. Kong, "Nonlinear fuzzy model predictive iterative learning control for drum-type boilerturbine system", *Journal of Process Control* , vol. 23, pp. 1023-1040, 2013.

[19] X. Wu, J. Shen, Y. Li, K. Lee, "Fuzzy modeling and predictive control of superheater steam temperature for power plant", *ISA Transactions* , vol. 56, pp. 241-251, 2015.

[20] H. Peng, T. Ozaki, V. H. Ozaki, Y. Toyoda, "A nonlinear exponential ARX model-based multivariable generalized predictive control strategy for thermal power plants", *IEEE Trans. Control System Technology*, vol. 10, No. 2, 2002.

[21] J. Hlava, J. Opalka, "Model predictive control of power plant superheater comparison of multi model and nonlinear approaches", *18th International conference on methods & models in automation & robotics*, pp. 331-316, 2013.

[22] X. Kong, X. Liu, K. Lee, "Nonlinear multivariable hierarchical model predictive control for boiler-turbine system", *Energy*, vol. 93, pp. 309-322, 2015.

[23] L. Pan, J. Luo, C. Cao, J. Shen, "$\mathcal{L}_1$ adaptive control for improving load-following capability of nonlinear boilerturbine units in the presence of unknown uncertainties", *Simulation Modelling Practice and Theory*, vol. 57, pp. 26-44, 2015.

[24] J. Wu, J. Shen, M. Krug, S. K. Nguang, Y. Li, "GA-based nonlinear predictive switching control for a boiler-turbine system", *J Control Theory Appl*, vol. 10, No. 1, pp. 100-106, 2012.

[25] F. Fang, L. Wei, "Backstepping-based nonlinear adaptive control for coal-fired utility boilerturbine units", *Applied Energy*, vol. 88, pp. 814-824, 2011.

[26] Y. Wan, J. Zhao, G. M. Dimirovski, "Nonlinear adaptive control for multi-machine power systems with boiler-turbine-generator unit", *Int. Trans. Electr. Energ. Syst.*, vol. 25, pp. 859-875, 2015.

[27] R. N. Silva, P. O. Shirley, J. M. Lemos, A. C. Goncalves, "Adaptive regulation of super-heated steam temperature: a case study in an industrial boiler", *Control Engineering Practice*, vol. 8, pp. 1405-1415, 2000.

[28] D. Li, H. Zeng, Y. Xue, X. Jiang, "Multivariable nonlinear control design for boiler-turbine units", *Proceedings of the 6th world congress on intelligent control and automation*, pp. 7518-7522, 2006.

[29] X. Liu, F. Lara-Rosano, C. W. Chan, "Neurofuzzy network modelling and control of steam pressure in 300 MW steam-boiler system", *Engineering applications of artificial intelligence*, vol. 16, pp. 431-440, 2003.

[30] Y. Wang, X. Yu, "New coordinated control design for thermal-power-generation units", *IEEE Trans. of Industrial Electronics*, vol. 57, No. 11, pp. 3848-3856, 2010.

[31] M. Ataei, R. Hooshmand, S. G. Samani, "A coordinated MIMO control design for a power plant using improved sliding mode controller", *ISA Transactions*, vol. 53, pp. 415-422, 2014.

[32] G. Liang, W. Li, Z. Li, "Control of superheated steam temperature in large-capacity generation units based on active disturbance rejection method and distributed control system", *Control Engineering Practice*, vol. 21, pp. 268-285, 2013.

[33] Y. Daren, X. Zhiqiang, "Nonlinear coordinated control of drum boiler power unit based on feedback linearization", *IEEE Trans. on Energy Conversion*, vol. 20, No. 1, 2005.

[34] T. Yu, K. W. Chan, J. P. Tong, B. Zhou, D. H. Li, "Coordinated robust nonlinear boiler-turbine-generator control systems via approximate dynamic feedback linearization", *Journal of Process Control*, vol. 20, pp. 365-374, 2010.

[35] K. Fregene, D. Kennedy, "Stabilizing control of a high-order generator model by adaptive feedback linearization", *IEEE Trans. on Energy Conversion*, vol. 18, No. 1, 2003.

[36] R. D. Bell, K. J. Astrom, "Dynamic models for boilerturbine alternator units: data logs and parameter estimation for a 160MW unit", *Tech. Rep. Report LUTFD2/(TFRT-3192)/1-137*, Department of Automatic Control, Lund Institute of Technology, Lund, Sweden, 1987.

[37] F. P. De Mello, "Boiler models for system dynamic performance studies", *IEEE Transactions on Power Systems*, vol. 6, pp.66-74, 1991.

[38] A. Isidori, *Nonlinear Control Systems*, 3rd Ed., London: Springer-Verlag, 1995.

[39] S. Sastry, *Nonlinear Systems: Analysis, Stability, and Control*, Springer, 1999.

[40] C. Kravaris, P. Daoutidis, R. Wright, "Output feedback control of Nonminimum-Phase Nonlinear Processes", *Chem. Eng. Sci.*, vol. 49, No. 13, pp. 2107-2122, 1994.

[41] C. Kravaris, R. Wright, "Deadtime Compensation for Nonlinear Processes", *AIChE J.*, vol. 35, pp. 1535-1542, 1987.

[42] B. Chen, X. Liu, K. Liu, C. Lin, "Novel adaptive neural control design for nonlinear MIMO time-delay systems", *Automatica*, vol. 45, pp.1554-1560, 2009.

[43] Y. Li, C. Ren, S. Tong, "Adaptive fuzzy backstepping output feedback control for a class of MIMO time-delay nonlinear systems based on high-gain observers", *Nonlinear Dyn.*, vol 67, pp.1175-1191, 2011.

[44] Z. Du, Z. Qu, "Improved adaptive fuzzy control for MIMO nonlinear time-delay systems, *J Control Theory Appl.*, vol. 2, pp.278-282, 2011.

[45] R. Wright, C. Kravaris, "Nonlinear decoupling control in the presence of sensor and actuator deadtimes", *Chem. Eng. Sci.*, vol. 58, pp. 3243-3256, Feb. 2003.

[46] K. J. Astrom, R. D. Bell, "Drum Boiler Dynamics", *Automatica*, vol. 36, pp. 363-378, 2000.

[47] K. J. Astrom, K. Eklund, "A simple non-linear drum boiler model",*Int. J. Control*, vol. 22, No. 5, pp. 739-740.

[48] R. D. Bell, K. J. Astrom, "Dynamics Models for Boiler-Turbine-Alternator Units: Data Logs and Parameter Estimation for a 160 MW Unit", Technical Report TFRT-3192, Lund Inst. of Technology, 1987.

[49] M. , Mikofski, "$IAPWS\_IF97$ functional form with no slip", MATLAB central: File exchange, 2014.

[50] M. Affandi, N. Mamat, S. Kanafiah, N. Khalid, "Simplified Equations for Saturated Steam Properties for Simulation Purpose", *Procedia Engineering*, vol. 53, pp. 722-726, 2013.

[51] H. Spliethoff, *Power Generation from Solid Fuels*, Springer, 2010.

[52] N. Jerome, W. Ray, "High-Performance Multivariable Control Startegies for Systems Having Time Delays", *AIChE J.*, vol. 32, No. 6, 1986.

[53] *Boiler Control Handbook*, 3rd edition. Spring House, PA: Moore Products Company, 1973.

[54] "Drum Level Control Systems in the Process Industries", *ABB Instrumentaion*, 1997.

[55] M. Iacob, G. Andreescu, "Drum-boiler control system employing shrink and swell effect remission in thermal power plants", *3rd International Congress on Ultra Modern Telecommunications and Control Systems and Workshops*, pp. 1-8, 2011.

[56] K. Rayaprolu, *Boilers for power and process*, CRC Press, 2009.

[57] *Steam, its generation and use*, 41st Ed., Ohio: The Babcock & Wilcox Company, 2005.

[58] P. Basu, C. Kefa, L. Jestin, "Boilers and Burners; Design and Theory", New York: Springer, 2000.

[59] J. G. Singer, *Combustion fossil power*, 4th Ed., Combustion Engineering Inc., 1991.

[60] K. C. Weston, *Energy conversion*, Brooks/Cole publishing, 2000.

[61] S. Lu, B. W. Hogg, "Dynamic nonlinear modeling of power plant by physical principles and neural networks", *Electrical Power and Energy Systems*, vol. 22, pp.67-78, 2000.

[62] R. N. Silva, P. N. Shirley, A. J. , Goncalves, J. M. Lemos, "Model of a power plant superheating system", *Proceedings Control 98*, Coimbra, Portugal, pp.471-476, 1998.

[63] O. ,R. ,I. ,Mohamed, *Study of energy efficient supercritical coal-fired power plant dynamic responses and control strategies*, PhD Thesis, The University Of Birmingham, UK, 2012.

[64] T. K. Roy, M. A. Mahmud, W. X. Shen, A. M. T. Oo, "A nonlinear adaptive backstepping approach for coordinated excitation and steam-valving control of synchronous generators", *10th Asian Control Conference (ASCC)*, pp. 1-6, 2015.

[65] H. Liu, S. Li, T. C, "Intelligent decoupling control of power plant main steam pressure and power output", *Int. J. Elec. Power*, vol. 25, pp.809-819, 2003.

[66] S. Lu, B. W. Hogg, "Predictive co-ordinated control for power-plant steam pressure and power output", *Control Eng. Pract.*, vol. 5, pp.79-84, 1997.

[67] R. Garduno-Ramirez, K. Lee, "Compensation of control-loop interaction for power plant wide-range operation", *Control Eng. Pract.*, vol. 13, pp.1475-1487, 2005.

[68] S. Lu, B. W. Hogg, "Predictive co-ordinated control for power-plant steam pressure and power output", *Control Eng. Pract.*, vol. 5, pp.79-84, 1997.

[69] R. Garduno-Ramirez, K. Lee, "Compensation of control-loop interaction for power plant wide-range operation", *Control Eng. Pract.*, vol. 13, pp.1475-1487, 2005.

[70] S. Matsumura, K. Ogata, S. Fujii, H. Shioya, H. Nakamura, "Adaptive control for the steam temperature of thermal power plants", *Control Eng. Practice*, vol. 2, No.4, pp.567-575, 1994.

Appendix A

Feedback Linearization

A.1 Control method

Feedback linearization is an approach that involves the design of a state feedback control law that results in a fully linearized system or a linear input/output closed-loop response [38, 39]. To illustrate this concept, consider a MIMO nonlinear system:

$$\begin{aligned} \frac{dx}{dt} &= f(x) + g_1(x)u_1 + \cdots + g_m(x)u_m \\ y_1 &= h_1(x), \ldots, y_m = h_m(x) \end{aligned} \tag{A.1}$$

with $x \in \Re^n$, f, g smooth vector fields on $\Re^m$, and h_i smooth functions. Assume that each output y_i has a finite relative degree r_i, and the decoupling (also called characteristics) matrix

$$C(x) = \begin{bmatrix} L_{g_1} L_f^{r_1-1} h_1(x) & \ldots & L_{g_m} L_f^{r_1-1} h_1(x) \\ \vdots & & \vdots \\ L_{g_1} L_f^{r_m-1} h_m(x) & \ldots & L_{g_m} L_f^{r_m-1} h_m(x) \end{bmatrix}$$

(where L_f and L_{g_i} denote Lie derivative operators) is nonsingular. Then, the state feedback control law:

$$u = C(x)^{-1} \begin{bmatrix} \dfrac{v_1 - \sum_{k=0}^{r_1} \beta_{1k} L_f^k h_1(x)}{\beta_{1r_1}} \\ \vdots \\ \dfrac{v_m - \sum_{k=0}^{r_m} \beta_{mk} L_f^k h_m(x)}{\beta_{mr_m}} \end{bmatrix} \tag{A.2}$$

results in the following decoupled linear input/output closed-loop system:

$$\begin{bmatrix} \sum_{k=0}^{r_1} \beta_{1k} y_1^{(k)}(t) \\ \vdots \\ \sum_{k=0}^{r_m} \beta_{mk} y_m^{(k)}(t) \end{bmatrix} = \begin{bmatrix} v_1 \\ \vdots \\ v_m \end{bmatrix}$$

where $\beta_{1k}, \ldots, \beta_{mk}$ are tunable parameters and $v_1, \ldots, v_m$ are reference inputs.

Each input/output pair can then be controlled using an external SISO controller with integral action. Note that when the total relative degree is the same as the order of the system, i.e., $\Sigma_i r_i = n$, not only is the input/output response linear but the overall closed loop system is fully linearized.

Unmeasured process states can be estimated through appropriate observers. A particular implementation of a static state feedback control with open loop observers [40], termed model state feedback structure, involves utilizing an online simulation of the process model to estimate the model state (Fig. 2). The model state is then utilized in two ways: 1) It goes through the model output map to generate the model output. 2) It is fed back to the static state feedback law. In the feedback loop, the difference between the model output and the process output corrects the required set point. The

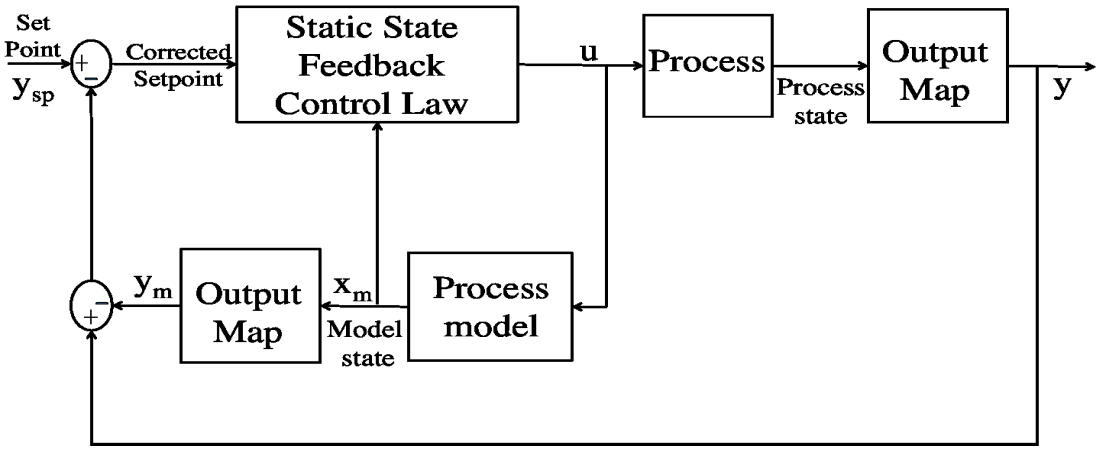

Figure A.1: Model state feedback structure.

required control action is then generated from the static state feedback law utilizing the fed back model state and corrected set point and, in the absence of model-process mismatches, the following response is induced:

$$y_i(t) + \sum_{k=1}^{r_i} \beta_{ik} \frac{d^k y_i(t)}{dt^k} = y_{i_{sp}}(t) \qquad i = 1, \ldots, m \tag{A.3}$$

obtained from the control law of (10) with $\beta_{i0} = 1$ and the corrected setpoint:

$$v_i(t) = y_{i_{sp}}(t) - y_i(t) + y_{i_{model}}(t) \qquad i = 1, \ldots, m$$

This strategy, under the conditions that the process model is exponentially stable, the coefficients β_{ik} are chosen so that the poles of the closed loop response are in the left hand side of the complex plane, and the process zero dynamics is locally asymptotically stable results in local asymptotic stability of the closed-loop system and incorporates integral action to enforce zero steady state error in the presence of step-like disturbances. For details see [40].

Appendix B

MATLAB m-files codes for the control strategies implementation

B.1 M-files coded for chapter 2 case studies

- Process dynamics.
- State feedback control.
- Open loop observer.
- PI-GMDC observer.
- Applied power set point changes.

```
function [sys,x0,str,ts] = vdv_sfune(t,x,u,flag,x0,efb,ef) %
% Represents the power plant dynamics as discussed in Chapter 2.
switch flag

% %******************************
case 0 % initialization;
% %******************************

sizes = simsizes; sizes.NumContStates = 2; sizes.NumDiscStates = 0;
sizes.NumOutputs = 2; sizes.NumInputs = 4; sizes.DirFeedthrough = 0;
sizes.NumSampleTimes = 1; sys = simsizes(sizes);
str = []; ts=[0 0];

%******************************
case 1 % derivatives;
%******************************

E = x(2) ; P=x(1);

%Inputs
%******************************
us = u(1); qe=u(2); efb=u(3);ef=u(4);

%parameters
%******************************
mt=300e3;
cp=0.5;
Pc=22.055;
Tc=647.126;
Hcr=2086;
k=341.0485;
delH=24190;
Tcond=9.4185+273.15;
Pcond=0.00118;
Tsup=535+273.15;
mnk=[-5, -4, -2, -1, -1, 0, 1,3,7,9; 1, 1, 0, 0, 1, 0, 0, 1, 1, 2; -7.23E-03,
1.77E-02, 7.11E-02, 4.87E-01, -3.60E-02, 9.93E-01, -5.50E-03, -1.45E-01, -
9.03E-03, -9.70E-02];
hf=1030.96;
Vwt=63.9059;
Vt=89;
Vst=Vt-Vwt;

%******************************
%Saturated Steam and water properties
%******************************
Tsat=IAPWS_IF97('Tsat_p',P);
h_w=IAPWS_IF97('hL_p',P);
h_s=IAPWS_IF97('hV_p',P);
rho_w=1/(IAPWS_IF97('vL_p',P));
rho_s=1/(IAPWS_IF97('vV_p',P));
dt_s=IAPWS_IF97('dTsatdpsat_p',P);
d_hw=IAPWS_IF97('dhLdp_p',P);
d_hs=IAPWS_IF97('dhVdp_p',P);
d_vL=IAPWS_IF97('dvLdp_p',P);
d_rho=-d_vL*rho_w^2;
```

```
d_vS=IAPWS_IF97('dvVdp_p',P);
d_rhos=-d_vS*rho_s^2;
%*******************************

%*******************************
%Superheated enthalpy calculation.
%*******************************

for i=1:10

HP(i)=(Tc/Tsup)^mnk(1,i)*(P/Pc)^mnk(2,i)*mnk(3,i);
LP(i)=(Tc/Tcond)^mnk(1,i)*(Pcond/Pc)^mnk(2,i)*mnk(3,i);
end

h_sup=Hcr*sum(HP);
h_lp=1843.474;

%*******************************
% functions
%*******************************

Q=efb*delH*qe;
hc=(h_s-h_w);
e1=rho_w*Vwt*d_hw+mt*cp*dt_s+rho_s*Vst*d_hs+hc*Vst*d_rhos-Vt;
qs=(k*P/(Tsup)^0.5)*us;
dPdt=1/e1*(Q+qs*(hf-h_s));
dEdt=qs*ef*(h_sup-h_lp)*0.001/0.4-E/0.4;
sys = [dPdt; dEdt];

%*******************************
case 3 % outputs;
%*******************************

    sys = [x(1);x(2)];
case {2, 4, 9}
    sys = [];
otherwise
error(['unhandled flag = ',num2str(flag)]);
end
```

```
function [us,qe]= shift(b11, b21,vii,vi, E, P, stt)
%#codegen

% Chapter 2: Static state feedback for controlling boiler pressure and power
%generation.

% %*******************************
%Parameters%
%*******************************
mt=300e3;
cp=0.5;
Pc=22.055;
Tc=647.126;
Hcr=2086;
ef=0.725;
k=341.0485;
efb=0.88;
delH=24190;
Tcond=9.4185+273.15;
Pcond=0.00118;
Tsup=535+273.15;
mnk=[-5, -4, -2, -1, -1, 0, 1,3,7,9; 1, 1, 0, 0, 1, 0, 0, 1, 1, 2; -7.23E-03,
1.77E-02, 7.11E-02, 4.87E-01, -3.60E-02, 9.93E-01, -5.50E-03, -1.45E-01, -
9.03E-03, -9.70E-02];
hf=1030.96;
Vwt=63.9059;
Vt=89;
Vst=Vt-Vwt;

******************
%Saturated steam and water properties
%*******************************
h_w=stt(1);
h_s=stt(2);
rho_w=stt(3);
rho_s=stt(4);
dt_s=stt(5);
d_hw=stt(6);
d_hs=stt(7);
d_rho=stt(8);
d_rhos=stt(9);

% %*******************************
%Superheated steam enthalpy calculation:
% %*******************************

HP=zeros(10,1);
LP=zeros(10,1);

for i=1:10
HP(i)=(Tc/Tsup)^mnk(1,i)*(P/Pc)^mnk(2,i)*mnk(3,i);
LP(i)=(Tc/Tcond)^mnk(1,i)*(Pcond/Pc)^mnk(2,i)*mnk(3,i);
end

h_sup=Hcr*sum(HP);
h_lp=1843.474;
```

```
% %*******************************
% functions
% %*******************************

hc=(h_s-h_w);
e1=rho_w*Vwt*d_hw+mt*cp*dt_s+rho_s*Vst*d_hs+hc*Vst*d_rhos-Vt;
%Characteristic Matrix
A=[k*(hf-h_s)*P/(e1*Tsup^0.5) efb*delH/e1; ef*(h_sup-
h_lp)*0.001/0.4*(k*P/(Tsup^0.5)) 0];
y = inv(A)*[(vi-P)/b11; (vii-(1-b21/0.4)*E)/b21];
%Control actions
us=y(1);
qe=y(2);
```

```
function [sys,x0,str,ts] = vdv_sfune(t,x,u,flag,x0,efb,ef) %
% Represents the power plant dynamics as discussed in Chapter 2.
switch flag

% %******************************
case 0 % initialization;
% %******************************

sizes = simsizes; sizes.NumContStates = 2; sizes.NumDiscStates = 0;
sizes.NumOutputs = 2; sizes.NumInputs = 4; sizes.DirFeedthrough = 0;
sizes.NumSampleTimes = 1; sys = simsizes(sizes);
str = []; ts=[0 0];

%******************************
case 1 % derivatives;
%******************************

E = x(2) ; P=x(1);

%Inputs
%******************************
us = u(1); qe=u(2); efb=u(3);ef=u(4);

%parameters
%******************************
mt=300e3;
cp=0.5;
Pc=22.055;
Tc=647.126;
Hcr=2086;
k=341.0485;
delH=24190;
Tcond=9.4185+273.15;
Pcond=0.00118;
Tsup=535+273.15;
mnk=[-5, -4, -2, -1, -1, 0, 1,3,7,9; 1, 1, 0, 0, 1, 0, 0, 1, 1, 2; -7.23E-03,
1.77E-02, 7.11E-02, 4.87E-01, -3.60E-02, 9.93E-01, -5.50E-03, -1.45E-01, -
9.03E-03, -9.70E-02];
hf=1030.96;
Vwt=63.9059;
Vt=89;
Vst=Vt-Vwt;

%******************************
%Saturated Steam and water properties
%******************************
Tsat=IAPWS_IF97('Tsat_p',P);
h_w=IAPWS_IF97('hL_p',P);
h_s=IAPWS_IF97('hV_p',P);
rho_w=1/(IAPWS_IF97('vL_p',P));
rho_s=1/(IAPWS_IF97('vV_p',P));
dt_s=IAPWS_IF97('dTsatdpsat_p',P);
d_hw=IAPWS_IF97('dhLdp_p',P);
d_hs=IAPWS_IF97('dhVdp_p',P);
d_vL=IAPWS_IF97('dvLdp_p',P);
d_rho=-d_vL*rho_w^2;
```

```
d_vS=IAPWS_IF97('dvVdp_p',P);
d_rhos=-d_vS*rho_s^2;
%*******************************

%*******************************
%Superheated enthalpy calculation.
%*******************************

for i=1:10

HP(i)=(Tc/Tsup)^mnk(1,i)*(P/Pc)^mnk(2,i)*mnk(3,i);
LP(i)=(Tc/Tcond)^mnk(1,i)*(Pcond/Pc)^mnk(2,i)*mnk(3,i);
end

h_sup=Hcr*sum(HP);
h_lp=1843.474;

%*******************************
% functions
%*******************************

Q=efb*delH*qe;
hc=(h_s-h_w);
e1=rho_w*Vwt*d_hw+mt*cp*dt_s+rho_s*Vst*d_hs+hc*Vst*d_rhos-Vt;
qs=(k*P/(Tsup)^0.5)*us;
dPdt=1/e1*(Q+qs*(hf-h_s));
dEdt=qs*ef*(h_sup-h_lp)*0.001/0.4-E/0.4;
sys = [dPdt; dEdt];

%*******************************
case 3 % outputs;
%*******************************

    sys = [x(1);x(2)];
case {2, 4, 9}
    sys = [];
otherwise
error(['unhandled flag = ',num2str(flag)]);
end
```

```
%Power plant open loop observer utilized for the PI-GMDC controller.

function [sys,x0,str,ts] = vdv_sfune(t,x,u,flag,x0) %

switch flag
%************************
case 0 % initialization;
%************************
sizes = simsizes; sizes.NumContStates = 8; sizes.NumDiscStates = 0;
sizes.NumOutputs = 2; sizes.NumInputs = 4; sizes.DirFeedthrough = 0;
sizes.NumSampleTimes = 1; sys = simsizes(sizes);
str = []; ts=[0 0];
%***************************
case 1 % derivatives;
%***************************

%Inputs:
%*********************************
us = u(1); qe=u(3); usd=u(2); qed=u(4);

%Parameters:
%*********************************
Ps=13.729;
Es=80;

%Functions
%***********************************
dx1dt=-0.0025*x(1)-0.1027*usd;
dx2dt=-2.5*x(2)+471.6128*usd;
dx3dt=-0.0025*x(3)-0.5421*usd;
dx4dt=-0.0025*x(4)+0.0082*qed;
dx7dt=dx1dt+dx4dt;
dx5dt=-2.5*x(5)-0.0433*qed;
dx6dt=-0.0025*x(6)+0.0433*qed;
dx8dt=dx2dt+dx3dt+dx5dt+dx6dt;
x(7)=x(1)+x(4);
x(8)=x(2)+x(3)+x(5)+x(6);

sys = [dx1dt,dx2dt,dx3dt,dx4dt,dx5dt,dx6dt,dx7dt,dx8dt];

%************************************
case 3 % outputs;
%************************************
    sys = [x(7);x(8)];
case {2, 4, 9}
    sys = [];
otherwise
error(['unhandled flag = ',num2str(flag)]);
end
```

```
%************************************************************
%Multiple power step changes applied for narrow range testing.
%************************************************************

function y = fcn(u)
%#codegen
t=50;
y=(80.0791);
k=floor(u);
if k>=150&&k<=5550
 y = (86.6784);
elseif k>=5550&&k<=10950
y=(82.6784);
elseif k>10950
    y=(78.6784);
end


%************************************************************
%Ramping of power set point applied in Chapter 2.
%************************************************************

function y = fcn(u)
%#codegen
y= 80.0791;
yss=y;
k=floor(u);
%power ramping at 2%/min.
if k>=50&&k<=25.8333*60

 y = (3.2/60)*(k-50)+yss;
 elseif k>25.8333*60&&k<=7200
      y = ( 3.2/60)*(25.8333*60-50)+yss;
elseif k>7200&&k<=8700
    y=(( 3.2/60)*(25.8333*60-50)+yss)-(3.2/60)*(k-7200);
elseif k>8700
    y=yss;
end


%************************************************************
%"Worst case scenario multiple step changes of power set point applied in
Chapter 2.
%************************************************************

function y = fcn(u)
%#codegen

y= 80.0179;
yss=y;
k=floor(u);
%Wide multiple step changes
if k>=50&&k<=1250
 y = 32+yss;
 elseif k>=1250&&k<=2450
 y=yss;
```

```
 elseif k>=2450&&k<=3650
      y = yss+32;
       elseif k>3650
 y=yss;

end


%************************************************************
%"Worst case scenario random fluctuations in deadtime.
%************************************************************
function y = fcn(u)
%#codegen

y=90;
k=floor(u);
if k>=1500&&k<=2500

 y = 80;
elseif k>=2500&&k<=4000
y=110;
elseif k>=4000&&k<=10000
y=120;
elseif k>=10000&&k<=13000
y=95;
elseif k>=13000&&k<=17000
y=120;
elseif k>=17000&&k<=25000
y=115;
elseif k>=25000&&k<=45000
y=100;
elseif k>=45000&&k<=65000
y=90;
elseif k>65000
    y=120;
end
```

B.2 M-files coded for chapter 3 case studies

- Process dynamics.
- State feedback control (same as in Chapter 2).
- Open loop observer (same as in Chapter 2).
- PI-GMDC observer (same as in Chapter 2).
- Applied power set point changes (same as in Chapter 2).

```
%Power plant dynamics; boiler pressure, drum level, power generation.

function [sys,x0,str,ts] = phase21(t,x,u,flag,x0,efb,ef)
switch flag

%******************************
case 0 % initialization;
%******************************
sizes = simsizes; sizes.NumContStates = 5; sizes.NumDiscStates = 0;
sizes.NumOutputs = 8; sizes.NumInputs = 5; sizes.DirFeedthrough = 0;
sizes.NumSampleTimes = 1; sys = simsizes(sizes);
str = []; ts=[0 0];

%******************************
case 1 % derivatives;
%******************************

%variables
%******************************
E = x(5) ; P=x(1); Vwt=x(2); a=x(3); Vsd=x(4);

% manipulated variables & Disturbances
%******************************
us = u(1); qe=u(2); efb=u(3);ef=u(4); qf=u(5);

%******************************
%Model parameters
%******************************
mt=300e3;
cp=0.5;
Pc=22.055;
Tc=647.126;
Hcr=2086;
k=341.0485;
delH=24190;
Tcond=9.4185+273.15;
Pcond=0.00118;
Tsup=535+273.15;
mnk=[-5, -4, -2, -1, -1, 0, 1,3,7,9; 1, 1, 0, 0, 1, 0, 0, 1, 1, 2; -7.23E-03,
1.77E-02, 7.11E-02, 4.87E-01, -3.60E-02, 9.93E-01, -5.50E-03, -1.45E-01, -
9.03E-03, -9.70E-02];
hf=1030.96;
Vt=89;
Vst=Vt-Vwt;
Vr=38;
%Vdc=11;
Vd=40;
mr=160e3;
b=0.3;
Ad=20;
Adc=0.3809;
g=9.81;
ki=25;
Td=12;
md=140000;
V0sd=7.793;
```

```
Vdc=11;


%******************************                                    132
%Saturated steam and water properties
%******************************
Tsat=IAPWS_IF97('Tsat_p',P);
h_w=IAPWS_IF97('hL_p',P);
h_s=IAPWS_IF97('hV_p',P);
rho_w=1/(IAPWS_IF97('vL_p',P));
rho_s=1/(IAPWS_IF97('vV_p',P));
dt_s=IAPWS_IF97('dTsatdpsat_p',P);
d_hw=IAPWS_IF97('dhLdp_p',P);
d_hs=IAPWS_IF97('dhVdp_p',P);
d_vL=IAPWS_IF97('dvLdp_p',P);
d_rho=-d_vL*rho_w^2;
d_vS=IAPWS_IF97('dvVdp_p',P);
d_rhos=-d_vS*rho_s^2;

%Superheated steam enthalpy calculation
%******************************
for i=1:10

HP(i)=(Tc/Tsup)^mnk(1,i)*(P/Pc)^mnk(2,i)*mnk(3,i);
LP(i)=(Tc/Tcond)^mnk(1,i)*(Pcond/Pc)^mnk(2,i)*mnk(3,i);
end

h_sup=Hcr*sum(HP);
h_lp=1843.474;

%******************************
%functions
%******************************

%algebraic equations
%******************************
Q=efb*delH*qe;
qs=(k*P/(Tsup)^0.5)*us;
eta=a*(rho_w-rho_s)/rho_s;
av=(rho_w/(rho_w-rho_s))*(1-(rho_s/((rho_w-rho_s)*a))*log(1+(rho_w-
rho_s)/rho_s*a));
davp=1/(rho_w-rho_s)^2*(rho_w*d_rhos-
rho_s*d_rho)*(1+(rho_w/rho_s)*(1/(1+eta))-
(rho_s+rho_w)/(eta*rho_s)*log(1+eta));
dava=(rho_w/(rho_s*eta))*(1/eta*log(1+eta)-1/(1+eta));
Vwd=Vwt-Vdc-(1-av)*Vr;
hc=h_s-h_w;
e11=rho_w-rho_s;
e12=Vwt*d_rho+Vst*d_rhos;
e21=rho_w*h_w-rho_s*h_s;
e22=Vwt*(h_w*d_rho+rho_w*d_hw)+Vst*(h_s*d_rhos+rho_s*d_hs)-Vt+mt*cp*dt_s;
e32=(rho_w*d_hw-a*hc*d_rho)*(1-av)*Vr+((1-
a)*hc*d_rhos+rho_s*d_hs)*av*Vr+(rho_s+(rho_w-rho_s)*a)*hc*Vr*davp-
Vr+mr*cp*dt_s;
e33=((1-a)*rho_s+a*rho_w)*hc*Vr*dava;
```

```
e42=Vsd*d_rhos+(1/hc)*(rho_s*Vsd*d_hs+rho_w*Vwd*d_hw-Vsd-
Vwd+md*cp*dt_s)+a*(1+b)*Vr*(av*d_rhos+(1-av)*d_rho+(rho_s-rho_w)*davp);
e43=a*(1+b)*(rho_s-rho_w)*Vr*dava;
e44=rho_s;
a11=e22-e12*e21/e11;
qdc2=2*rho_w*Adc*(rho_w-rho_s)*g*av*Vr/ki;
qdc=qdc2^0.5;
qr=qdc-Vr*(av*d_rhos+(1-av)*d_rho+(rho_w-rho_s)*davp)*(1/a11*(Q+(hf-
e21/e11)*qf-(h_s-e21/e11)*qs))+(rho_w-rho_s)*Vr*dava*1/e33*(Q-a*hc*qdc-
e32*(1/a11*(Q+(hf-e21/e11)*qf-(h_s-e21/e11)*qs)));
qsd=rho_s/Td*(Vsd-V0sd)+a*qdc+a*b*(qdc-qr);

% Model eqns
%*******************************
dPdt=1/a11*(Q+(hf-e21/e11)*qf-(h_s-e21/e11)*qs);
dVwdt=1/e11*(qf-qs-e12*(1/a11*(Q+(hf-e21/e11)*qf-(h_s-e21/e11)*qs)));
dadt=1/e33*(Q-a*hc*qdc-e32*(1/a11*(Q+(hf-e21/e11)*qf-(h_s-e21/e11)*qs)));
dvsdt=1/e44*(rho_s/Td*(V0sd-Vsd)+(hf-h_w)/hc*qf-e42*(1/a11*(Q+(hf-
e21/e11)*qf-(h_s-e21/e11)*qs))-e43*(1/e33*(Q-a*hc*qdc-e32*(1/a11*(Q+(hf-
e21/e11)*qf-(h_s-e21/e11)*qs)))));
dEdt=qs*ef*(h_sup-h_lp)*0.001/0.4-E/0.4;

sys = [dPdt; dVwdt; dadt; dvsdt; dEdt];

%*******************************
case 3 % outputs;
%*******************************
rho_w=1/(IAPWS_IF97('vL_p',x(1)));
rho_s=1/(IAPWS_IF97('vV_p',x(1)));
av=(rho_w/(rho_w-rho_s))*(1-(rho_s/((rho_w-rho_s)*x(3)))*log(1+(rho_w-
rho_s)/rho_s*x(3)));
Ad=20;
Vsz=(x(4)-2.9474297);
Vwz=(x(2)-63.9059);
    Vdc=11;
Vwd=x(2)-Vdc-(1-av)*38-25.0702;
sys = [x(1);Vwd; Vsz; ((Vsz+Vwd)/Ad);x(5); x(4);x(2);x(3)];
case {2, 4, 9}
    sys = [];
    otherwise

error(['unhandled flag = ',num2str(flag)]);
end
```

B.3 M-files coded for chapter 4 case studies

- Process dynamics.
- State feedback control for boiler pressure and power generation control.
- Open loop observer for boiler pressure and power generation.
- State feedback control for superheated steam temperature control.
- Open loop observer for superheated steam temperatures.
- State feedback control for reheated steam temperature control.
- Open loop observer for reheated steam temperatures.
- Applied power set point changes.

```
function [sys,x0,str,ts] = process15mTc3(t,x,u,flag,x0) %
switch flag

%**************************
case 0 % initialization;
%**************************

sizes = simsizes; sizes.NumContStates = 11; sizes.NumDiscStates = 0;
sizes.NumOutputs = 11; sizes.NumInputs = 7; sizes.DirFeedthrough = 0;
sizes.NumSampleTimes = 1; sys = simsizes(sizes);
str = []; ts=[0 0];

%**************************
case 1 % derivatives;
%**************************

%Variables
%**************************

%pressure
P=x(1);

%platen SH
Tw_PSH=x(2);
hout_PSH=x(3);

%SH 1
Tw_SH1=x(4);
hout_SH1=x(5);

%SH 2
Tw_SH2=x(6);
hout_SH2=x(7);

%REHEATER
Tw_RH=x(8);
hout_RH=x(9);

%HP turbine
E_HP=x(10);
E_LP=x(11);

%inputs
%**************************
us = u(1); qfuel=u(2); efb=u(3);qat1=u(4); u_RH=u(5); qat2=u(6); a2=u(7);

%parameter
%**************************
mt=300e3;
cp=0.5;
Tsup=535+273.15;
k=327.057;
delH=29163.6516;
k_RH=1635.28;
```

```
hf=IAPWS_IF97('h_pT',13.78,275+273.15);
Vwt=63.9059;
Vt=89;
Vst=Vt-Vwt;
qfg=12.84353295*qfuel;

%******************************
%Steam and water properties
%******************************
Tsat=IAPWS_IF97('Tsat_p',P);
h_w=IAPWS_IF97('hL_p',P);
h_s=IAPWS_IF97('hV_p',P);
rho_w=1/(IAPWS_IF97('vL_p',P));
rho_s=1/(IAPWS_IF97('vV_p',P));
dt_s=IAPWS_IF97('dTsatdpsat_p',P);
d_hw=IAPWS_IF97('dhLdp_p',P);
d_hs=IAPWS_IF97('dhVdp_p',P);
d_vL=IAPWS_IF97('dvLdp_p',P);
d_rho=-d_vL*rho_w^2;
d_vS=IAPWS_IF97('dvVdp_p',P);
d_rhos=-d_vS*rho_s^2;

% functions
%*************************

%Boiler

Q=efb*delH*qfuel;
hc=(h_s-h_w);
e1=rho_w*Vwt*d_hw+mt*cp*dt_s+rho_s*Vst*d_hs+hc*Vst*d_rhos-Vt;

%Superheaters

hin_SH1=h_s;
Tin_SH1=IAPWS_IF97('T_ph',P,h_s);%kJ/kg
hat1=815; %kJ/kg
hat2=815; %kJ/kg
cpw=0.5; %kJ/kgK
rhow=8060; %kg/m3
V_PSH=6.884632408; %m3
V_SH1=13.99808183; %m3
V_SH2=11.13423406; %m3
V_RH=74.38189113; %m3
Vw_PSH=0.672327384; %m3
Vw_SH1=1.367000178; %m3
Vw_SH2=1.087327545; %m3
Vw_RH=7.263856556;


%platen SH

ebolt=0.7;
 sigma=5.67E-08;     %W/m2K4
  Tg_PSH=(1568.15+1758.15)/2;  % K
Ar=151;
```

```
   heff_PSH=11.080;

%SH 1
Tg_SH1=(1230.25+670.75)/2; %K

hweff_SH1=13.117;%W/(K kg/s^0.6)
heff_SH1=17.28154188;%W/(

%SH2

Tg_SH2=(1230.25+1568.15)/2; %K
hweff_SH2=3.355;%W/(K kg/s^0.6)
heff_SH2=11.015;
a=(1-a2); %bypass factor

%REHEATER

Tg_RH=(1568.15+1071.75)/2; %K
hweff_RH=7.574;
heff_RH=9.797309476;
Prh=P/5; %MPa

%Attemperators

qs=(k*P/(IAPWS_IF97('T_ph',P,hout_PSH))^0.5)*us;

%AT1
qst_SH1=qs;%kg/s
qst_SH2=qst_SH1+qat1;
hin_SH2=(hout_SH1*qst_SH1+hat1*qat1)/(qat1+qst_SH1)

%AT2
qst_PSH= qs+qat1+qat2;
qst_RH=(k_RH*Prh/(IAPWS_IF97('T_ph',Prh,hout_RH))^0.5)*u_RH+qat1+qat2;
hin_PSH=(hout_SH2*qst_SH2+hat2*qat2)/(qat2+qst_SH2)

%Reheater inlet conditions
Tout_PSH=IAPWS_IF97('T_ph',P,hout_PSH);
sin_Tb=XSteam('s_pT',P*10,Tout_PSH-273.15);
hisen_RH=XSteam('h_ps',P/5*10,sin_Tb);
hin_RH=0.725*(hisen_RH-hout_PSH)+hout_PSH;
Tin_RH=IAPWS_IF97('T_ph',P/5,hin_RH);

%Turbine 2 outlet conditions
Tout_RH=IAPWS_IF97('T_ph',P/5,hout_RH);
sin_Tb2=XSteam('s_pT',P/5*10,Tout_RH-273.15);
hisen_Tb2=XSteam('h_ps',0.1787,sin_Tb2);
hout_Tb2=0.725*(hisen_Tb2-hout_RH)+hout_RH;

%%Steam Correlations
h=[hin_PSH hout_SH1 hin_SH2 hout_SH2 hout_RH];
P2=[ones(1,4)*P Prh];

%Superheated steam temperature
```

```
T=IAPWS_IF97('T_ph',P2,h);
Tin_PSH=T(1);
Tout_SH1=T(2);
Tin_SH2=T(3);

Tout_SH2=T(4);
Tout_RH=T(5);
T1=[Tin_PSH Tout_PSH Tin_SH1 Tout_SH1 Tin_SH2 Tout_SH2 Tin_RH Tout_RH];
P1=[ones(1,6)*P Prh Prh];

%density of steam
rho=1./(IAPWS_IF97('v_pT',P1,T1));
rhoin_PSH=rho(1);
rhoout_PSH=rho(2);
rhoin_SH1=rho(3);
rhoout_SH1=rho(4);
rhoin_SH2=rho(5);
rhoout_SH2=rho(6);
rhoin_RH= rho(7);
rhoout_RH= rho(8);

%*************************
%model subequations
%*************************

%platen superheater

T_PSHa=(Tin_PSH+Tout_PSH)/2;
Qw_PSH=Ar*ebolt*sigma*(Tg_PSH^4-Tw_PSH^4)*1e-3;
Q_PSH=heff_PSH*qst_PSH^0.8*(Tw_PSH-T_PSHa);

%SH1
T_SH1a=(Tin_SH1+Tout_SH1)/2;
Q_SH1=heff_SH1*qst_SH1^0.8*(Tw_SH1-T_SH1a);
Qw_SH1=hweff_SH1*(a*qfg)^0.6*(Tg_SH1-Tw_SH1);

%SH2
T_SH2a=(Tin_SH2+Tout_SH2)/2;
Q_SH2=heff_SH2*qst_SH2^0.8*(Tw_SH2-T_SH2a);
Qw_SH2=hweff_SH2*(a*qfg)^0.6*(Tg_SH2-Tw_SH2);

%REHEATER

T_RHa=(Tin_RH+Tout_RH)/2;
Q_RH=heff_RH*qst_RH^0.8*(Tw_RH-T_RHa);
Qw_RH=hweff_RH*(a2*qfg)^0.6*(Tg_RH-Tw_RH);

%*************************
%models
%*************************

%boiler
dPdt=1/e1*(Q+qst_SH1*(hf-h_s));
```

```
%platen superheater

%Gas-wall side

dTw_PSHdt=(Qw_PSH-Q_PSH)/(rhow*Vw_PSH*cpw);

%steam side
rho_PSHa=(rhoin_PSH+rhoout_PSH)/2;
dh_PSHdt=(Q_PSH-qst_PSH*(hout_PSH-hin_PSH))/(rho_PSHa*V_PSH);

%SH1

%Gas-wall side

dTw_SH1dt=(Qw_SH1-Q_SH1)/(rhow*Vw_SH1*cpw);

%steam side
rho_SH1a=(rhoin_SH1+rhoout_SH1)/2;
dh_SH1dt=(Q_SH1-qst_SH1*(hout_SH1-hin_SH1))/(rho_SH1a*V_SH1);

%SH2

%Gas-wall side

dTw_SH2dt=(Qw_SH2-Q_SH2)/(rhow*Vw_SH2*cpw);

%steam side
rho_SH2a=(rhoin_SH2+rhoout_SH2)/2;
dh_SH2dt=(Q_SH2-qst_SH2*(hout_SH2-hin_SH2))/(rho_SH2a*V_SH2);

%REHEATER

%Gas-wall side

dTw_RHdt=(Qw_RH-Q_RH)/(rhow*Vw_RH*cpw);

%steam side
rho_RHa=(rhoin_RH+rhoout_RH)/2;
dh_RHdt=(Q_RH-qst_RH*(hout_RH-hin_RH))/(rho_RHa*V_RH);

%Turbine
dEdt=qst_PSH*(0.001*(hout_PSH-hin_RH))/0.4-E_HP/0.4;
dE2dt=qst_RH*(0.001*(hout_RH-hout_Tb2))/0.4-E_LP/0.4;

sys = [dPdt;dTw_PSHdt;dh_PSHdt;dTw_SH1dt; dh_SH1dt;dTw_SH2dt;
dh_SH2dt;dTw_RHdt; dh_RHdt; dEdt; dE2dt];

%*************************
case 3 % outputs;
%*************************
        sys =
[x(1);x(2);x(3);x(4);x(5);x(6);x(7);x(8);x(9);x(10)+x(11);x(10)];
case {2, 4, 9}
```

```
    sys = [];
otherwise
error(['unhandled flag = ',num2str(flag)]);
end
```

```
function [us,qe]= shift(b11, b21,vii,vi, E, P, stt)
%#codegen
%Static state feedback for controling boiler pressure and power generation
%as discussed in Chapter 4.
mt=300e3;
cp=0.5;
efb=0.4517;
k=327.057;%
delH=29163.6516;
k_RH=1635.28;
Tsup=535+273.15;
hf=1207.9;
Vwt=63.9059;
Vt=89;
Vst=Vt-Vwt;

%*******************************
%Steam and water properties
%*******************************
h_w=stt(1);
h_s=stt(2);
rho_w=stt(3);
rho_s=stt(4);
dt_s=stt(5);
d_hw=stt(6);
d_hs=stt(7);
d_rho=stt(8);
d_rhos=stt(9);
hisen_RH=stt(10);
hout_PSH=stt(11);
hisen_Tb2=stt(12);
hout_RH=stt(13);
%*******************************

%reheater inlet/outlet conditions
%*******************************

hin_RH=0.725*(hisen_RH-hout_PSH)+hout_PSH;
hout_Tb2=0.725*(hisen_Tb2-hout_RH)+hout_RH;



qat1=2.794; %kg/s
qat2=2.794;

% functions
hc=(h_s-h_w);
e1=rho_w*Vwt*d_hw+mt*cp*dt_s+rho_s*Vst*d_hs+hc*Vst*d_rhos-Vt;
A=[k*(hf-h_s)*P/(e1*Tsup^0.5) efb*delH/e1; (hout_PSH-
hin_RH)*0.001/0.4*(k*P/(Tsup^0.5))+(hout_RH-
hout_Tb2)*0.001/0.4*(k_RH*(P/5)/(Tsup^0.5)) 0];
y = A\[(vi-P)/b11; (vii-(E)-b21*(-E/0.4+(qat1+qat2)*(hout_PSH-
hin_RH)*0.001/0.4+(qat1+qat2)*(hout_RH-hout_Tb2)*0.001/0.4))/b21];
%control actions
us=y(1);
qe=y(2);
```

```
function [sys,x0,str,ts] = process15mE2(t,x,u,flag,x0) %
%Observer for boiler pressure and power generation
switch flag
%******************************
case 0 % initialization;
%******************************
sizes = simsizes; sizes.NumContStates = 3; sizes.NumDiscStates = 0;
sizes.NumOutputs = 2; sizes.NumInputs = 5; sizes.DirFeedthrough = 0;
sizes.NumSampleTimes = 1; sys = simsizes(sizes);
str = []; ts=[0 0];
%******************************
case 1 % derivatives;
%******************************

% states
%******************************
E_HP = x(2) ; P=x(1); E_LP=x(3);

% Inputs
%******************************
us = u(1); qe=u(2); efb=u(3); qat1=u(4); qat2=u(5);

%parameter
%******************************
mt=300e3;
cp=0.5;
Pc=22.055;
Tc=647.126;
Hcr=2086;
k=327.057;%
delH=29163.6516;
k_RH=1635.28;
Tsup=535+273.15;
hf=IAPWS_IF97('h_pT',13.78,275+273.15);
Vwt=63.9059;
Vt=89;
Vst=Vt-Vwt;

%******************************
%Steam and water properties
%******************************
Tsat=IAPWS_IF97('Tsat_p',P);
h_w=IAPWS_IF97('hL_p',P);
h_s=IAPWS_IF97('hV_p',P);
rho_w=1/(IAPWS_IF97('vL_p',P));
rho_s=1/(IAPWS_IF97('vV_p',P));
dt_s=IAPWS_IF97('dTsatdpsat_p',P);
d_hw=IAPWS_IF97('dhLdp_p',P);
d_hs=IAPWS_IF97('dhVdp_p',P);
d_vL=IAPWS_IF97('dvLdp_p',P);
d_rho=-d_vL*rho_w^2;
d_vS=IAPWS_IF97('dvVdp_p',P);
d_rhos=-d_vS*rho_s^2;
hout_PSH=IAPWS_IF97('h_pT',P,Tsup);
Prh=P/5;
hout_RH=IAPWS_IF97('h_pT',P/5,Tsup);
```

```
%steam flow rates
qs=(k*P/(Tsup)^0.5)*us;
qat1=2.794; %kg/s
qat2=2.794; %kg/s
qst_SH1=qs;
qst_PSH=qs+qat1+qat2;%kg/s
qst_RH=(k_RH*Prh/(IAPWS_IF97('T_ph',Prh,hout_RH))^0.5)*us+qat1+qat2;

%turbine calculations
%Reheater inlet conditions

sin_Tb=XSteam('s_pT',P*10,535);
hisen_RH=XSteam('h_ps',P/5*10,sin_Tb);
hin_RH=0.725*(hisen_RH-hout_PSH)+hout_PSH;

%Turbine 2 outlet conditions

sin_Tb2=XSteam('s_pT',P/5*10,535);
hisen_Tb2=XSteam('h_ps',0.1787,sin_Tb2);
hout_Tb2=0.725*(hisen_Tb2-hout_RH)+hout_RH;

% functions
Q=efb*delH*qe;
hc=(h_s-h_w);
e1=rho_w*Vwt*d_hw+mt*cp*dt_s+rho_s*Vst*d_hs+hc*Vst*d_rhos-Vt;
dPdt=1/e1*(Q+qst_SH1*(hf-h_s));
dEdt=qst_PSH*(0.001*(hout_PSH-hin_RH))/0.4-E_HP/0.4;
dE2dt=qst_RH*(0.001*(hout_RH-hout_Tb2))/0.4-E_LP/0.4;
sys = [dPdt; dEdt; dE2dt];

%******************************
case 3 % outputs;
%******************************
    sys = [x(1);x(2)+x(3)];
case {2, 4, 9}
    sys = [];
otherwise
error(['unhandled flag = ',num2str(flag)]);
end
```

```
function [q1,q2]= shift(us, P,g11, g21, v1,v2,qfuel, stt, x_p)
%#codegen
%static state feedback for controlling superheated steam temperatures.
%parameters
%*******************************
k=327.057;
hat1=815;
hat2=815;
V_PSH=6.884632408; %m3
V_SH2=11.13423406; %m3
heff_PSH=11.080;  %W/(K kg/s^0.8)
heff_SH2=11.015;
T_PSHa=x_p(6);
T_SH2a=x_p(7);
Tw_PSH=x_p(1);
Tw_SH2=x_p(4);
h_PSH=x_p(2);
h_SH2=x_p(5);
h_SH1=x_p(3);
hin_SH2=x_p(8);
hin_PSH=x_p(9);
rhoin_PSH=stt(3);
rhoout_PSH=stt(1);
rhoin_SH2=stt(4);
rhoout_SH2=stt(2);
Tsup=stt(5);

%functions
%*****************************
rho_PSHa=(rhoin_PSH+rhoout_PSH)/2;
rho_SH2a=(rhoin_SH2+rhoout_SH2)/2;
%characteristic matrix
Lg2h1=(1/(rho_PSHa*V_PSH))*(0.8*heff_PSH*(Tw_PSH-T_PSHa)*(k*P*us/Tsup^0.5)^(-
0.2)-(h_PSH-hin_PSH));
Lg3h1=(1/(rho_PSHa*V_PSH))*(0.8*heff_PSH*(Tw_PSH-T_PSHa)*(k*P*us/Tsup^0.5)^(-
0.2)-(h_PSH-hin_PSH));
Lg2h2=(1/(rho_SH2a*V_SH2))*(0.8*heff_SH2*(Tw_SH2-T_SH2a)*(k*P*us/Tsup^0.5)^(-
0.2)-(h_SH2-hin_SH2));

A=[  Lg2h1 Lg3h1; Lg2h2 0];
L1=(1/g11)*(v1-h_PSH-(g11/(rho_PSHa*V_PSH)*(heff_PSH*(Tw_PSH-
T_PSHa)*(k*P*us/Tsup^0.5)^0.8-(k*P*us/Tsup^0.5)*(h_PSH-hin_PSH))));
L2=(1/g21)*(v2-h_SH2-(g21/(rho_SH2a*V_SH2)*(heff_SH2*(Tw_SH2-
T_SH2a)*(k*P*us/Tsup^0.5)^0.8-(k*P*us/Tsup^0.5)*(h_SH2-hin_SH2))));

%manipulated variables
y = (A)\[L1; L2];

q1=y(1);
q2=y(2);
```

```
function [sys,x0,str,ts] = process_Tcntrl2(t,x,u,flag,x0) %
switch flag
%**************************
case 0 % initialization;
%**************************
sizes = simsizes; sizes.NumContStates = 8; sizes.NumDiscStates = 0;
sizes.NumOutputs = 12; sizes.NumInputs = 7; sizes.DirFeedthrough = 1;
sizes.NumSampleTimes = 1; sys = simsizes(sizes);
str = []; ts=[0 0];
%**************************
case 1 % derivatives;
%*********************************

% States
%*********************************
Tw_PSH=x(1);
hout_PSH=x(2);

%SH 1
Tw_SH1=x(3);
hout_SH1=x(4);

%SH 2
Tw_SH2=x(5);
hout_SH2=x(6);

%REHEATER
Tw_RH=x(7);
hout_RH=x(8);

% Inputs
%*********************************

us = u(1); qfuel=u(2);qat1=u(3);qat2=u(4); a1=u(5); P=u(6); u_RH=u(7);
mt=300e3;
cp=0.5;
k=327.057;
delH=29163.6516;
k_RH=1635.28;
hf=IAPWS_IF97('h_pT',13.78,275+273.15);
Vwt=63.9059;
Vt=89;
Vst=Vt-Vwt;
efb=0.4517;
a=(1-a1);
qfg=12.84353295*qfuel;

%*****************************
%Steam and water properties
%*****************************
Tsat=IAPWS_IF97('Tsat_p',P);
h_w=IAPWS_IF97('hL_p',P);
h_s=IAPWS_IF97('hV_p',P);
rho_w=1/(IAPWS_IF97('vL_p',P));
rho_s=1/(IAPWS_IF97('vV_p',P));
```

```
dt_s=IAPWS_IF97('dTsatdpsat_p',P);
d_hw=IAPWS_IF97('dhLdp_p',P);
d_hs=IAPWS_IF97('dhVdp_p',P);
d_vL=IAPWS_IF97('dvLdp_p',P);
d_rho=-d_vL*rho_w^2;
d_vS=IAPWS_IF97('dvVdp_p',P);
d_rhos=-d_vS*rho_s^2;


% functions
%**********************************

%Superheaters

hin_SH1=h_s;
Tin_SH1=IAPWS_IF97('T_ph',P,h_s);%kJ/kg
hat1=815; %kJ/kg
hat2=815; %kJ/kg
cpw=0.5; %kJ/kgK
rhow=8060; %kg/m3
V_PSH=6.884632408; %m3
V_SH1=13.99808183; %m3
V_SH2=11.13423406; %m3
V_RH=74.38189113;
Vw_PSH=0.672327384; %m3
Vw_SH1=1.367000178; %m3
Vw_SH2=1.087327545; %m3
Vw_RH=7.263856556;

%platen SH
ebolt=0.7;
 sigma=5.67E-08;     %W/m2K4
  Tg_PSH=(1568.15+1758.15)/2;  % K
Ar=151;
heff_PSH=11.080;

%SH 1
Tg_SH1=(1230.25+670.75)/2; %K

hweff_SH1=13.117;%W/(K kg/s^0.6)
heff_SH1=17.28154188;%W/(

%SH 2

Tg_SH2=(1230.25+1568.15)/2; %K

 %bypass factor

hweff_SH2=3.355;%W/(K kg/s^0.6) 4.991827971
heff_SH2=11.015;

%REHEATER

Tg_RH=(1568.15+1071.75)/2; %K
```

```
hweff_RH=7.574;
heff_RH=9.797309476;
Prh=P/5; %MPa
Tsupc=535+273.15;

%Attemperators

qs=(k*P/(IAPWS_IF97('T_ph',P,hout_PSH))^0.5)*us;

%AT1
qst_SH1=qs;%kg/s

qst_SH2=qst_SH1+qat1;

%AT2

qst_PSH= qs+qat1+qat2;
qst_RH=qst_PSH;
hin_SH_2=(hout_SH1*qst_SH1+hat1*qat1)/(qat1+qst_SH1);
hin_PSH_2=(hout_SH2*qst_SH2+hat2*qat2)/(qat2+qst_SH2);

%Reheater inlet conditions
Tout_PSH=IAPWS_IF97('T_ph',P,hout_PSH);
sin_Tb=XSteam('s_pT',P*10,Tout_PSH-273.15);
hisen_RH=XSteam('h_ps',P/5*10,sin_Tb);
hin_RH=0.725*(hisen_RH-hout_PSH)+hout_PSH;
Tin_RH=IAPWS_IF97('T_ph',P/5,hin_RH);

%%Steam Correlations

h=[hin_PSH_2 hout_SH1 hin_SH_2 hout_SH2 hout_RH];

P2=[ones(1,4)*P Prh];

%Superheated steam temperature

T=IAPWS_IF97('T_ph',P2,h);
Tin_PSH=T(1);
Tout_SH1=T(2);
Tin_SH2=T(3);

Tout_SH2=T(4);
Tout_RH=T(5);
T1=[Tin_PSH Tout_PSH Tin_SH1 Tout_SH1 Tin_SH2 Tout_SH2 Tin_RH Tout_RH];
P1=[ones(1,6)*P Prh Prh];

%density of steam

rho=1./(IAPWS_IF97('v_pT',P1,T1));
rhoin_PSH=rho(1);
rhoout_PSH=rho(2);
rhoin_SH1=rho(3);
rhoout_SH1=rho(4);
rhoin_SH2=rho(5);
```

```
rhoout_SH2=rho(6);
rhoin_RH= rho(7);
rhoout_RH= rho(8);

%model subequations

%platen superheater

T_PSHa=(Tin_PSH+Tout_PSH)/2;
Qw_PSH=Ar*ebolt*sigma*(Tg_PSH^4-Tw_PSH^4)*(1e-3);
Q_PSH=heff_PSH*qst_PSH^0.8*(Tw_PSH-T_PSHa);

%SH1
T_SH1a=(Tin_SH1+Tout_SH1)/2;
Q_SH1=heff_SH1*qst_SH1^0.8*(Tw_SH1-T_SH1a);
Qw_SH1=hweff_SH1*(a*qfg)^0.6*(Tg_SH1-Tw_SH1);

%SH2
T_SH2a=(Tin_SH2+Tout_SH2)/2;
Q_SH2=heff_SH2*qst_SH2^0.8*(Tw_SH2-T_SH2a);
Qw_SH2=hweff_SH2*(a*qfg)^0.6*(Tg_SH2-Tw_SH2);

%REHEATER

T_RHa=(Tin_RH+Tout_RH)/2;
Q_RH=heff_RH*qst_RH^0.8*(Tw_RH-T_RHa);
Qw_RH=hweff_RH*(a1*qfg)^0.6*(Tg_RH-Tw_RH);

%model

%platen superheater

%Gas-wall side

dTw_PSHdt=(Qw_PSH-Q_PSH)/(rhow*Vw_PSH*cpw);

%steam side
rho_PSHa=(rhoin_PSH+rhoout_PSH)/2;
dh_PSHdt=(Q_PSH-qst_PSH*(hout_PSH-hin_PSH_2))/(rho_PSHa*V_PSH);

%SH1

%Gas-wall side

dTw_SH1dt=(Qw_SH1-Q_SH1)/(rhow*Vw_SH1*cpw);

%steam side
rho_SH1a=(rhoin_SH1+rhoout_SH1)/2;
dh_SH1dt=(Q_SH1-qst_SH1*(hout_SH1-hin_SH1))/(rho_SH1a*V_SH1);

%SH2

%Gas-wall side
```

```
dTw_SH2dt=(Qw_SH2-Q_SH2)/(rhow*Vw_SH2*cpw);

%steam side
rho_SH2a=(rhoin_SH2+rhoout_SH2)/2;
dh_SH2dt=(Q_SH2-qst_SH2*(hout_SH2-hin_SH_2))/(rho_SH2a*V_SH2);


%REHEATER

%Gas-wall side

dTw_RHdt=(Qw_RH-Q_RH)/(rhow*Vw_RH*cpw);

%steam side
rho_RHa=(rhoin_RH+rhoout_RH)/2;
dh_RHdt=(Q_RH-qst_RH*(hout_RH-hin_RH))/(rho_RHa*V_RH);

sys = [dTw_PSHdt;dh_PSHdt;dTw_SH1dt; dh_SH1dt;dTw_SH2dt; dh_SH2dt;dTw_RHdt;
dh_RHdt];%dhin_SH2;dhin_PSH; dh_PSHa; dh_SH2a];

%**********************************
case 3 % outputs;
%**********************************

    k=327.057;
    Tsup=(IAPWS_IF97('T_ph',u(6),x(2)));
 qs=(k*u(6)/Tsup^0.5)*u(1);

 hin_SH2=(qs*x(4)+815*u(3))/(qs+u(3));
 hin_PSH=((qs+u(3))*x(6)+815*u(4))/(qs+u(3)+u(4));
 Tin_SH2=IAPWS_IF97('T_ph',u(6),hin_SH2);
 Tin_PSH=IAPWS_IF97('T_ph',u(6),hin_PSH);
% %Reheater inlet conditions
 Tout_PSH=IAPWS_IF97('T_ph',u(6),x(2));
 Tout_SH2=IAPWS_IF97('T_ph',u(6),x(6));
 T_PSHa=(Tin_PSH+Tout_PSH)/2;
 T_SH2a=(Tin_SH2+Tout_SH2)/2;

 sys = [x(1);x(2);x(4);x(5);x(6);hin_SH2; hin_PSH;T_PSHa; T_SH2a; x(7);
x(8);x(3)];
    case {2, 4, 9}
    sys = [];
otherwise
error(['unhandled flag = ',num2str(flag)]);
end
```

```
function gm  = shift(us, P,g31, g32, v1,qfuel, h_RH, stt,Tw_RH,qat1,qat2)

%#codegen
%static state feedback for controlling reheated steam temperature.
%Parameters
k=1635.28;
cpw=0.5; %kJ/kgK
rhow=8060; %kg/m3
V_RH=74.38189113;
Vw_RH=7.263856556;
efb=0.4517;

qfg=12.84353295*qfuel;

if qat1<0
    qat1=0;
end
if qat2<0
    qat2=0;
end

%REHEATER

Tg_RH=(1568.15+1071.75)/2; %K
hweff_RH=7.574;
heff_RH=9.797309476
Prh=P/5;
rhoin_RH=stt(6);
rhoout_RH=stt(5);
dV_RHdh=stt(4);
T_RHa=stt(1);
Tout_RH=stt(7);
hin_RH=stt(3);
dTdh=stt(2);

%functions
rho_RHa=(rhoin_RH+rhoout_RH)/2;
Lfh=1/(rho_RHa*V_RH)*(heff_RH*(Tw_RH-
T_RHa)*((k*Prh*us/Tout_RH^0.5)+qat1+qat2)^(0.8)-
(k*Prh*us/Tout_RH^0.5+qat1+qat2)*(h_RH-hin_RH));

dLfh=[1/(rho_RHa*V_RH)*heff_RH*((k*Prh*us/Tout_RH^0.5)+qat1+qat2)^(0.8)
1/(rho_RHa*V_RH)*(-heff_RH/2*((k*Prh*us/Tout_RH^0.5)+qat1+qat2)^(0.8)*dTdh-
(k*Prh*us/Tout_RH^0.5)+qat1+qat2)+dV_RHdh/2*1/V_RH*(heff_RH*(Tw_RH-
T_RHa)*((k*Prh*us/Tout_RH^0.5)+qat1+qat2)^(0.8)-
(k*Prh*us/Tout_RH^0.5+qat1+qat2)*(h_RH-hin_RH))];

f=[-1/(rhow*cpw*Vw_RH)*(heff_RH*(Tw_RH-
T_RHa)*(k*Prh*us/Tout_RH^0.5+qat1+qat2)^(0.8));1/(rho_RHa*V_RH)*(heff_RH*(Tw_
RH-T_RHa)*((k*Prh*us/Tout_RH^0.5)+qat1+qat2)^(0.8)-
(k*Prh*us/Tout_RH^0.5+qat1+qat2)*(h_RH-hin_RH))];

g=[1/(rhow*cpw*Vw_RH)*(hweff_RH*qfg^0.6*(Tg_RH-Tw_RH));0];

m0=dLfh*f;
```

```
m1=dLfh*g;
a=1/g32*(v1-h_RH-(g31*Lfh+g32*m0))/m1;

if a<=0
    gm=0;
else
gm=a^(1/.6);
end
```

```
function [sys,x0,str,ts] = process_Tcntrl3(t,x,u,flag,x0) %
switch flag
%*******************************
case 0 % initialization;
%*******************************
sizes = simsizes; sizes.NumContStates = 8; sizes.NumDiscStates = 0;
sizes.NumOutputs = 2; sizes.NumInputs = 7; sizes.DirFeedthrough = 0;
sizes.NumSampleTimes = 1; sys = simsizes(sizes);
str = []; ts=[0 0];

%*******************************
case 1 % derivatives;
 %*******************************

% States
%*******************************

%platen SH
Tw_PSH=x(1);
hout_PSH=x(2);

%SH 1
Tw_SH1=x(3);
hout_SH1=x(4);

%SH 2
Tw_SH2=x(5);
hout_SH2=x(6);

%REHEATER
Tw_RH=x(7);
hout_RH=x(8);

%Inputs
%*******************************
us = u(1); qfuel=u(2);qat1=u(3);qat2=u(4); a1=u(5); P=u(6); u_RH=u(7);

%parameters
%*******************************
mt=300e3;
cp=0.5;
k=327.057;
delH=29163.6516;
k_RH=1635.28;
Tsup=535+273.15;
hf=IAPWS_IF97('h_pT',13.78,275+273.15)
Vwt=63.9059;
Vt=89;
Vst=Vt-Vwt;
efb=0.4517;
a=(1-a1);
qfg=12.84353295*qfuel;

%*******************************
%Steam and water properties
```

```
%*******************************
Tsat=IAPWS_IF97('Tsat_p',P);
h_w=IAPWS_IF97('hL_p',P);
h_s=IAPWS_IF97('hV_p',P);
rho_w=1/(IAPWS_IF97('vL_p',P));
rho_s=1/(IAPWS_IF97('vV_p',P));
dt_s=IAPWS_IF97('dTsatdpsat_p',P);
d_hw=IAPWS_IF97('dhLdp_p',P);
d_hs=IAPWS_IF97('dhVdp_p',P);
d_vL=IAPWS_IF97('dvLdp_p',P);
d_rho=-d_vL*rho_w^2;
d_vS=IAPWS_IF97('dvVdp_p',P);
d_rhos=-d_vS*rho_s^2;

%functions
%*******************************

%Superheaters

hin_SH1=h_s;
Tin_SH1=IAPWS_IF97('T_ph',P,h_s);%kJ/kg
hat1=815; %kJ/kg
hat2=815; %kJ/kg
cpw=0.5; %kJ/kgK
rhow=8060; %kg/m3
V_PSH=6.884632408; %m3
V_SH1=13.99808183; %m3
V_SH2=11.13423406; %m3
V_RH=74.38189113;
Vw_PSH=0.672327384; %m3
Vw_SH1=1.367000178; %m3
Vw_SH2=1.087327545; %m3
Vw_RH=7.263856556;


%platen SH

ebolt=0.7;
 sigma=5.67E-08;     %W/m2K4
  Tg_PSH=(1568.15+1758.15)/2;  %1591.15 K
Ar=151;
   heff_PSH=11.080;


%SH 1
Tg_SH1=(1230.25+670.75)/2; %K
hweff_SH1=13.117;%W/(K kg/s^0.6)
heff_SH1=17.28154188;%W/(

%SH 2
Tg_SH2=(1230.25+1568.15)/2; %K
hweff_SH2=3.355;%W/(K kg/s^0.6) 4.991827971
heff_SH2=11.015;

%REHEATER
```

```
Tg_RH=(1568.15+1071.75)/2; %K
hweff_RH=7.574;
heff_RH=9.797309476;

Prh=P/5; %MPa

%Attemperators

qs=(k*P/(IAPWS_IF97('T_ph',P,hout_PSH))^0.5)*us;

%AT1
qst_SH1=qs;%kg/s
qst_SH2=qst_SH1+qat1;
hin_SH2=(hout_SH1*qst_SH1+hat1*qat1)/(qat1+qst_SH1);
hin_PSH=(hout_SH2*qst_SH2+hat2*qat2)/(qat2+qst_SH2);

%AT2
qst_PSH= qs+qat1+qat2;
qst_RH=(k_RH*Prh/(IAPWS_IF97('T_ph',Prh,hout_RH))^0.5)*u_RH+qat1+qat2;

%Reheater inlet conditions
Tout_PSH=IAPWS_IF97('T_ph',P,hout_PSH);
sin_Tb=XSteam('s_pT',P*10,Tout_PSH-273.15);
hisen_RH=XSteam('h_ps',P/5*10,sin_Tb);
hin_RH=0.725*(hisen_RH-hout_PSH)+hout_PSH;
Tin_RH=IAPWS_IF97('T_ph',P/5,hin_RH);

%%Steam Correlations

h=[hin_PSH hout_SH1 hin_SH2 hout_SH2 hout_RH];
P2=[ones(1,4)*P Prh];

%Superheated steam temperature

T=IAPWS_IF97('T_ph',P2,h);
Tin_PSH=T(1);
Tout_SH1=T(2);
Tin_SH2=T(3);
Tout_SH2=T(4);
Tout_RH=T(5);
T1=[Tin_PSH Tout_PSH Tin_SH1 Tout_SH1 Tin_SH2 Tout_SH2 Tin_RH Tout_RH];
P1=[ones(1,6)*P Prh Prh];

%density of steam

rho=1./(IAPWS_IF97('v_pT',P1,T1));
rhoin_PSH=rho(1);
rhoout_PSH=rho(2);
rhoin_SH1=rho(3);
rhoout_SH1=rho(4);
rhoin_SH2=rho(5);
rhoout_SH2=rho(6);
rhoin_RH= rho(7);
rhoout_RH= rho(8);
```

```
%model subequations
%*******************************

%platen superheater

T_PSHa=(Tin_PSH+Tout_PSH)/2;
Qw_PSH=Ar*ebolt*sigma*(Tg_PSH^4-Tw_PSH^4)*1e-3;
Q_PSH=heff_PSH*qst_PSH^0.8*(Tw_PSH-T_PSHa);

%SH1
T_SH1a=(Tin_SH1+Tout_SH1)/2;
Q_SH1=heff_SH1*qst_SH1^0.8*(Tw_SH1-T_SH1a);
Qw_SH1=hweff_SH1*(a*qfg)^0.6*(Tg_SH1-Tw_SH1);

%SH2
T_SH2a=(Tin_SH2+Tout_SH2)/2;
Q_SH2=heff_SH2*qst_SH2^0.8*(Tw_SH2-T_SH2a);
Qw_SH2=hweff_SH2*(a*qfg)^0.6*(Tg_SH2-Tw_SH2);

%REHEATER

T_RHa=(Tin_RH+Tout_RH)/2;
Q_RH=heff_RH*qst_RH^0.8*(Tw_RH-T_RHa);
Qw_RH=hweff_RH*(a1*qfg)^0.6*(Tg_RH-Tw_RH);

%model
%*******************************

%platen superheater

%Gas-wall side

dTw_PSHdt=(Qw_PSH-Q_PSH)/(rhow*Vw_PSH*cpw);

%steam side
rho_PSHa=(rhoin_PSH+rhoout_PSH)/2;
dh_PSHdt=(Q_PSH-qst_PSH*(hout_PSH-hin_PSH))/(rho_PSHa*V_PSH);

%SH1

%Gas-wall side

dTw_SH1dt=(Qw_SH1-Q_SH1)/(rhow*Vw_SH1*cpw);

%steam side
rho_SH1a=(rhoin_SH1+rhoout_SH1)/2;
dh_SH1dt=(Q_SH1-qst_SH1*(hout_SH1-hin_SH1))/(rho_SH1a*V_SH1);

%SH2

%Gas-wall side
```

```
dTw_SH2dt=(Qw_SH2-Q_SH2)/(rhow*Vw_SH2*cpw);

%steam side
rho_SH2a=(rhoin_SH2+rhoout_SH2)/2;
dh_SH2dt=(Q_SH2-qst_SH2*(hout_SH2-hin_SH2))/(rho_SH2a*V_SH2);


%REHEATER

%Gas-wall side

dTw_RHdt=(Qw_RH-Q_RH)/(rhow*Vw_RH*cpw);

%steam side
rho_RHa=(rhoin_RH+rhoout_RH)/2;
dh_RHdt=(Q_RH-qst_RH*(hout_RH-hin_RH))/(rho_RHa*V_RH);

sys = [dTw_PSHdt;dh_PSHdt;dTw_SH1dt; dh_SH1dt;dTw_SH2dt; dh_SH2dt;dTw_RHdt;
dh_RHdt];

%*******************************
case 3 % outputs;
%*******************************

        sys = [x(7);x(8)];

    case {2, 4, 9}
    sys = [];
otherwise
error(['unhandled flag = ',num2str(flag)]);
end
```

```
%Power set point ramping down at 2%/min.

function y = fcn(u)
%#codegen
y= 46.36+113.5;
yss=y;
k=floor(u);
if k>=150&&k<=987.5
 y = yss-(3.2/60)*(k-150);
 elseif k>987.5
      y = yss-( 3.2/60)*(987.5-150);
end


%Power set point wide range multiple step changes.

function y = fcn(u)
%#codegen
y= 46.36+113.5;
yss=y;
k=floor(u);
if k>=50&&k<=1550
y = yss-32;
 elseif k>=1550&&k<=3050
 y=yss;
 elseif k>=3050&&k<=4550
      y = yss-32;
elseif k>=4550
    y=yss
end


%Deadtime fluctuations for power set point wide range multiple step changes.

function y = fcn(u)
%#codegen
t=1500;
y=90;

k=floor(u);
if k>=1500&&k<=2500
 y = 80;
elseif k>=2500&&k<=4000
y=110;
elseif k>=4000&&k<=5500
y=120;
elseif k>=5500&&k<=7500
y=90;
elseif k>=7500&&k<=10000
y=85;
elseif k>=10000&&k<=13000
y=95;
elseif k>=13000&&k<=17000
y=120;
elseif k>=17000&&k<=25000
y=115;
```

```
elseif k>=25000&&k<=45000
y=100;
elseif k>=45000&&k<=65000
y=90;
elseif k>65000
    y=120;
end
```